Zircon provenance of Devonian deposits in Western Norway

By

Leif-Erik Rydland Pedersen

01.06.2011

Department of Earth Science, University of Bergen

2011

Master Thesis

Abstract

The provenance of the Devonian deposits of western Norway has been studied by detrital zircon geochronology. These deposits are found in the Fensfjorden -, Solund -, Kvamshesten -, Hornelen - and Smøla basin. A total of 9 samples were collected, and extracted for detrital zircons (n = 713), which were analyzed with laser ablation ICP-MS to determine their U/Pb age.

The detrital U/Pb zircon ages provide three distinct groups: ~400-500 Ma, 900-1200 Ma, and 1400-1700 Ma, which are correlated rocks formed during Caledonian, Sveconorwegian, and Gothian orogeny, respectively.

The zirkon population of the samples from the Fensfjorden and the Solund basins, which are the two southernmost basins, are dominated by Sveconorwegian zircons. The Lindås Nappe (Middle Allochthon) appears to be the most likely source of these zircons. To the north there is a marked change to more Gothian zircons in the Kvamshesten basin. This is consistent with the Gothian ages reported from the Middle Allochthon in this area (the Dalsfjord Suite). Assuming that the Middle Allochthon is the main source of the Proterozoic zircons of these basins, then this supports a marked change in the ages of the Middle Allochton form an Sveconorwegian-dominated Lindås Nappe in the south - to a Gothian-dominated Dalsfjord Nappe towards the north.

In the Hornelen and Smøla basins there are a large component of Caledonian zircons with the Upper Allochthon as a main source. In the Hornelen basin in particular, there is a population of zircons with a young Caledonian age (410 – 415 Ma). Potential source rocks for this component is as yet only reported from the Middle/Lower Allochthons in the footwall of the Nordfjord-Sogn Detachment Zone and from the Western Gneiss Region.

Acknowledgements

This master thesis is a part of the Source to Sink cooperation between University of Bergen and Statoil.

I would like to thank my supervisors Prof. Jan Kosler (UIB) and Hege Fonneland (Statoil), for excellent scientific guidance during these two years.
Martina, Siv, and Ole are thanked for their patience and helpfulness during the process of sample preparation and analyses.

I would also like to thank Eivind and Einar for all the funny moments we've had in "tarmen".

Last but not least I want to thank my dad for everything he have taught me, and all the great discussions we've had!

Contents

Introduction

In Neoproterozoic to mid Phanerozoic times, the Iapetus Ocean separated the continents of Laurentia and Baltica situated in the southern hemisphere. This came to an end when the two continents collided in the end of the Silurian period, forming the Caledonian orogeny.

The Caledonian orogeny appears to have started by the initiation of subduction and formation of volcanic arcs at around the Cambrian-Ordovician boundary. This was followed by 50 million years of crustal accretion and formation of ophiolite complexes, arc sequences, granitic batholiths, and arc-continent collisional events. The Solund-Stavfjord Ophiolite complex (443 Ma) that forms the substrate to one of the West Norwegian Devonian basins represents the last remnant of the Iapetus oceanic crust preserved in the orogen.

The oceanic accretionary stage of the orogeny was followed by mid Silurian to Early Devonian continent-continent collision between Laurentia and Baltica. Exotic terranes consisting of outer Baltic margin with sedimentary cover, Iapetus oceanic crust with sedimentary cover, island arcs and pieces of Laurentia were then thrusted onto the Baltic margin, while some parts of the this margin became subducted to ultra-high pressure metamorphic conditions.

After the orogenic peak and maximum topographic elevation in the Early Devonian, the orogen started to collapse by backsliding of the allochthons along numerous detachment zones. In Western Norway the Nordfjord-Sogn Detachment Zone is the most prominent. During this backsliding, parts of the subducted Baltic basement were exhumed from eclogite facies conditions at around 80 km depth, and brought in tectonic contact with Caledonian allochthons that have only experienced greenschist facies conditions (8 – 50 km depth).

During the collapse, the terrestrial sedimentary sequences of Devonian age were formed. They were deposited in extensional tectonic basins in the hanging walls of the detachment zones, and the continued opening of accommodation space by westward backsliding resulted in vast stratigraphical basin thicknesses. The Devonian sedimentary sequences were deposited on different allochtons in the hanging wall, and they represent a window into the Devonian paleogeology of

western Norway. As these sedimentary sequences are closely associated in space and time with detachment faults that accommodated several tens of kilometers of footwall exhumation during the orogenic collapse, the provenance of these basins may potentially provide information on this exhumation history.

In this master thesis, I report the U/Pb zircon provenance ages of sandstones from Devonian basins of Western Norway. The provenance of five different basins has been constrained by acquiring U/Pb age data by laser ablation ICP-MS from 713 zircons extracted from 9 samples. In an attempt to improve the knowledge on the orogenic collapse from the changing Devonian paleogeology of Western Norway, the provenance signatures of the different Devonian basins are compared, and potential sources from different tectonic units are defined and discussed.

The Geology of Western Norway

The Caledonian orogeny of western Norway is composed of three principal components: 1) an autochthonous gneiss complex, called the Western Gneiss Region, that consists of late Precambrian and lower Paleozoic meta sediments and Precambrian crystalline rocks; 2) a stack of Caledonian Nappes comprising both slices of the continental margin as well as exotic oceanic terrains; and 3) late Caledonian mollase sequences of Devonian age (Fig. 1).

Proterozoic Basement

Western Gneiss Region (WGR) represents the northwestern part of southwestern Scandian Domain, which is dominated by rocks that formed during the Gothian orogeny (1750 - 1500 Ma). The WGR consists mainly of migmatic orthogneisses that range from dioritic to granitic composition. In the northwestern part of the WGR, mafic gneisses, amphibolites, ultramafic rocks and paragneisses are abundant, but supracrustal rocks are volumetricly insignificant (Skår & Pedersen 2003 and references therein).

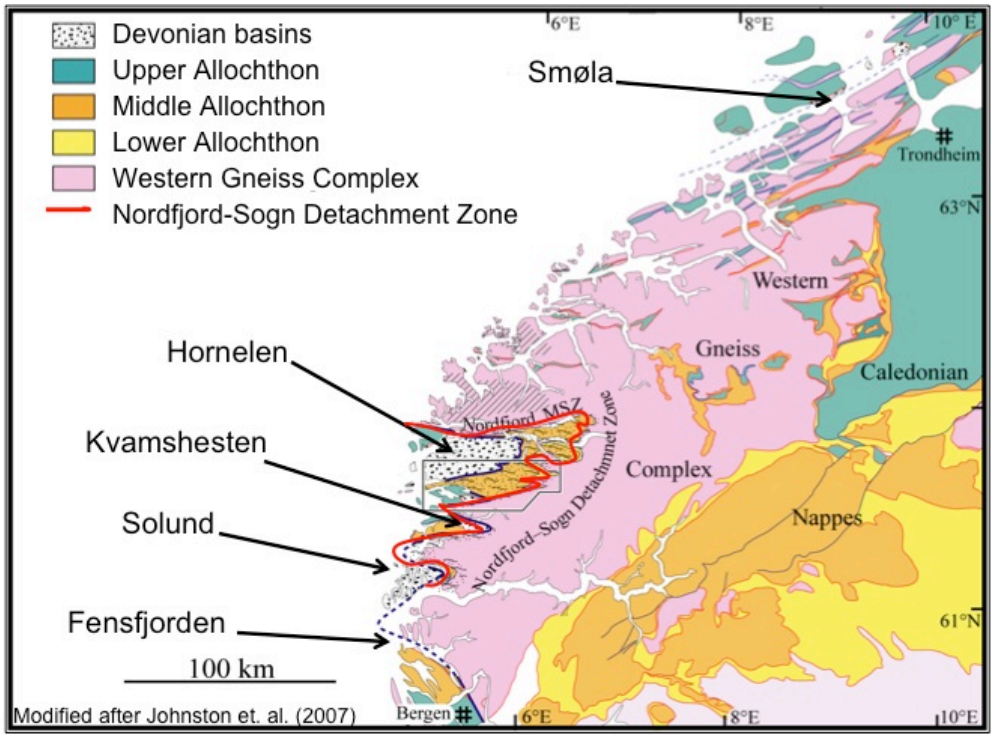

Figure 1. *Overview of the geology in southwestern Norway. Far thrusted exotic nappes to the east, Western Gneiss Region exposed in central parts , and the Devonian basins are along the coast situated on the top of different nappes (Modified after Johnston et al. 2007).*

Age determinations from the WGR suggest that it becomes younger towards the south and the west, with an age range of 1686-1653 Ma in the northern part to 1641 Ma in the south (Skår & Pedersen 2003 and references therein). Numerous granitic plutons intruded into the WGR during the Sveconorwegian orogeny (1250-900 Ma), and they are mainly found in the central part of the WGR (Fig. 2).

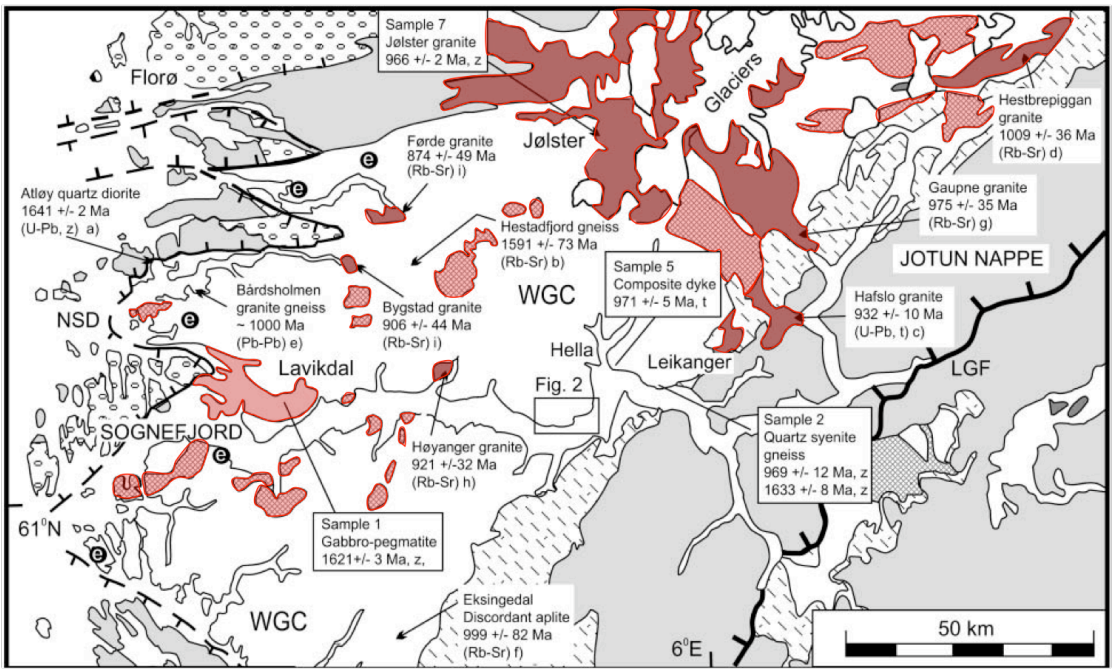

Figure 2. *Geological map of the southern part of Western Gneiss Region. Legend: Predominately Gothian Gneisses of granitic to dioritic composition, as well as gneiss-migmatites and amphibolite colored in white; Sveconorwegian plutons colored in red; Lower Allochthon with black dashed lines; Middle Allochthon colored light grey; Devonian Sedimentary rocks with elliptic circles. (modified from Skår & Pedersen 2003).*

The 40Ar/39Ar muscovite cooling ages in WGR are diachronous, from ~400 Ma in the east to ~374 Ma in the west (Hacker 2007), indicating the WNW parts of the WGR were at deeper levels when the muscovite in the eastern part of the WGR reached its closing temperature (400 °C). The WGR appears to have been first exhumed from the upper mantle depth as one unit, and was further exhumed by unroofing progressively from east to west (Johnston 2007; Kylander et al. 2008 and references therein).

Allochthons

The Caledonian nappe stack in Norway is divided into four tectonic units: 1) the Lower Allochthon; 2) the Middle Allochthon; 3) the Upper Allochthon; and 4) the Uppermost Allochthon (Gee et al. 1985). Of these, only the Lower, Middle and Upper Allochthons are exposed in Western Norway (Fig. 1). In the coastal region where the Devonian basins are located, these allochthons are exposed in the Nordfjord-Sogn area and in the Bergen area, - where they constitute the minor and major Bergen Arcs. In both areas the allochthons are bound to the east by late orogenic detachment faults.

Lower Allochthon

The Lower Allochthon consists of lower Paleozoic and late Precambrian meta sediments, that together with Precambrian crystalline rocks are interpreted to originate from the continental margin of Baltica as a basement-cover pair (Roberts & Gee 1985). In the study area there are two groups that belong to this allochthon:

1) The Askvoll Group that is found east of the Kvamshesten Devonian basin, and that consists of mylonitic gneisses dated by the U/Pb-zircon medthod to 1641± 23 Ma (Skår et al. 1994).

2) The Svartekari Group that is exposed south of Hornelen, and that is made of muscovite-rich ortho- and paragneisses. The orthogneisses have been dated to 1604 Ma, which is interpreted as corresponding to the igneous crystallization of the protolith, with a Caledonian lower concordia intercept (Johnston 2006).

Middle Allochthon

The Middle Allochthons consists of what is thought to be the outer continental margin of Baltica and its sedimentary cover, made of late Precambrian and lower Paleozoic meta sediments, mafic dikes, and Precambrian crystalline rocks (Roberts & Gee 1985). The crystalline rocks are exposed within the Lindås Nappe, the Dalsfjord Suite and the Eikefjord Group.

The Lindås Nappe is situated within the Bergen Arcs just south of the Fensfjorden basin, and consists of Proterozoic anortosite- mangerite-charnockite granite suite and banded gneiss complexes (Bingen 2001 and references therein), with local Caledonian eclogite and amphibolite overprint in the west (Bingen 2001). The Dalsfjord Suite, which is located in the Kvamshesten area, has been correlated with the Jotun Complex and to some extent with the Lindås Nappe (Corfu & Andersen 2002). The complex is composed of monzonitic to syenitic rocks with minor gabbroic and anorthositic units (Kolderup 1922, 1928). A monzonite sample has been dated to 1634 ± 3 Ma, while a crosscutting gabbro formed at 1464 ± 6 Ma (Corfu & Andersen 2002). Both rocks show a strong Sveconorwegian overprint. The Eikefjord Group consists of two orthogneiss suites; fined-grained biotite gneisses associated with anorthosite layers and boudins and albite schists associated with megacrystic augen gneisses. The biotite gneiss yielded discordant zircon U/Pb ages, 1543 and 1000 Ma (Johnston 2006). The Eikefjord Group, Lindås Nappe, Dalsfjord Complex and Jotun Nappe are correlated with each other due to similarities in the rock compositions and age spectra (Bingen 2001; Corfu & Andersen 2002; Johnston 2006; Lundmark et al. 2007).

Metasedimentary sequences within the Middle Allochthon are associated with the Dalsfjord Suite and with the Hyllestad Complex. The Høyvik Group unconformably overlay the Dalsfjord Suite (Andersen et al. 1990). This group consists of late Precambrian to Ordovician quartzites and meta-arkoses with local schist and marbles. At Ordovician times the rocks of the Høyvik Group experienced greenschist facies metamorphism (Andersen et al. 1998). The Høyvik Group is again unconformably overlain by the Herland Group, which is interpreted to represent continental margin deposits. It represents a transgressive sequence composed of conglomerates, metasandstones, and carbonates (Brekke & Solberg 1987). Pentemerides fossils within the group provide an age constraint of 428-423 Ma (Wenlock) for sediment deposition (Andersen et al. 1990).

The Hyllestad Complex that is cropping out east of the Solund basin consists of psammite, mafic schist, metapelite, semipelite and amphibolite, assumed to be of

Eocambrian age (Tillung 1999). This complex is strongly mylonitized and is also considered to be a part of the NSDZ (Norton 1987).

The Lykkebø Group consists of quartzites interlayed with pelitic schist. Zircon population U-Pb ages cluster around 1700-1600 Ma and 1000 Ma and support the interpretation that these sediments represent the Precambrian cover of the Eikefjord Group, correlating both groups to the Dalsfjord Suite and Høyvik Group as a basement-cover pair (Johnston 2006; Corfu & Andersen 2002).

Upper Allochthon

The Upper Allochthon is made of oceanic crust, sediments and island arcs that formed in the Iapetus Ocean. The Sunnfjord Melange, which consists of carbonate-bearing greenschist and conglomerates, is considered to be the terrane-link between Middle and Upper Allochthon (Alsaker & Furnes 1994; Andersen et al. 1990).

The Solund-Stavfjord Ophiolite Complex (S-SOC) crops out northwest of Solund and west of the Kvamshesten Devonian basin. The ophiolite complex has yielded an U/Pb age of 443 ± 3 Ma (Dunning & Pedersen 1988). The younger Stavenes Group is situated northwest of the Kvamshesten Devonian basin, and consists of metagreywackes with local intrusions, volcanoclastics, and pillow lavas. The unit lies conformably on the S-SOC, and the metagreywackes are considered to represent its sedimentary cover (Furnes et al. 1990). Provenance study of the cover units yielded U/Pb ages of 492-462, 1959-1024, and 2495 Ma (Pedersen & Dunning 1993).

The Lifjorden Complex is located east of the Solund Devonian basin, and consists mainly of meta-graywacke, greenschist and greenstones (Tillung 1999), and is intruded by the Sogneskollen Gronodiorite dated to 434 ± 4 Ma (Hacker et al. 2003). The rock composition and deformation suggest that the Lifjorden Complex can be correlated with the Stavenes Group (Furnes et al. 1990). The Sunnarvik Group consists of metavolcanic rocks intruded by keratophyric dikes, with a quartzite and schist cover, and is located south of Hornelen. Two samples have been dated from this group; an intrusion with a 556 Ma age, and a

sandstone yielding zircon age clusters around 1500 Ma and 1000 Ma (Johnston 2006).

Bremangerlandet west of Hornelen consists of two tectonostratigraphical units; the lower "oceanic terrain", consisting of metamorphic igneous rocks, that is in thrust contact to the overlying sedimentary Kalvåg Melange. The latter is of Ordovician-Silurian age and has been intruded by the Bremanger Granodiorite and the Gåsøy intrusion, which yields ages of 443 ± 4 and 440 ± 5 Ma, respectively (Hansen et al. 2002).

Devonian Detachment Zones

The formation of the Devonian basins in Western Norway is linked to extensional tectonics. The collapse of the Caledonian orogeny started in the early Devonian times, around 400 Ma shortly after the peak metamorphism (Fossen 1992). A simplified model proposed by Fossen (2000) divides the extensional history into three different modes as illustrated in figure 3: Mode 1 involves reactivation of the basal décollement zone leading to hinterland directed transport of the orogenic wedge; Mode 2 is development of the W-NW dipping extensional shear zones cutting into the basement, while Mode 3 represents the formation of brittle faults with some semi ductile elements.

There are three detachment shear zones (Mode 2) that have played a key role in the deposition of the Devonian basins in western Norway: The Nordfjord-Sogn Detatchement Zone, The Fensfjorden fault, and the Høybakken Detachement Zone.

The Nordfjord-Sogn Detachment Zone (NSDZ) is the largest of the Caledonian extensional shear zones in terms of thickness, offset and strain. The NSDZ is a 2-6 km wide, low-angle ductile shear zone that extends ~100 km along strike - from the Solund region in the south to Sørøyane UHP domain in the north (Fig. 1). The zone is characterized by top to the west asymmetric extensional shear fabrics found in rocks of all tectonostratigraphic levels, and is broadly centered within the Lower and Middle Allochthons (Johnston et al. 2007). The lower part

of the NSDZ (Lower/Middle Allochthon-southern WGC; footwall) reached amphibolite and locally eclogite facies, whereas the structurally higher parts of Middle and Upper Allochthon (the hanging wall) were only exposed to greenschist facies conditions. Ar/Ar muscovite ages show that the lower part of the NSDZ went through the muscovite blocking temperature at a later stage than the upper parts (402-396 and 419-417 Ma respectively; Johnston et al. 2007). The displacement by the NSDZ is suggested to be around 50-100 km (Norton 1986; Fossen 2000).

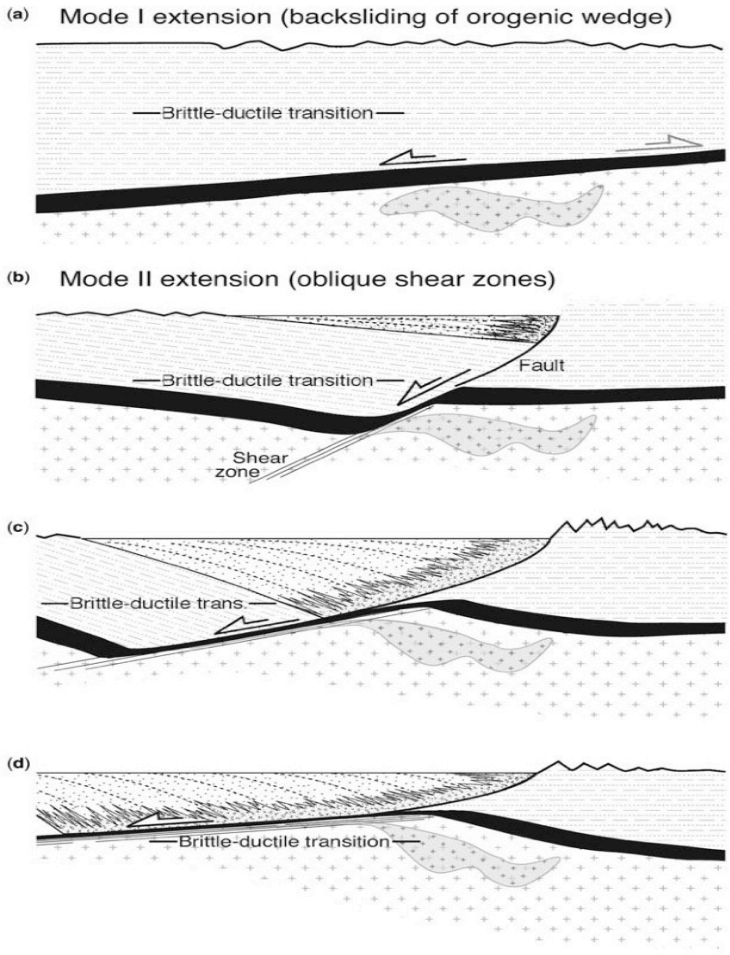

Figure 3. *Illustration of the two first modes of extensional tectonics during the end of the Caledonian orogeny. A) Mode 1 is reactivation of the basal thrust zone into a low angled detachment zone. B) Mode 2 corresponds to the initiation of steeper dipping shear zones that rotate to lower angle with increasing strain, leading to development (c-d) of hanging wall basins with very thick stratigraphic sequence (Fossen 2010).*

To the south, the NSDZ extends into the Bergen Arc region, where the Fensfjorden fault is regarded to be a branch of the NSDZ (Norton 1986, 1987; Milnes et *al.* 1988; Wenneberg & Milnes 1994).

The Devonian deposits in the Smøla region are associated with the Høybakken Detachement Zone (Fig. 4). In this area, the extensional regime differed significantly from that of the NSDZ (Fossen 2010 and references therein). Whereas the extension along the NSDZ is westward directed, the extension in this northern area was bidirectional (Fig. 4). There, two detachment zones formed (Høybakken and Kollstraumen) with a SW and NE dip direction, respectively (Braathen et al. 2000). This bidirectional extension exhumed the Central Norway basement window (CNBW), which triggered magmatic activity and the formation of granite bodies (Braathen et al. 2000).

The hanging wall of the Høybakken detachment consists of Caledonian nappes and plutons in addition to the Devonian basin. The Høybakken detachment zone consists of a 2-3 km thick package of mylonites with a 20-degree SE dip (Séranne 1992). These detachment zones experienced greenschist to amphibolite facies metamorphic conditions (Braathen et al. 2000).

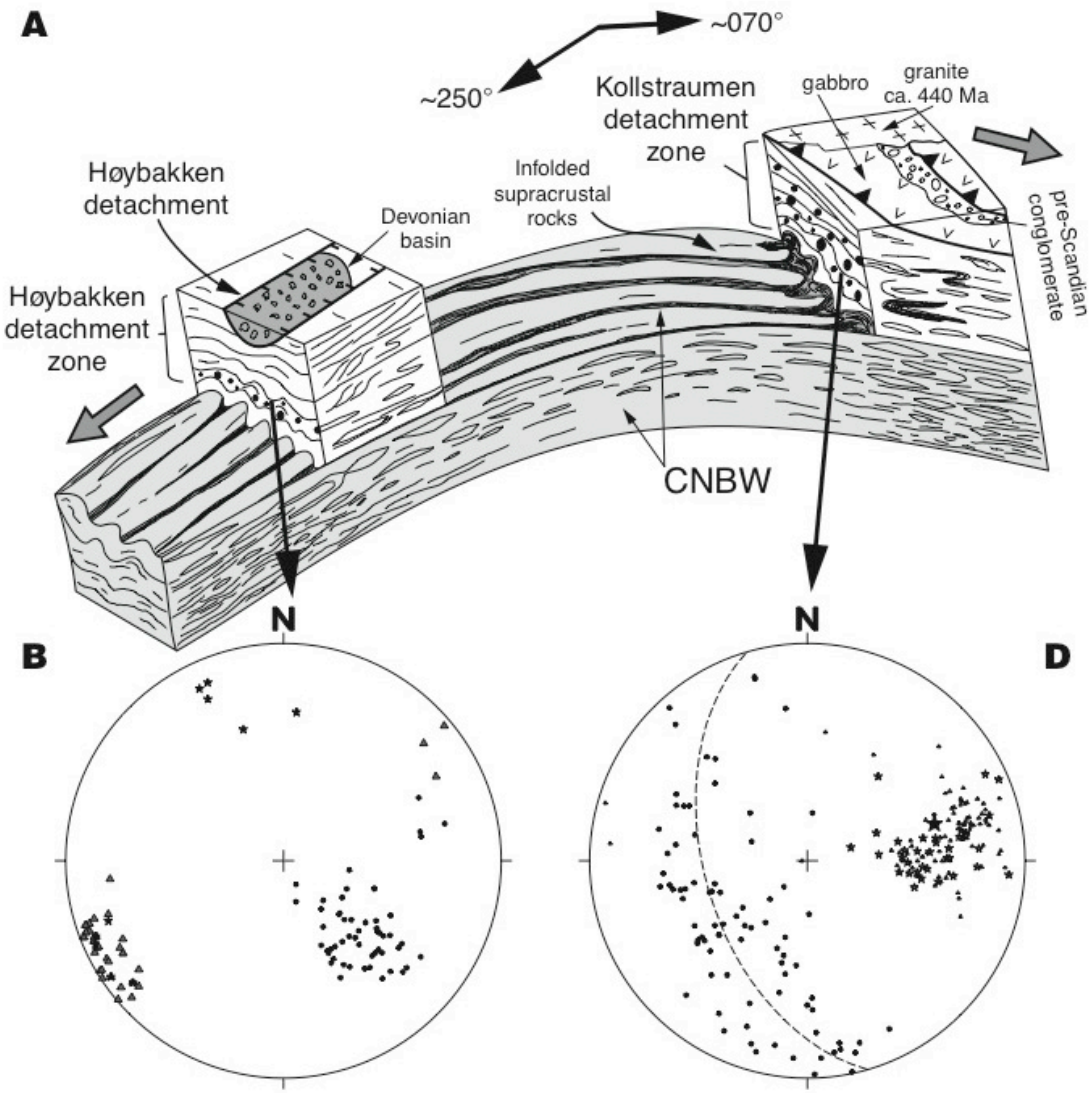

Figure 4. *Block diagram that illustrates the bidirectional extensional regime provided by the Høybakken and the Kollstraumen detatchement zones. This lead to exhumation of the CNBW and formation of Devonian basins on the Høybakken hanging wall (Braathen et al. 2000).*

The Devonian Basins and sample locations

Five Devonian basins are located along the west coast of Norway: From south to north these are: The Fensfjorden, Solund, Kvamshesten, Håsteinen, and the Hornelen basins (Fig. 5, a). In addition, there is also the Røragen basin close to Røros, and The Smøla basin northwest of Trondheim (Fig. 5, b). All these sedimentary basins are composed of continental clastic sedimentary rocks. Studies of plant fossils and crossopterygian fish in the early to middle twentieth century suggested a middle Devonian age (Jarvik 1949).

In the Hornelen and the Kvamshesten basins there are locally derived fanglomerates in the fringes and sandstone deposits in the central parts of the basin (Steel & Gloppen 1980). The other basins are mostly filled with unsorted and ungraded conglomerates interpreted as alluvial fan deposits (Seranne & Seguret 1987 and references therein). The stratigraphic thicknesses are unusually large compared to the size of the basins, as exemplified by a stratigraphic thickness of 25 km for the Hornelen basin that is only 18 km in width (Steel et al. 1977). The basins along the west coast mostly lie unconformably on the exotic nappes in the west, while the eastern part is in fault contact with the Nordfjord Sogn Detatchment Zone (NSDZ) that formed during collapse of the Caledonian orogeny (Norton 1986).

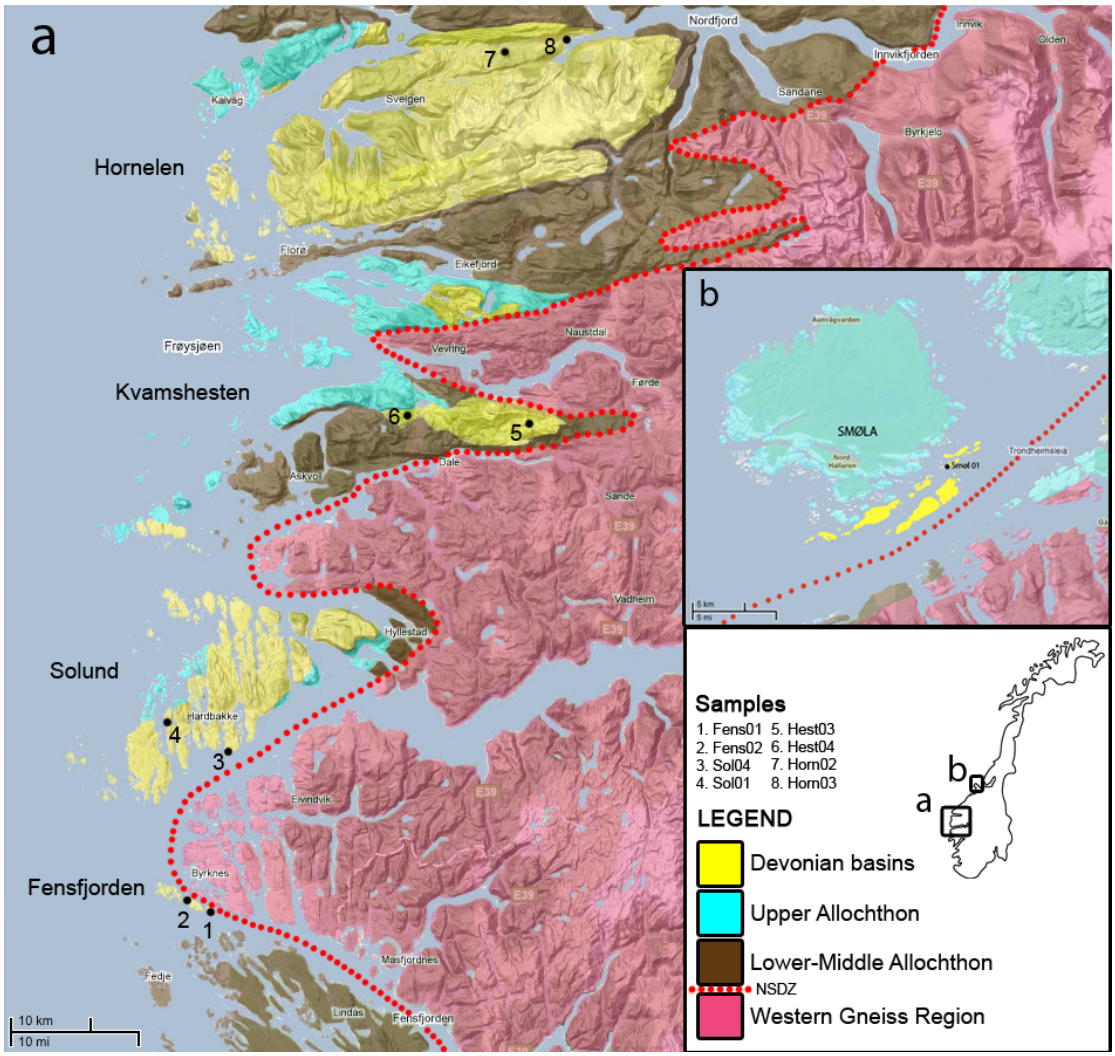

Figure 5. *Map of the Devonian basins of Western Norway with sample locations.*

The Devonian Basin of Fensfjorden

The Devonian rocks in the Fensfjorden area are located at the Ytre Byrknesøyene. These islands are situated just west of the Bergen Arc Shear Zone, which is the southern continuation of the NSDZ. The WGR is located east of the shear zone, whereas the Lindås Nappe is found south of the basin (Fig. 6). The Devonian deposits consist mainly of fanglomerates with some sandy to pebbly-conglomerate lenses, and the composition of the clasts are dominated by greenstone in the areas visited during sampling, but also numerous peridotite clast are found in the basin (Hövelmann & Austrheim 2009).

Two samples, a sandstone and a conglomerate, were collected from two different island (Fig. 5 and 6; sample Fens 01 and Fens 02).

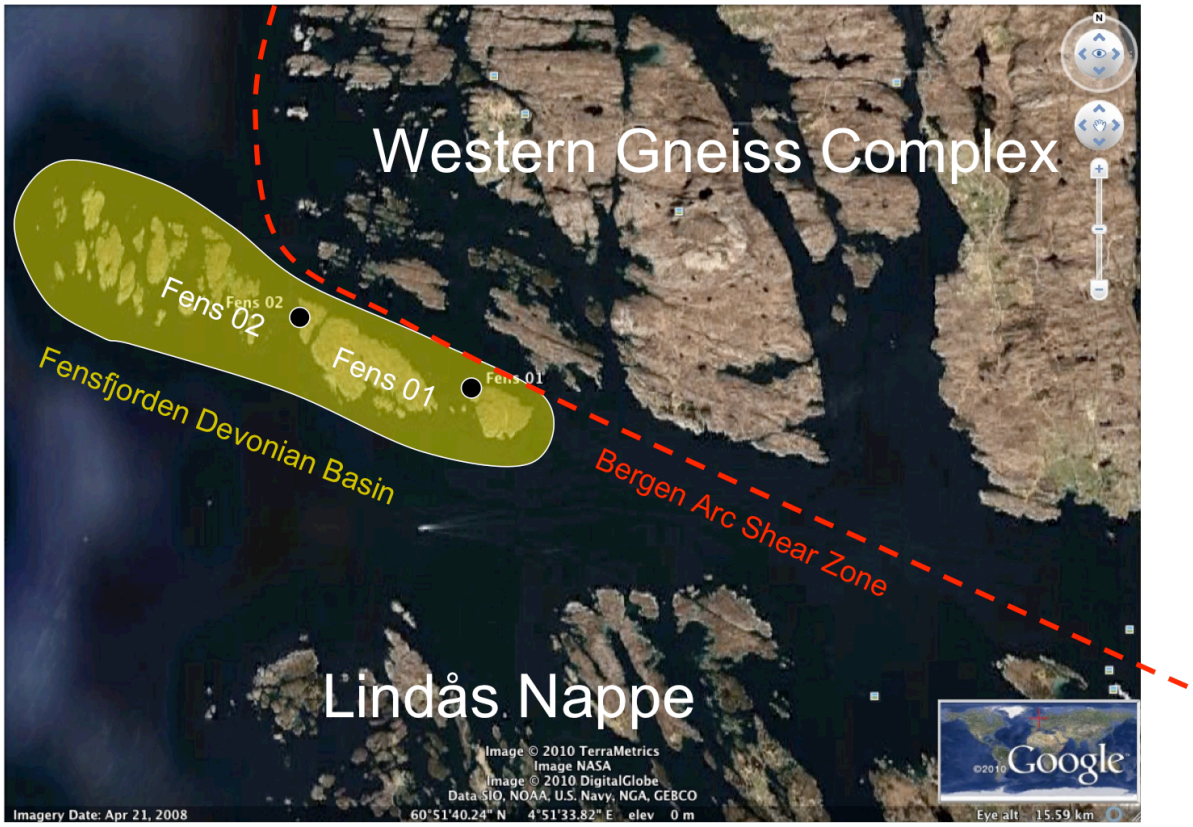

Figure 6. *A satellite image of the western part of Fensfjorden, with names of the tectonostratigraphic units in the area.*

The Devonian Basin of Solund

This basin is located north of Sognefjorden and is exposed within the Solund archipelago and the Værlandet area further north. The Solund basin is situated in the hanging wall of NSDZ which in this area consists of the Lifjorden complex (Upper Allochthon), the Sognekollen granodiorite, the Hyllestad complex (Lower/Middle Allochthon), and the Solund Stavfjord Ophiolite complex. The Solund basin is in primary contact with the Solund-Stavfjord Ophiolite complex to the west and northwest, and in fault contact (Solund Fault) with The Lifjorden complex to the east and southeast (cross section shown in Fig. 7). The WGR is located to the east, in the hanging wall of the NSDZ.

The Solund basin consists mainly of conglomerates with local sandstone bands, whereas fanglomerates, beccias and fluvial sandstone dominate in the Værlandet area. The clast material consists of greywacke, quartzite, siltstone, peridotite and gabbro believed to be of Cambro-Silurian age, as well as quartzites and gneisses of Precambrian origin (Hövelmann & Austrheim 2009; Seranne & Seguret 1987).

Pebbles of redish siltstones are present locally, and these are believed to represent fine distal facies of Devonian age derived from elsewhere in the basin (Seranne & Seguret 1987). The paleocurrents in the southern part of the basin (Solund archipelago) give an overall NW direction both on elongated pebble lineation, and trough cross bedding. In the Værlandet area the paleocurrents deciphered from the clasts mainly suggest a NW direction while the sandstones display directions of SW and SE (Nilsen 1968; Osmundsen and Andersen 2001).

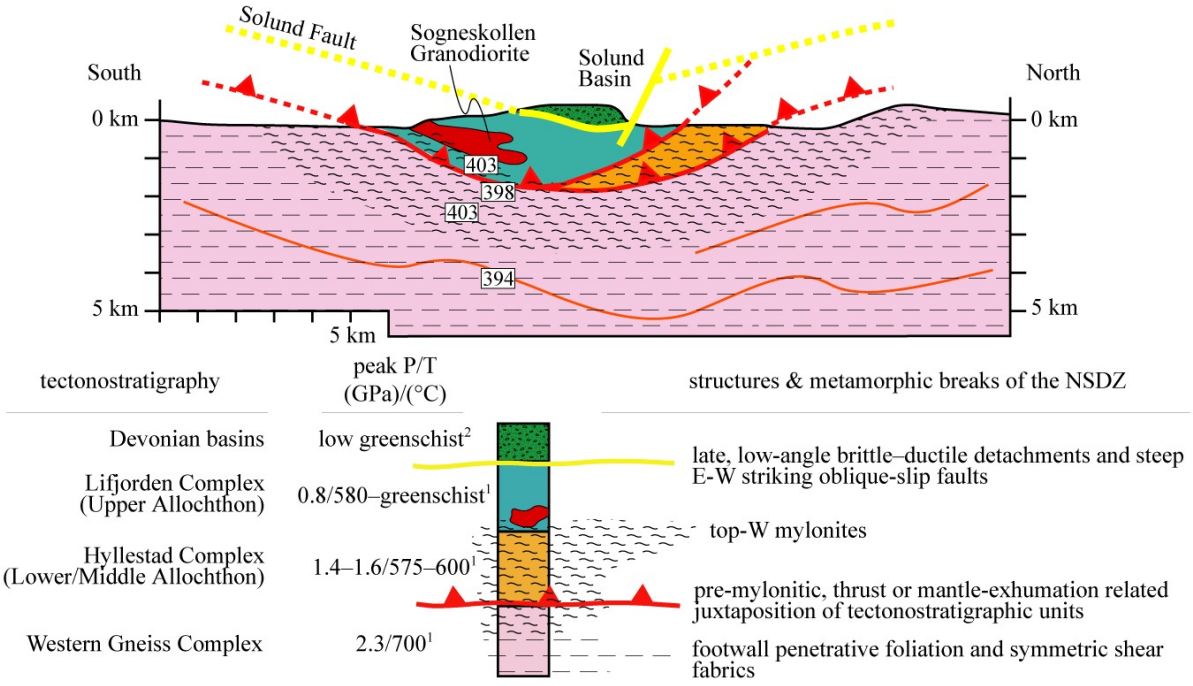

Figure 7. *South to north tectostratigraphical cross section of the eastern Solund Devonian Basin. The units in the hanging wall; Hyllestad Complex, Lifjord Complex, Sognekollen Granodiorite, and the Solund Basin. The foot wall consists of the Western Gneiss Region. The Solund Fault is separating the Solund Devonian Basin from underlying Lifjorden Complex. Nordfjord Sogn Detachement Fault shown in red (Johnston et al. 2007).*

The different paleocurrent directions were interpreted by Osmundsen and Andersen (2001) to reflect three different depositional systems. The NW directed paleocurrents in the Solund and Værlandet area are thought to be from the two main depositional systems: a conglomerate-dominated system sourced in the footwall, and a sandy system sourced from the hanging wall of a NW-dipping basin controlling fault. The third depositional system, indicated by the

SW-directed paleocurrents in sandstones in the Værlandet area, has its source along the NE basin margin (Fig. 8). Onlap relationship between Devonian strata and the basement, but also interfingering relationships between the main sedimentary units, indicate that the oldest Devonian rocks are found in the southwest (Osmundsen & Andersen 2001, and references therein).

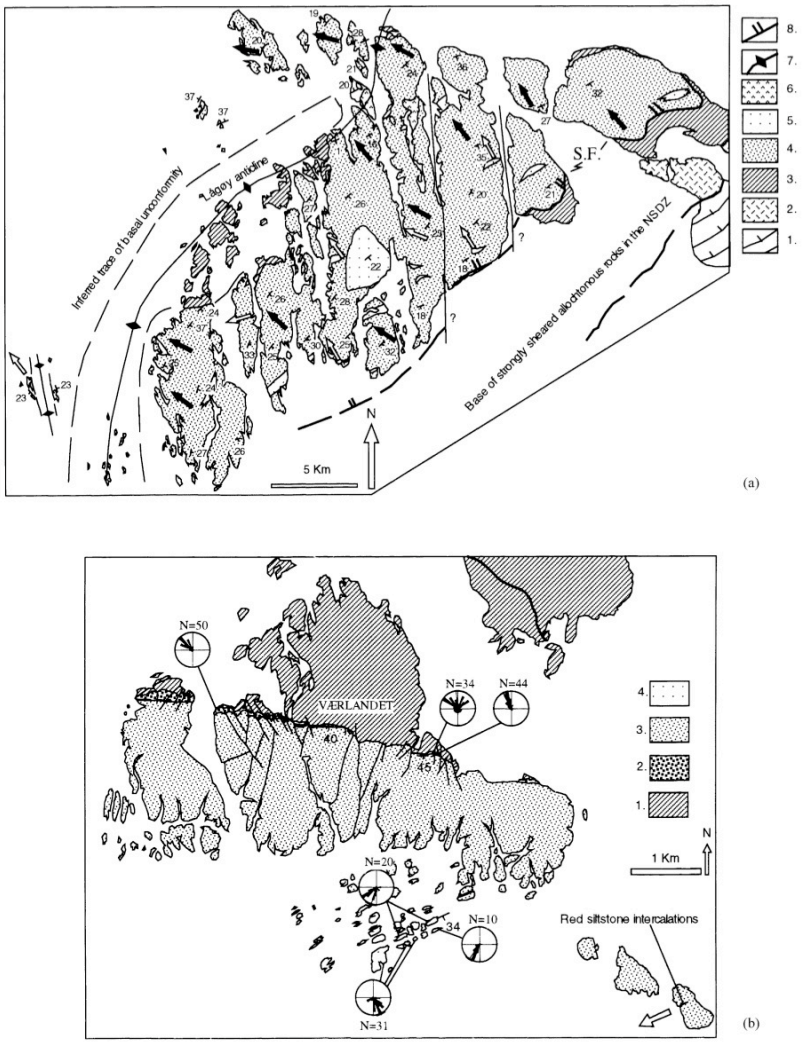

Figure 8. *Map of the Solund Basin. a) the Solund archipelago b) Værlandet area. Paleocurrents are shown as arrows; Filled arrows represent elongated pebble lineation, while unfilled arrows represent readings of trough cross-bedding. Legend in a): 1. WGR; 2. Sogneskollen Granodiorite; 3. Lifjorden Complex in the east, Solund-Stavfjord ophiolite complex in the west; 4. Devonian conglomerates; 5. Devonian sandstones; 6. Gabbroic bodies, interpreted as landslide (Bryhni and Skjerlie (1975); 7. Lågøy anticline; 8. Solund fault. Legend in b): 1. Caledonian allochthon; 2. Monomict breccias; 3. Conglomerates; 4. Fluvial channel sandstones (P.T. Osmundsen & T.B. Andersen 2001)*

Two samples, a sandstone and a conglomerate were taken from two different parts of the basin within the conglomerate unit (Fig. 8, a; Fig. 5, Sol 01 and Sol 04).

The Devonian Basin of Kvamshesten

The Kvamshesten basin is located just south of the Førdefjord. It is in primary contact with the Dalsfjord Suite (Middle Allochthon) and the Solund-Stavfjord Ophiolite Complex (Upper Allochthon) to the west. Together with the Høyvik Group (Middle Allochthon) and Askvoll Group (Lower/Middle Allochthon), these rock units make up the hanging wall of NSDZ in this area. The Dalsfjord Fault separates the Dalsfjord Complex from the Askvoll Group, and terminates down in the NSDZ (Fig. 9).

The sedimentology in the Kvamshesten basin can be divided into three main facies: 1) Fanglomerates that are present along the northern and southern rims; 2) fluvial sandstones in the central parts; and 3) floodplain siltstone (Fig. 12). The pebbles in the southern fan system and breccias in the central basin are reported to consist mainly of syenitic gneisses, granites, gabbro, anorthosite and diorite from the underlying Dalsfjord Suite (Osmundsen et al. 1998).

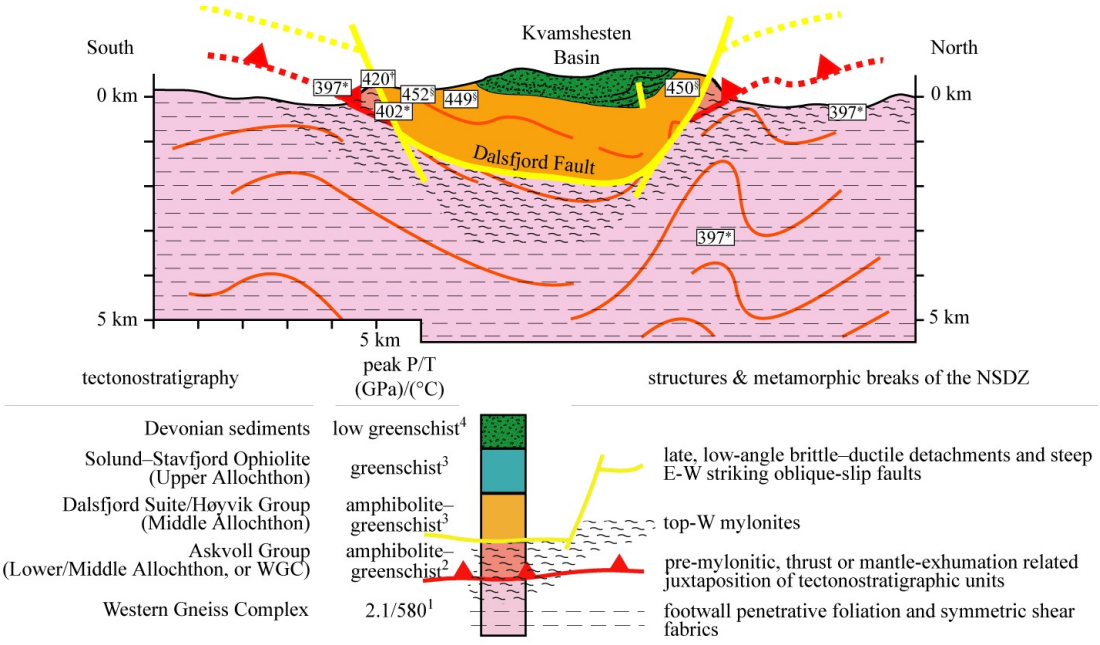

Figure 9. *South to north tectostratigraphical cross section of the eastern Kvamshesten Devonian Basin. The units shown in the hanging wall; Dalsfjord Suite, Askvoll Group and the Kvamshesten Basin. The foot wall constitutes of the WGR. The Dalsfjord Fault is shown*

in yellow, separating the Dalsfjorden Suite from the underlying Askvoll Group and WGR. Nordfjord Sogn Detachement Fault is shown in red (Johnston et al. 2007)

In the Kvamshesten basin several large blocks crop out at different stratigraphic levels. The blocks consist of metamorphosed igneous and sedimentary rocks, derived from the underlying Sunnfjord Melange, Høyvik Group and Dalsfjord Suite (Osmundsen et al. 1998). The fanglomerates and fluvial sandstones come from two main terminal fan systems; one sourced in the hanging wall, and one in the basin-controlling fault in the footwall. During periods of rapid fault-controlled subsidence, the fluvial system sourced in the hanging wall migrated towards the footwall. When subsidence rates in the footwall decreased and/or the sediment influx from the footwall fan system increased, the footwall sourced material prograded into the basin. Thus the basin's depocenter migrated either towards the footwall or towards the basin center, depending on what system had favorable conditions. The shifts are recorded as stacking patterns (retrogradational or progradational) within the fanglomerate systems, and changes in paleocurrents (east or west) are interpreted from trough cross bedding in the sandstones at different stratigraphic levels (Osmundsen and Andersen 2001; Osmundsen et al. 2000).

Two sandstone samples were collected from opposite sides of the basin from rocks interpreted to be channel sandstones (Osmundsen et al. 2000; Fig. 10; Fig. 5, Hest 03 and Hest 04).

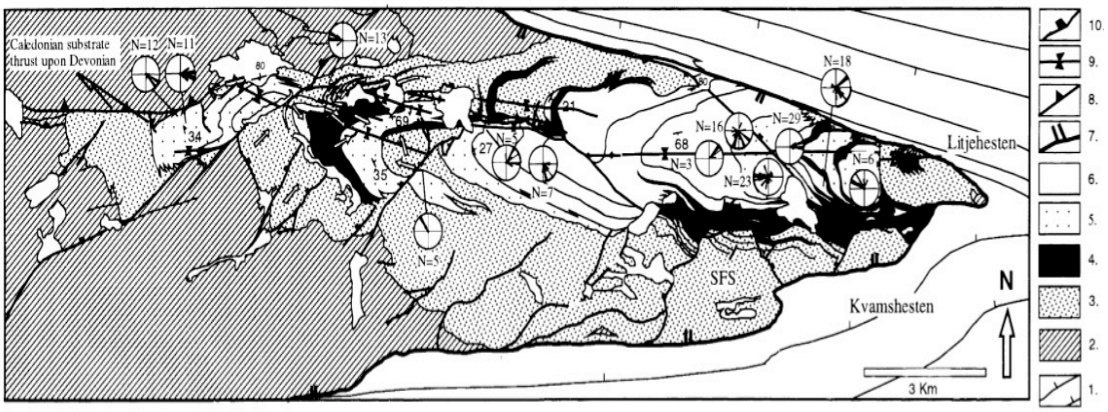

Figure 10. *Map of the Kvamshesten Basin. Paleocurrent indicators are shown as rose diagrams from trough cross beds in sandstone. Legend: 1. WGR; 2. Dalsfjord Suite in the north and south, Høyvik Group in the north, and Solund-Stavfjord ophiolite complex in the*

north west; 3. Devonian conglomerates and breccias; 4. Devonian floodplain/floodbasin; 5. Pebbly green multistorey channel sandstone and red fine sandstone 6. Multistory channel sandstones; 7. Dalsfjord Fault; 8. Thrust/reverse fault; 9. Fold axis; 10. Intrabasinal normal/oblique faults (Osmundsen et al. 2000)

The Devonian Basin of Hornelen

The Hornelen basin is located just south of Nordfjord, and it is the largest Devonian basin in Norway, with a stratigraphic thickness of ca. 25 km (Steel et al. 1977). The basin has fault contacts to the south and north (cross section shown in Fig. 11), and it has a thrust contact to the east, towards the Middle Allochthon (Steel et al. 1977; Osmundsen and Andersen 2001). It is situated on the top of the Eikfjord- and Lykkebø Groups (Middle Allochthon). In the west it has primary contact with Bremanger Granitoid Complex (Upper Allochthon) and the Kalvåg Melange (Middle Allochthon). Together with the Håsteinen Devonian basin, the Sunnarvik Complex (Upper Allochthon), Bremanger Granitoid Complex (Upper Allochthon), the Kalvåg Melange (Middle Allochthon), and the Svartekari Group, these rock units make up the hanging wall of the NSDZ in this area.

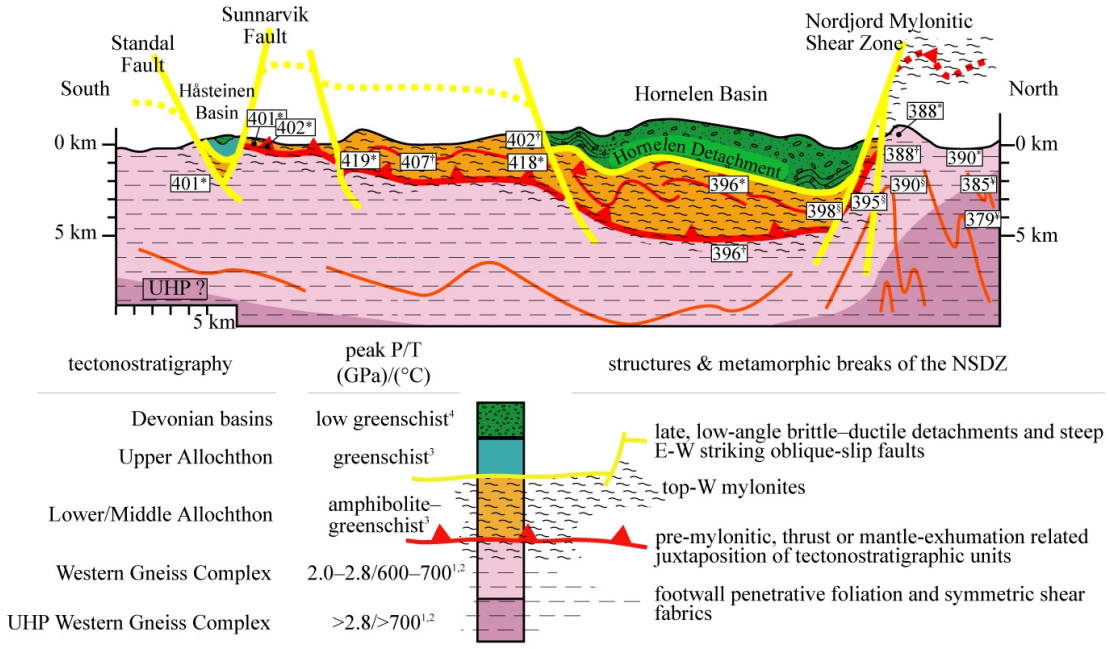

Figure 11. *South to north tectostratigraphical cross section of the eastern Hornelen- and Håsteinen Devonian Basins. The units shown in the hanging wall; Dalsfjord Suite, Hornelen basin, Håsteinen basin, and the Sunnarvik Complex. The foot wall consists of the WGR with UHP terraine north in the cross section. The Hornelen Detachment shown in yellow is*

separating the basin from the underlying Middle Allochthon. Nordfjord Sogn Detachement Fault is shown in red (Johnston et al. 2007)

The Hornelen basin is filled with three types of sediments; fanglomerates in the fringes of the basin, fluvial sandstones in the central parts, and floodplain deposits in one area in the northern part of the basin (Fig. 12). The fanglomerates in the northeast to northwest are relatively thick and steep dipping, as they are mainly debris flow deposits. The sedimentary fans in the south are bigger and dominated by stream-transported conglomerates (Osmundsen & Andersen 2001). The central parts of the basin are dominated by sandstones from an alluvial plain environment (Steel et al. 1977) and have westward trending paleocurrents, except in the northeastern part where it is more to the northwest (Fig. 12). Due to changes in the sediment supply versus the accommodation space available, the alluvial fans reached at times far into the basin, while the braided plain at other times almost covered the entire width of the basin (Steel et al. 1977; Anderson & Cross 2001).

The clasts along the northwestern and northern border of the basin consist mainly (80%) of quartz diorite, greenschist, gneiss, and quartzite, whereas gabbro, quartz diorite, quartzite and gneisses dominate the clasts along the northeastern border. In the south-southeastern part of the Hornelen basin the clast population is more dominated by quartzite and gneiss, in addition to more abundant meta-cherts (Cuthbert 1991). The sources of the clasts are intepreted to be in the nearby footwall complexes. The clasts do not contain any high-grade metamorphic rocks similar to those found in the WGR (Cuthbert 1991 and references therein).

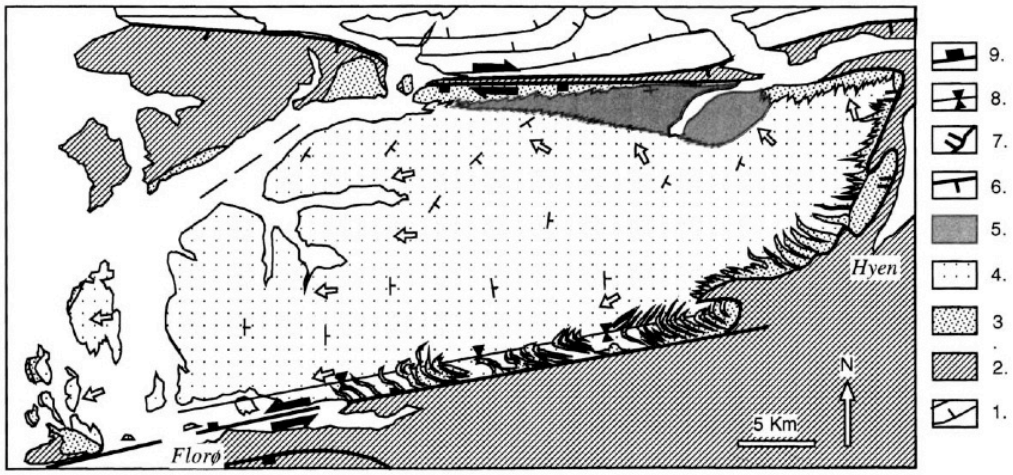

Figure 12. *Map of the Hornelen Devonian basin. Paleocurrent directions are shown as open arrows in sandy parts of the basin (Steel and Gloppen, 1980). Legend: 1. WGR; 2. Dalsfjord Suite in the south east, Bremanger Granitoid Complex and the Kalvåg Melange in the west; 3. Devonian conglomerates and breccias; 4. Devonian fluvial channel sandstones; 5. Devonian floodbasin/lacustrine sandstones, siltstones and mudstones (Osmundsen & Andersen 2001 and references therein)*

Two samples, a sandstone and a siltstone, were taken from the northern part interpreted as a floodbasin/lacustrine environment (Fig. 5; Horn 02 and Horn 03).

The Devonian Basin of Smøla

The Devonian basin of Smøla is situated west of Trondheim along the Møre-Trøndelag Fault Complex (Fig. 15). The Devonian rocks are exposed on many smaller islands that are located southeast of the island of Smøla. The biggest islands that make up the Devonian Smøla Group include the islands of Edøy, Glassøy and Kuli. Edøy consist of the Edøy Formation in the northwest and of the Kyrhaug Formation in the southeast, whereas Kuli and Glassøy make up the Glassøy Formation (Atakan 1989; Fig. 16). In the west, the basin lies unconformably upon rocks belonging to the Upper Allocthon. These rocks include plutons of mostly dioritic composition, in addition to volcanic and volcanoclastic rocks. Together with the Devonian Basin of Smøla, the plutonic, volanic and volcanoclastic rocks make up the hanging wall of the Høybakken detachment. The footwall in the southeast consists of Precambrian basement gneisses equivalent to the WGR, but the actual contact relationship cannot be seen due to the seaway separating the Devonian islands from the

mainland/basement. The NW-margin of the Devonian basin has been folded and inverted together with the basement, so that the actual margins of the Smøla Devonian basin during deposition and their geometry and possible type are not known (Atakan 1989).

The main infill of the Smøla Devonian basin is represented by conglomerates, but sandstone lenses also occur in several parts in the sedimentary sequence (Atakan 1989). The paleocurrents based on the clast analysis show an overall southern direction (Fig. 14). The main clast population of the Glassøy Formation is of dioritic, granitic, and volcanic composition, whereas the clasts in the Edøy Formation consist mainly of green- grey sandstone and granites (Atakan 1989).

One sample has been collected from a sandstone in the northeastern part of the basin (Fig. 5, Smøl 01).

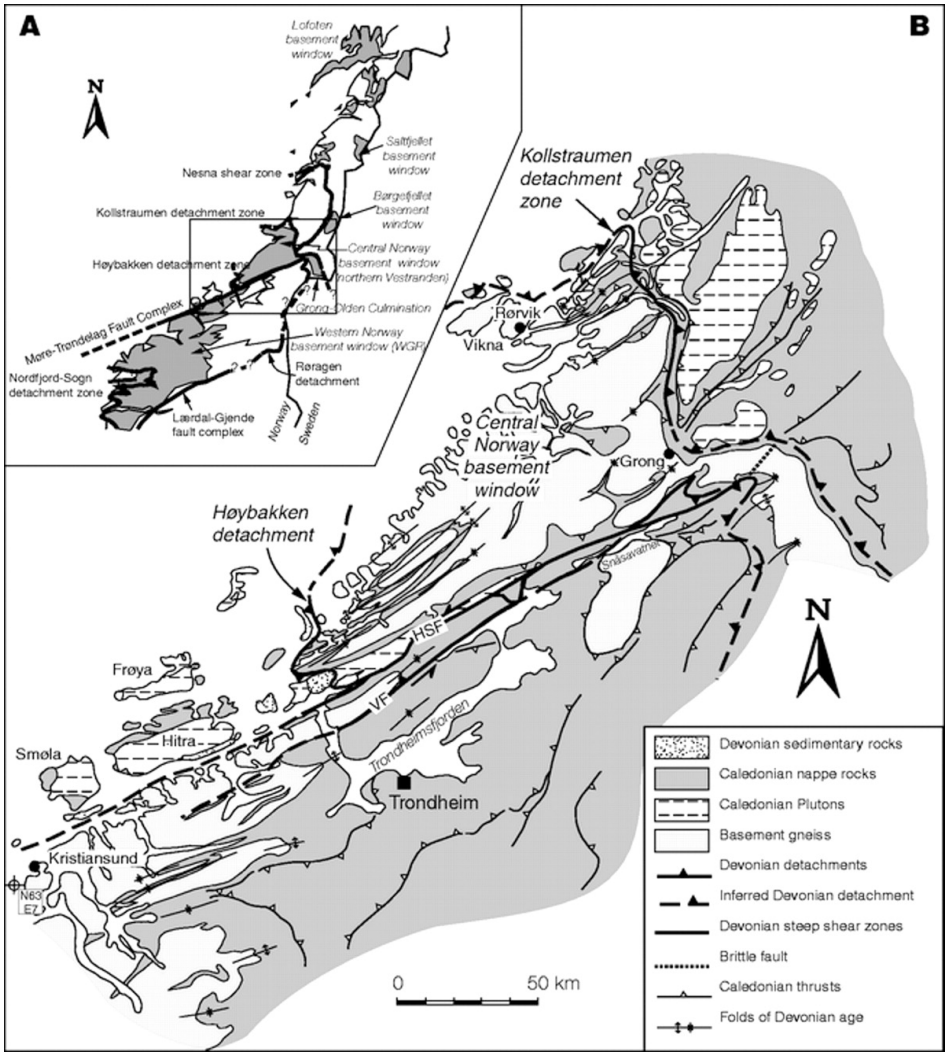

Figure 13. *A: Overview of the central parts of the Scandinavian Caledonides. Devonian shear zones and faults as bold black lines; B: Tectonic map of the squared area in A, showing a more detailed tectonic map. The Smøla Devonian basin is located just south of the Island of Smøla (Braathen et al. 2000).*

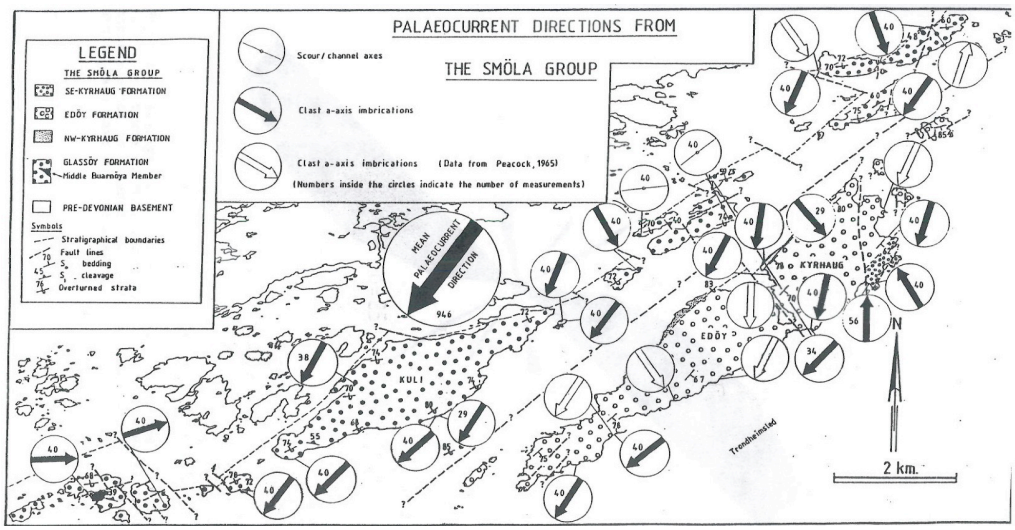

Figure 14. *Paleocurrent directions of the Smøla Devonian basin (Atakan 1989).*

Analytical Method

Sample preparation

A total of 11 samples from five different basins have been analysed in this study study. The samples were first cut to small pieces (<5*5cm) so that they could be crushed in the ''jaw crusher'' into fine gravel (<1*1cm), and then milled to sand (2-0.0625mm) in the ''Mill''. The milled sample was sieved with a 315-micron sieve, resulting in two size-fractions. The sample fraction <315 micron was taken into bowls and filled with water. The samples were then repeatedly washed in water to remove the fine size fraction that would clog the filters during separation in heavy liquids. The samples were then dried before the heavy liquid separation was initialized.

Since zircons have high density (4.66 g cm^{-3}), heavy liquid separation is a useful method to remove the light mineral fraction. The heavy liquid separation was done in two steps. The first separation was conducted with LST (liquid sodium heteropolytungstates), which has a density of 2.80 ± 0.02 g/mL. The sample then got mixed with the liquid. Minerals with a higher density than the liquid got separeated to the bottom of the funnel, and were filtered off. The heavy fraction was washed in distilled water and dried.

Diiodomethane (CH_2I_2) was used in the second heavy liquid separation. It has a density of 3.325 g/mL. The dried heavy fraction from the previous separation in LST was mixed with the heavy liquid, and the heavy fraction was filtered off. The heavy fraction was washed with acetone and air dried for further separation.

The sample was then run through a magnetic separator (Frantz Magnetic Barrier Laboratory Separator, Model LB-1) with a 1.0 A current to remove magnetic minerals.

After the magnetic separation, the non-magnetic fraction was studied under a microscope. The zircon grains were picked out with tweezers and attatched to a piece of 2-sided tape on a plate of glass. Approximately 150-250 zircon grains (Andersen 2004) were attached to the tape; the sample was mounted in a plastic ring and filled with epoxy. When the epoxy hardened, the sample was grinded

and polished so the internal zircons surfaces were exposed for laser ablation ICP-MS analysis.

Laser ablation ICP-MS dating of zircons

The zircons were mounted in 1 cm epoxy-filled blocks and polished to obtain even surfaces suitable for laser ablation ICP-MS analysis. Prior to analysis by laser ablation ICPMS, the sample surfaces were cleaned in DI water and ethanol. Isotopic analysis of zircons by laser ablation ICP-MS followed the technique described in Kosler et al. (2002). A Thermo-Finnigan Element 2 sector field ICP-MS coupled to a 193 ArF excimer laser (Resonetics RESOlution M50-LR) at Bergen University was used to measure Pb/U and Pb isotopic ratios in zircons. The sample introduction system was modified to enable simultaneous nebulisation of a tracer solution and laser ablation of the solid sample (Horn et al., 2000). Natural Tl ($^{205}Tl/^{203}Tl$ = 2.3871 - Dunstan et al., 1980), ^{209}Bi and enriched ^{233}U and ^{237}Np (>99%) were used in the tracer solution, which was aspirated to the plasma in an argon - helium carrier gas mixture through an Apex desolvation nebuliser (Elemental Scientific) and a T-piece tube attached to the back end of the plasma torch. A helium gas line carrying the sample from the laser cell to the plasma was also attached to the T-piece tube. The laser was set up to produce energy density of ca 80 J/cm^2 at a repetition rate of 5 Hz. The laser beam was imaged on the surface of the sample placed in the two-volume ablation cell, which was mounted on a computer-driven motorized stage of a microscope. During ablation the stage was moved beneath the stationary laser beam to produce a linear raster (ca 30-70 microns) in the sample. Typical acquisitions consisted of a 35 second measurement of analytes in the gas blank and aspirated solution, particularly ^{203}Tl - ^{205}Tl - ^{209}Bi -^{233}U - ^{237}Np, followed by measurement of U and Pb signals from zircon, along with the continuous signal from the aspirated solution, for another 120 seconds. The data were acquired in time resolved - peak jumping - pulse counting mode with 1 point measured per peak for masses 202 (flyback), 203 and 205 (Tl), 206 and 207 (Pb), 209 (Bi), 233 (U), 237 (Np), 238 (U), 249 (233U oxide), 253 (237Np oxide) and 254 (238U oxide). Raw data were corrected for dead time of the

electron multiplier and processed off line in a spreadsheet-based program (Lamdate - Kosler et al., 2002) and plotted on concordia diagrams using Isoplot (Ludwig, 1999). Data reduction included correction for gas blank, laser-induced elemental fractionation of Pb and U and instrument mass bias. Minor formation of oxides of U and Np was corrected for by adding signal intensities at masses 249, 253 and 254 to the intensities at masses 233, 237 and 238, respectively. No common Pb correction was applied to the data. Details of data reduction and corrections are described in Kosler et al. (2002) and Kosler & Sylvester (2003). Zircon reference material 91500 (1065 Ma - Wiedenbeck et al., 1995), GJ-1 (609 Ma – Jackson et al., 2004) and Plešovice (337 Ma - Slama et al., 2008) were periodically analysed during this study and they yielded mean ages of 1066.5±27.8, 604.4±13.7 and 344.8±9.9 Ma, respectively.

Uncertainty

There are many different factors that contribute to uncertainty in a U-Pb zircon provenance study. The most important are: natural bias of the detrital zircon record in the sample; contamination during sample preparation; human bias during picking of zircons, elemental fractionation of U and Pb, mass bias of ICPMS, and limited availability of suitable mineral standards to correct for the previous problems. Possible counter solutions to elemental fractionation and mass bias of ICPMS are described in depth in Kosler & Sylvester (2003).

During sample preparation, all samples were handled one at the time and with new paper sheets covering surfaces for each sample. The equipment that was in touch with the samples was washed/cleaned according to laboratory instructions. When picking zircons all shapes, sizes and colors were picked.

Results

In this study a total of 1356 zircon grains were analyzed. Of these, 643 measurements were not included in the interpretation for reasons listed below, leaving 713 measurements as the final data set that is reported and discussed here (Fig. 15; Appendix, Table 1-9).

The zircons that were not included in the final data set were removed due discordancy (more then a 50 Ma difference between the two U/Pb ages), or due to large analytical uncertainty (more than 100 Ma (1 sigma) for Proterozoic and Archean zircons, and more than 40 Ma (1 sigma) for Paleozoic zircons).

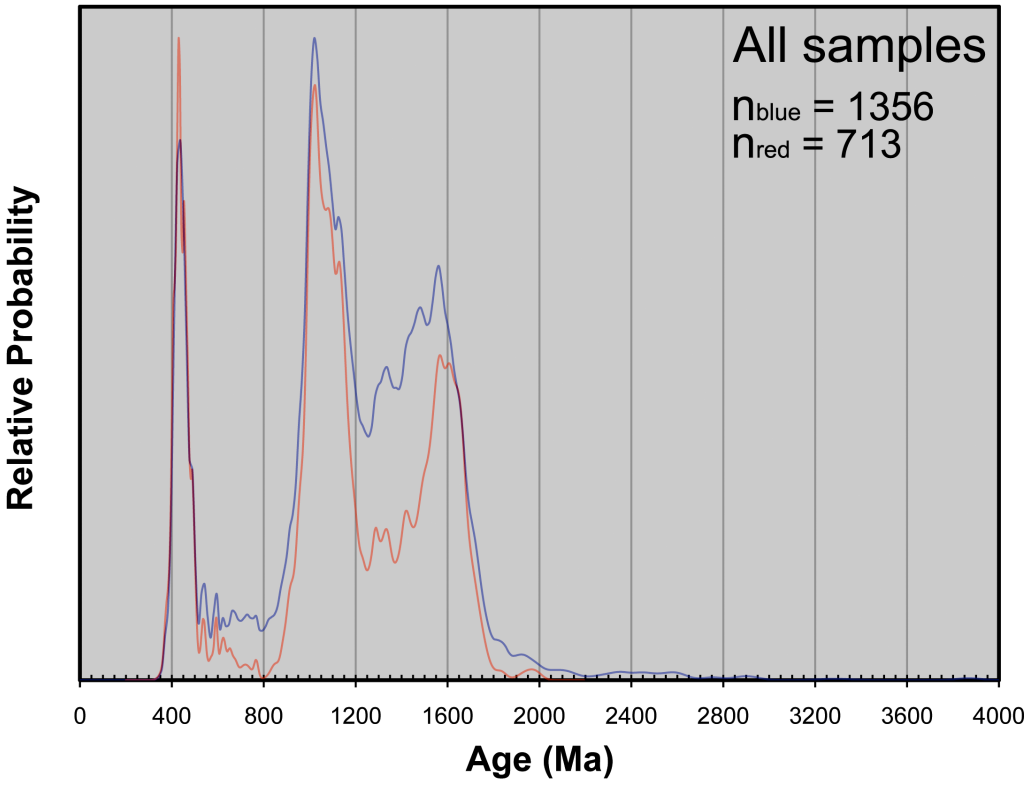

Figure 15. *Probability density plots showing all the measurements before data filtering in blue, and the final data set in red.*

The data have been plotted in a probability density plot before (blue) and after (red) filtering of the imprecise U/Pb ages (Fig. 15). Both plots show similar distribution of ages, but since the data filtering was based on absolute values of discordancy and uncertainty rather than on relative values, there was a small

bias favoring younger grains over older grains, but it has little effect on the final interpretation.

In the following section, the zircon provenance ages are presented for individual basins from south to north. For each sample analyzed, the results are shown graphically as concordia diagrams and as histograms combined with probability density plots. In the text the "age" always refers to the $^{238}U/^{206}Pb$ age, which is overall the most precise U-Pb chronometer for the LA-ICPMS measurements presented here.

The Fensfjorden Devonian Basin

Two samples have been analyzed from the Fensfjorden basin (Fens01 and Fens02); Fens 01 is a medium-grained sandstone from a sand lens, while Fens 02 is a fine-gravel orthoconglomerate from a lens of fine-medium gravel orthoconglomerates.

The zircon ages from **Fens01** (Fig. 16, a and b) are dominated by Mesoproterozoic ages (1000 – 1600Ma), with a total of 62 zircons within this age range (85%). The rest of the zircon grains have ages from the late Paleoproterozoic (1600 – 2500 Ma), 2 zircons (3%), early Neoproterozoic (542 – 1000 Ma), 8 zircons (11%), and one Silurian zircon with an age of 434 ± 16 Ma. The sample has a continuous distribution of ages from the youngest Neoproterozoic zircon, 916 ± 35 Ma, to the oldest Mesoproterozoic zircon, 1569 ± 91 Ma. The most prominent peaks in the probability-density plot are all between 1000-1200 Ma, and this age range contains ca. 60% of the dated zircon population.

The **Fens 02** sample (Fig. 16, c and d) is also dominated by zircon of Mesoproterozoic (1000 – 1600 Ma) and late Neoproterozoic (542 – 1000 Ma) ages. Zircons of this age-range make up as much as 96% of the zircon population. On the concordia diagram the zircons define a main cluster around 1100 Ma, and a minor cluster around 1400 Ma (Fig. 16, c). The remaining 4% of the sample consists of one grain with a late Paleoproterozoic age (1706 ± 79 Ma), and two grains of Paleozoic ages (501 ± 12 Ma and 472 ± 24 Ma).

The two samples show similar signatures, with the difference that Fens 01 has a continuous distribution of Mesoproterozoic ages.

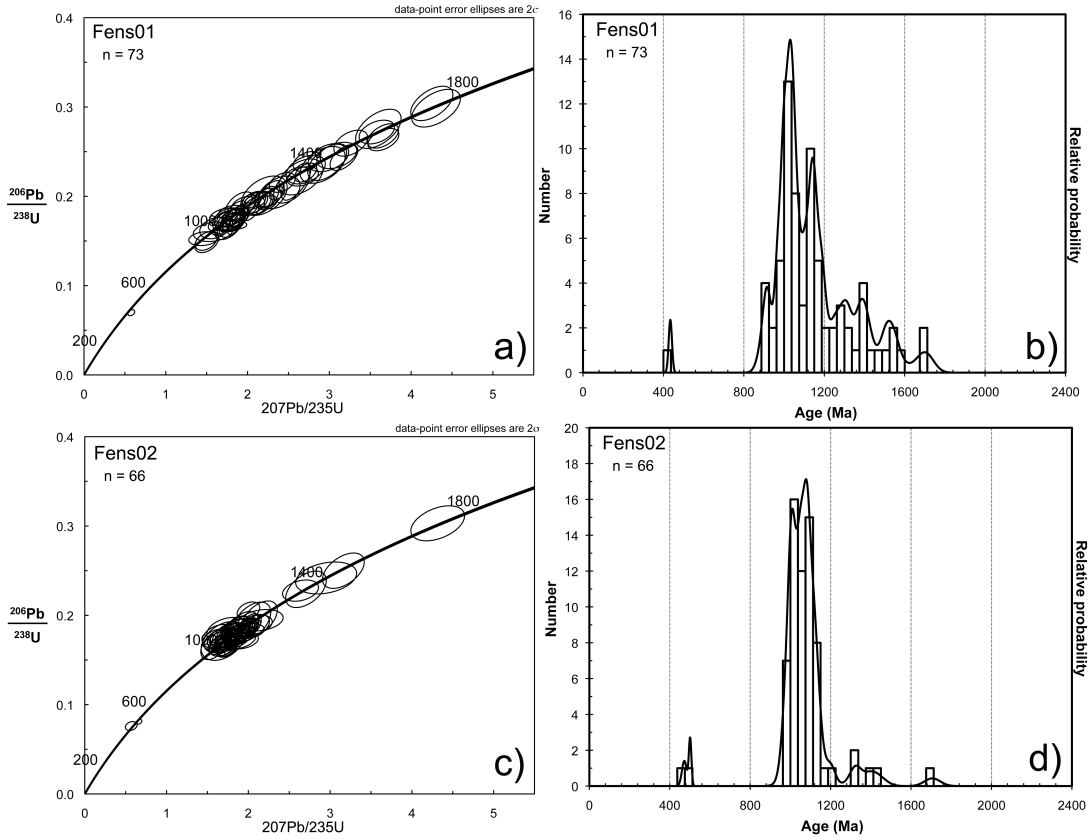

Figure 16. *Concordial plots (a,c) and corresponding histograms with probability density plots for samples Fens 01 and Fens 02, respectively. The error ellipses are 2σ..*

The Solund Devonian Basin

Two samples have been analyzed from the Devonian sedimentary basin in Solund: Sol 01, a fine-grained gravel conglomerate, and Sol 02, a medium-sandstone. **Sol 01** (Fig. 17, a and b) have a significant component of Mesoproterozoic (1000 – 1600 Ma) and late Neoproterozoic (542 – 1000 Ma) zircons. Approximately 93% of the dated grains lie within the 900 Ma to 1520 Ma age range. Within this range, the ages cluster densely between 880 and 1200 Ma (98 grains), and a lesser amount of grains plot between 1280 and 1520Ma (25 grains). The histogram shows that the largest peaks are all between 1000 and 1120 Ma (Fig. 17, b). The remaining 7% of the zircon population consists of

3 grains from the late Paleoproterozoic, two grains from upper Neoproterozoic, and 6 grains of early Devonian to late Cambrian age (410 – 496 Ma).

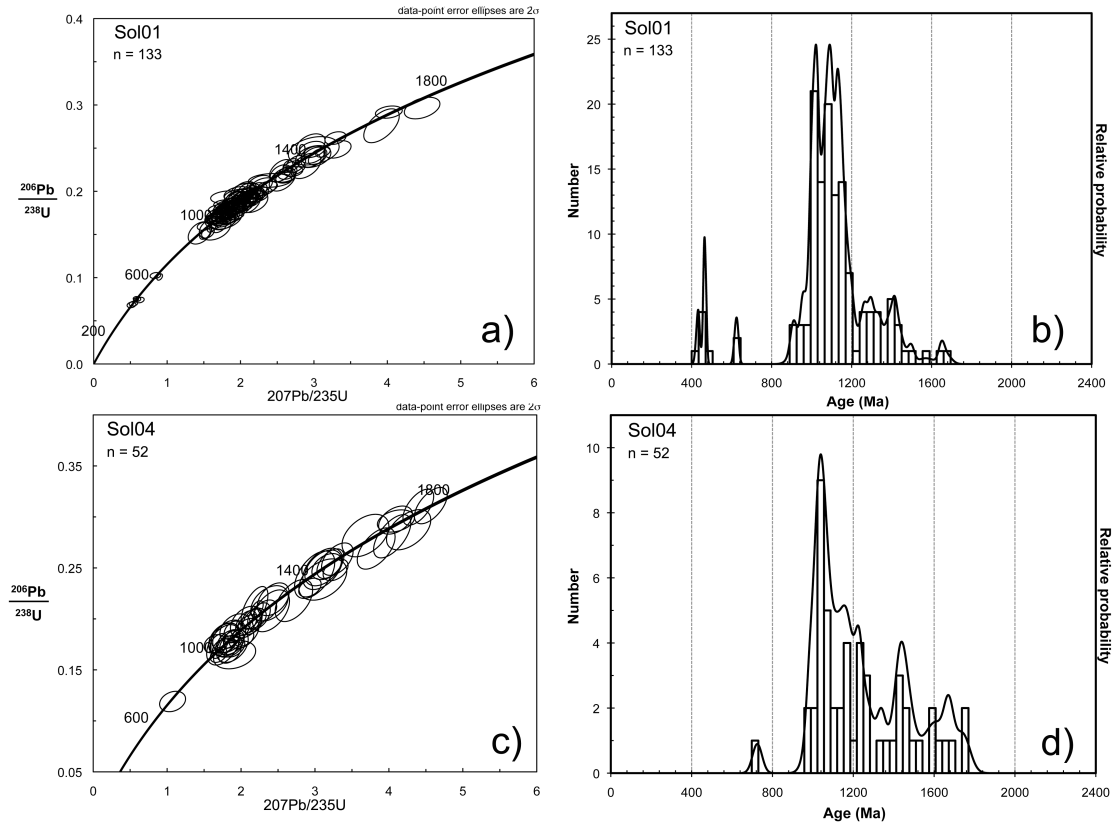

Figure 17. *Concordial plots (a,c) and corresponding histograms with probability density plots for samples Sol 01 and Sol 02, respectively. The error ellipses are 2σ.*

Except for a grain from the middle Neoproterozoic Era (725 ± 47 Ma), **Sol04** is completely dominated by early Neoproterozoic to late Paleoproterozoic ages. On the concordia diagram these form 3 clusters with corresponding peaks on the relative probability plot (Fig. 17, c and d):

1) A cluster containing 65% of the grains in the sample. Spanning from lower-Neoproterozoicum to middle-Mesoproterozoicum (960 – 1280Ma), which defines a prominent peak in the relative probability plot at 1000-1100Ma.

2) A cluster spanning from middle- to lower-Mesoproterozoicum (1320 - 1520Ma), containing 19% of the grains, which form a minor 1440 Ma peak in the relative probability plot.

3) A small cluster (14%) of zircons mostly from the upper Paleoproterozoic (1560 – 1800Ma).

The two samples show similar age patterns. The only notable difference is that sample Sol 01 contains a young zircon population (410 – 496 Ma) not recorded in sample Sol 04.

The Kvamshesten Devonian Basin

Two samples, Hest03 and Hest04, have been analyzed from the Kvamshesten basin. Both samples are sandstones with medium grain size.

The zircon ages from the **Hest 03** sample define 4 clusters on the Concordia diagram (Fig. 18, a). The oldest of these clusters consists of 75% of the dated zircon grains, and spans from the early Mesoproterozoicum to the late Paleoproterozoicum in age (ca 1460 – 1820Ma). Zircons of this age define the major peak in the relative probability plot (peak age of 1520 - 1680 Ma).

A slightly younger cluster, which contains 7% of the grains in the sample, is close to 1300 Ma and spans from 1200-1360 Ma (middle Mesoproterozoicum). A group of late Neoproterozoic to early Mesoproterozoic grains (960 – 1140Ma) cluster at around 1000 Ma, the population contains 9% of the analyzed grains in the sample. These two age clusters define minor peaks on the probability density plot.

In addition to zircon grains of Proterozoic age, the sample yielded some grains of Paleozoic age. This youngest group contains 9% of the zircons in the sample, and it spans from upper Ordovician to Lower Devonian ages, with the oldest and youngest grain being 450 ± 14 and 379 ± 36 Ma, respectively.

The Hest 04 zircons define two distinct age groups on the Concordia diagram. The most dominating cluster (Fig. 18, b), which contains 87% of the sample, spans from early Mesoproterozoicum to late Paleoproterozoicum (1280-1760Ma). Zircons of this age range define a single peak on the probability density plot with a peak age of ~1580 Ma. The smaller cluster is made out of the remaining 13% of the sample. These grains span from early Neoproterozoicum to late Mesoproterozoicum in age (~900-1100Ma).

The two samples show similar age patterns, although Hest 03 contains a young zircon population (379 ± 36 - 450 ± 14 Ma) in addition.

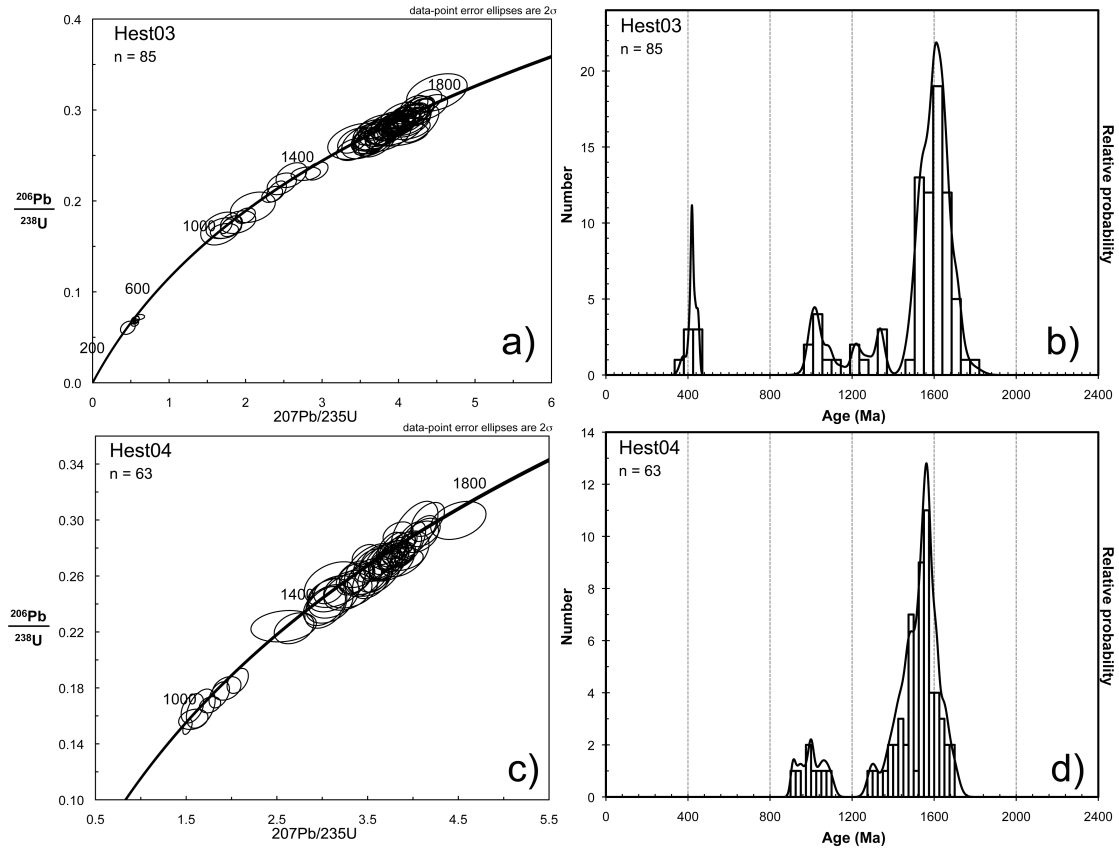

Figure 18. *Concordial plots (a,c) and corresponding histograms with probability density plots for samples Hest03 and Hest04, respectively. The error ellipses are 2σ.*

The Hornelen Devonian basin

Two samples, Horn 02 and Horn 03, have been analyzed from the Hornelen basin. The former is a fine-grained sandstone while the latter is a siltstone.

The zircon ages of **Horn02** can be divided into 3 clusters on the Concordia-diagram. The youngest cluster has a strong overlap, while the other two are distributed across a larger time period with a weaker overlap (Fig. 19, a). The cluster spanning from middle-Mesoproterozoic to late Paleoproterozoic (~1300-1780Ma) contains 47% of the grains in the sample, and have age maxima on the probability density plot between 1620 – 1700 Ma.

While the cluster spanning from early Neoproterozoic to middle Mesoproterozoic (~900 – 1220 Ma) contains 26% of the grains in the sample. The youngest cluster contains 24% of the sample grains, and it spans from early Devonian to Cambrian (407 ± 13 – 510 ± 38 Ma), with age peaks between 420

and 500 Ma on the relative probability curve. This cluster can be subdivided into three different age modes with calculated average ages of late Silurian/early Devonian (416 ± 13 Ma), early Ordovician (462 ± 17 Ma), and Cambrian (499 ± 23 Ma). Only one grain (711 ± 54 Ma) is not a part of any of the clusters mentioned above.

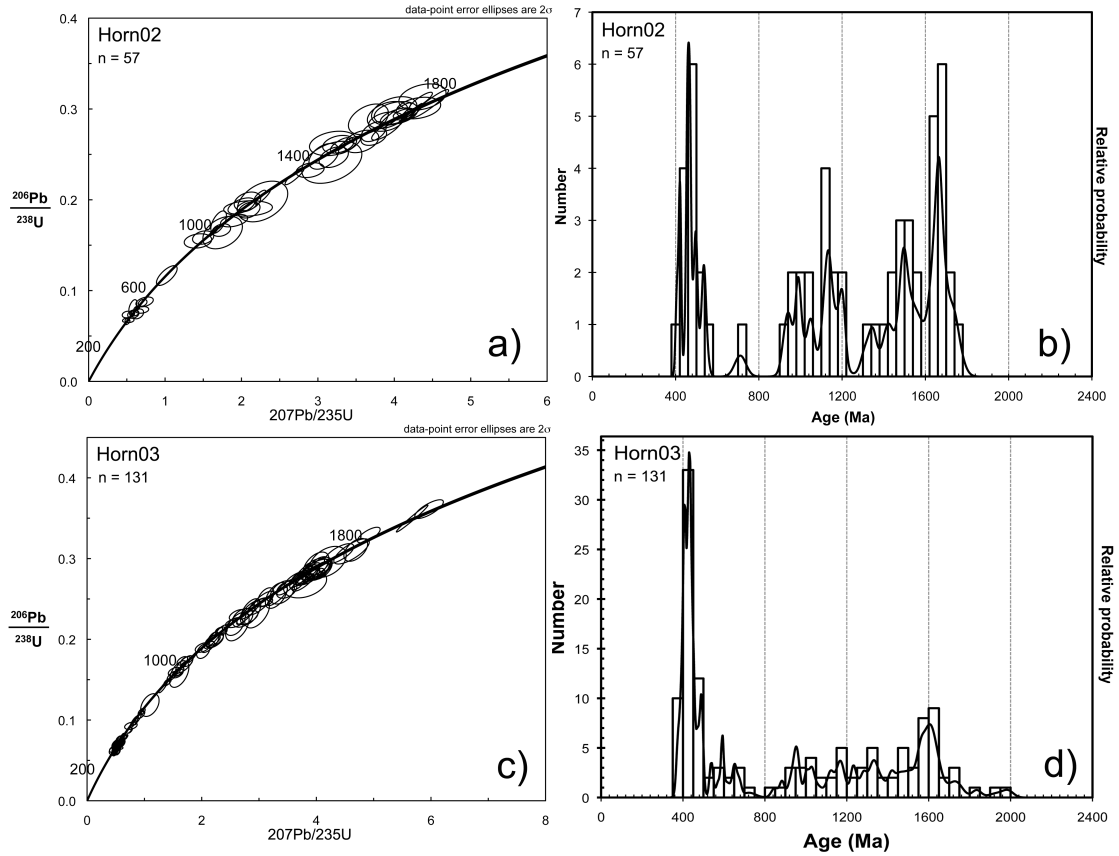

Figure 19. *Concordial plots (a,c) and corresponding histograms with probability density plots for samples Horn 02 and Horn 03, respectively. The error ellipses are 2σ.*

The zircon ages of the **Horn 03** sample can be divided into three clusters and a continuous distribution of grains on the Concordia-diagram (Fig. 19, c), the latter range from the early Neoproterozoic to the late Paleoproterozoic (1080 – 1760Ma), which makes 41% of the sample. The cluster at ~1000 Ma consists of 9% of the sample and spans from early Neoproterozoicum to late Mesoproterozoicum (800-1080Ma). The two other clusters span from Cambrian to late Neoproterozoicum (538 – 848Ma), and Devonian to Cambrian (373 – 496Ma). The former consists of 8% of the grains in the sample, while the latter consists of 40% and has a peak on the relative probability curve at ~420 Ma.

The remaining 2% of the sample are 3 zircon grains from the Paleoprotozoic (1800 – 2000Ma).

The two samples have similar zircon age distributions, with the exception of Horn 03 that contains a larger component of Devonian to Cambrian zircons.

The Smøla Devonian basin

A sandstone of medium grain size has been analyzed from the Smøla basin. On the Concordia-diagram (Fig. 20, a) the zircon ages define three clusters and 6 individual points. The most prominent cluster spans from Devonian to Cambrian (402 – 507Ma), containing 67% of the grains in the sample, and has age peaks on the relative probability curve between 440 and 470 Ma. The two other clusters span from early Neoproterozoic to late Mesoproterozoic (960 – 1040Ma), and within upper Paleoproterozoicum (1600 – 1700Ma), consisting of 8% and 6% of the grains in the sample, respectively. The individual grains yield ages of: 1951 ± 60 Ma, 1278 ± 29 Ma, 1429 ± 63 Ma, 841 ± 57 Ma, 767 ± 17 Ma, and 577 ± 37 Ma.

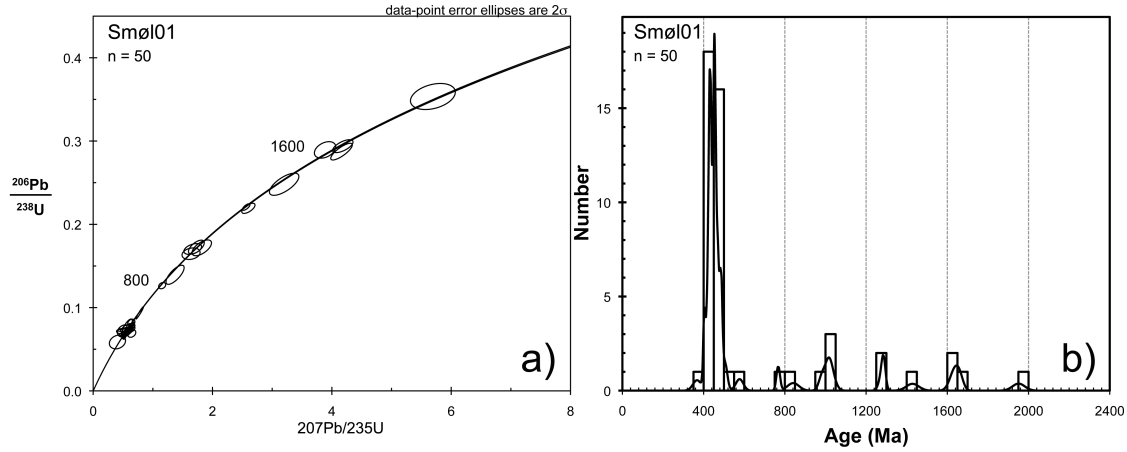

Figure 20. *Concordial plot (a) and corresponding histograms with probability density plots for sample Smøl 01. The error ellipses are 2σ.*

Discussion

Three major peaks appear on the relative probability plot when the zircon ages of the nine samples from the five Devonian basins are combined (Fig. 21): 1) Paleo to Mesoproterozoic grains with a peak at 1600 Ma; 2) late Mesoproterozoic to early Neoproterozoic grains with a peak at 1060 Ma; and 3) middle Neoproterozoic to early Devonian age grains with a maximum frequency between 400-500 Ma, with a relative probability peak at around 430 Ma.

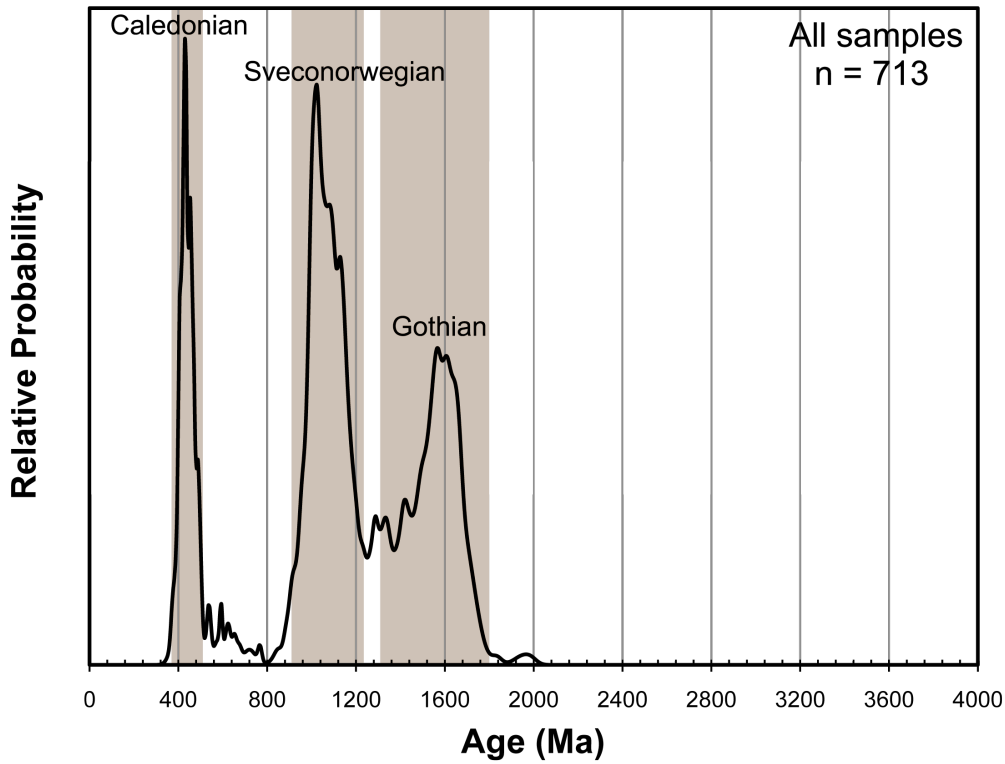

Figure 21. *A probability density plot showing all the measurements from the five Devonian basins. Relative probability peaks at ~430, ~1060, and ~1600 Ma. Time span of orogenies marked in light brown.*

These three age groups correspond with three different orogenies dominating the geology of southwest Norway (Fig. 21): **the Gothian orogeny (1300-1800Ma)**, **the Sveconorwegian orogeny (900-1250Ma)**, and the **Caledonian orogeny (400-500Ma)**. For the sake of simplicity, the zircon ages will from here on be correlated to these rock-forming events rather then names of time periods.

There is a variation in what age group is dominating the different basins, as shown in **figure 22**. Samples from individual basins consistently show similar age distributions from different stratigraphic levels within the basin. Also some basins show similar age distributions (Solund and Fensfjorden), whereas there are marked differences between others; e.g. Kvamshesten and Hornelen.

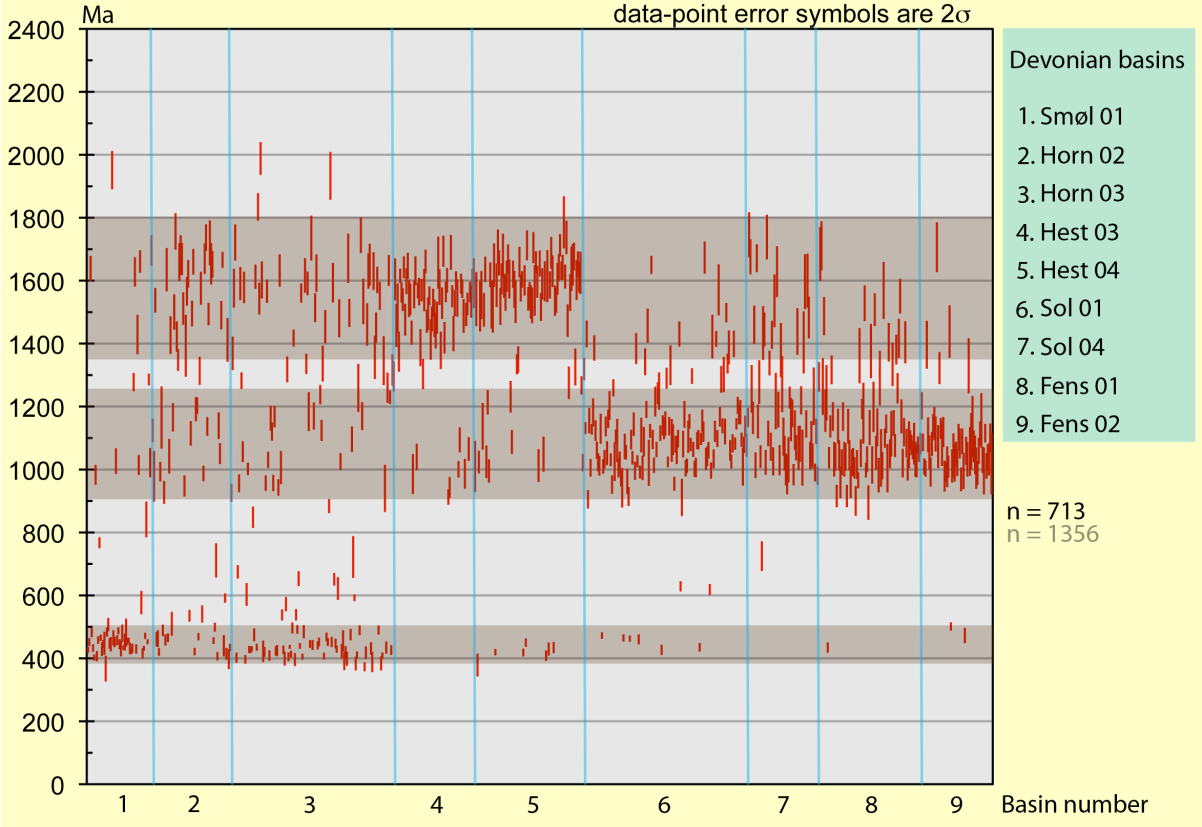

Figur 22. *An average plot of all the zircon 206Pb/238U ages with 2-sigma uncertainty. The ages are plotted basin wise starting with the most northwards basin of Smøla (1), going southwards to the most southern basin of Fensfjorden (8 and 9). Time span of orogenies marked in light brown.*

Zircon age distribution between basins and potential source rocks

Paleo- to Early Neoproterozoic zircons

The magmatism and continental growth that occurred during the Gothian and Sveconorwegian orogeny produced magmatic rocks ranging from 1800 – 900

Ma. The WGR, and the Lower- and Middle Allochthons are predominantly made up of rocks of this age range.

All basins have zircon populations that formed during the Gothian and the Sveconorwegian orogenies, but zircons of these ages totally predominate in the three southernmost basins (Fensfjorden, Solund and Kvamshesten).

Zircons formed during the Sveconorwegian orogeny dominate in the zircon populations in all four samples collected from the **Fensfjorden** and the **Solund** basins (77%), with the highest peaks at ~1060Ma. The Fensfjorden and the Solund basins consist mainly of conglomerates and breccias, showing that these zircons came from a nearby source.

The Bergen Arc Shear Zone separate the Fensfjorden basin from the WGR to the northeast, which in this region is dominated by rocks of presumably Gothian age (no major Sveconorwegian granites have been described from the region). The Lindås Nappe (Middle Allochthon; Fig. 6) is located just to the south of this basin. The radiometric ages available from this nappe suggests that it mainly is made up of intrusions and metamorphic rocks of Sveconorwegian age (age range from 921 to 1237 Ma; Bingen 2001). This correlates well with the ages of the dominant detrital zircons population within these basins (Fig. 22), and the Lindås Nappe seems as the most likely source of the main zircon population within the Fensfjorden and Solund samples.

The presence of ophiocarbonates (weathered peridotite) both in the Fensfjorden- and Solund basins shows that they received detritus from a similar source (Hövelmann & Austrheim 2009). The similar zircon patterns shown by the samples from the Fensfjorden and the Solund basins suggests in addition that the source region yielding Proterozoic zircons were similar for the two basins.

In the **Kvamshesten** basin just northeast of Solund (Fig. 5), there is a notable shift in the age signature relative to that documented in the two southern basins (Fig. 22). The Kvamshesten basin is also different in morphology from the southern basins, as the central part is made of fluvial sandstone (Fig. 10), whereas the fanglomerates are mainly in the fringes of the basin. The two samples, which are taken from different stratigraphic levels within the fluvial sandstone in the Kvamshesten basin, both contain large proportion of zircons

originating from a Gothian source rock (Fig. 22). Although it is possible that the sandstone in the central parts could have been transported from exotic source rocks that are not present in the nearby fans, this seems unlikely as the basin is interpreted to be closed during deposition (Osmundsen 1998). The underlying Dalsfjord Suite (Middle Allochton) has yielded Gothian ages (Corfu & Andersen 2002) - matching the predominating zircon populations of the samples from the basin. This appears as a likely source of the major zircon population of these sediments.

The shift in the dominating detrital zircon age between the Solund-Fensfjorden basins and the Kvamshesten basin from Sveconorwegian to Gothian (Fig. 22) suggests that here is a marked change in the proportion of Gothian and Sveconorvegian rocks in the Lindås Nappe to the Dalsfjorden Suite. This shift is consistent with the U-Pb ages reported from these nappe units. Lundmark et al. (2007) proposed that the difference in age signature within the Middle Allochthonous rocks indicated that the Lindås Nappe could have experienced a higher degree of Sveconorwegian overprint due to a deeper crustal position at that time compared to the Dalsfjord and Jotun nappes.

Middle to Late Neoproterozoic zircons

This time span (542 – 850 Ma) is dominated by magmatism caused by extensive rifting of Laurentia, which locally lead to the opening of the Iapetus Ocean (Rankin 1976). Rocks from this event are mainly found in the Seve-Kalak nappes located in central Norway. The upper part of the Kalak nappes are intruded by minor granites, pegmatite bodies and leucosomes formed between 876 – 825 Ma and 711 - 680 Ma (Corfu et al. 2007; Kirkland et al. 2006; 2008). Also found in the Kalak Nappe is the Seiland Igneous Province dated to have formed between 571 and 561 Ma followed by an event of syenite pegmatites at 531 – 523 Ma (Pedersen et al. 1989; Roberts et al. 2006;). In southern Norway (Telemark area), the Fen Complex represents another alkaline intrusive unit that formed between 580-540 Ma (Andersen & Taylor 1988), where the rift-related magmas intruded the Precambrian basement gneisses. In the Seve nappe a sheeted dyke complex and a granite pluton are reported with ages of 608 and 845 Ma,

respectively (Svennings 2001; Paulsson & Andréasson 2002). Also a keratophyric dike intruding the Sunnarvik complex in the Hornelen area yields an age of 556 Ma (Johnston 2007). These different ages are all represented among the 16 zircons (8%) from the Hornelen samples, as well as ages (590 – 670 Ma) not recorded in any potential source rock (Fig. 23).

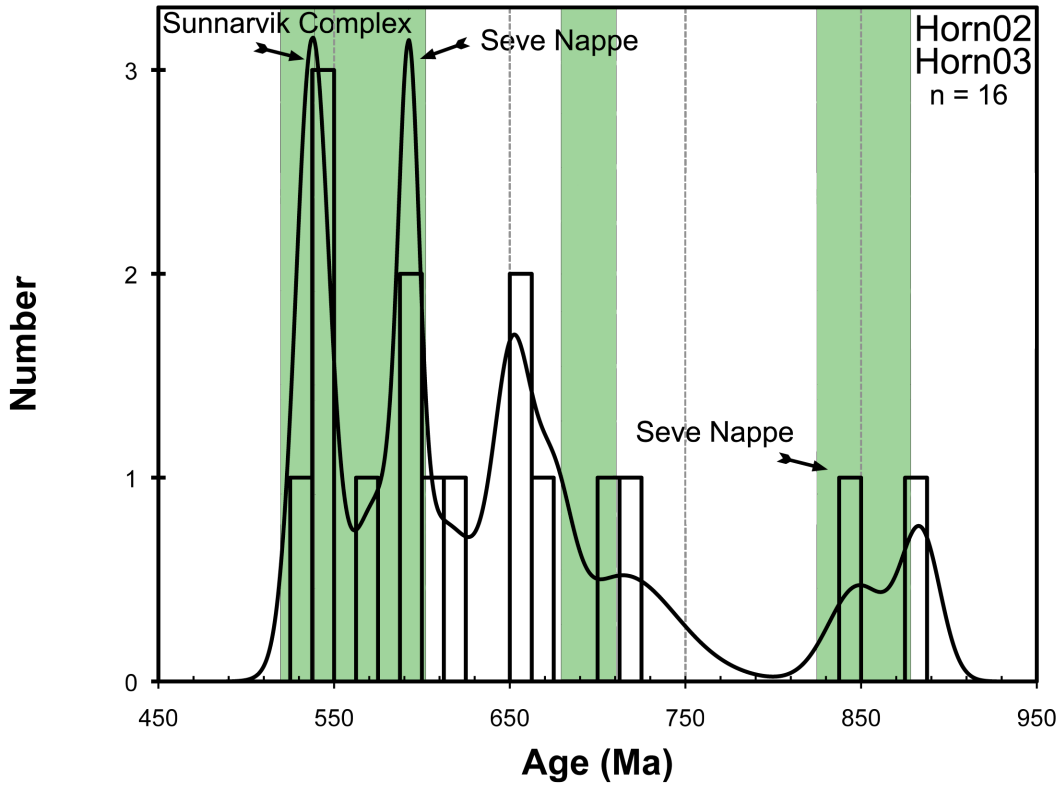

Figur 23. *A probability density plot with histogram showing 16 zircons of Cryogenian or Ediacaran ages from the Hornelen basin. Relative probability peaks at ~510, ~595, 655, and 880 Ma. The y-axis represents the relative probability and number of zircon grains. Green columns mark magmatic events recorded in the Seve-Kalak nappes and in the Precambrian basement of southern Norway (Fen Complex).*

Apart from the Sunnarvik Complex, there are to my knowledge no known rock units of this age in the potential source area of the Hornelen basin. This indicates that the rift-related magmatic rocks of Cryogenian or Ediacaran age are more widespread in southern Norway than presently known. Alternatively, grains of this age range may stem from re-sedimented sedimentary rocks that had a much wider source region than the Devonian basins.

The Late Cambrian to Early Devonian zircons

There is a marked increase in zircons of Caledonian age when going from the Solund/Fensfjorden/Kvamshesten basins to the Hornelen basin (Fig. 22). Whereas the main zircon populations of the Solund/Fensfjorden/Kvamshesten samples mainly are of Sveconorwegian and Gothian ages (96.3 % and 95.27 %), the Hornelen samples have a very pronounced Caledonian component (35%). In addition to the samples analysed in this study, a prominent Caledonian component is also present in a sample from a distal-sandstone near the stratigraphic base of Hornelen (data from Johnston 2006).

Going from Devonian basin of Hornelen to the Devonian basin of **Smøla,** the Caledonian component increases from 35% to 69% (Fig. 22). There is accordingly a significant variation within the Caledonian component between the different basins, with an apparent increase in this component towards the north.

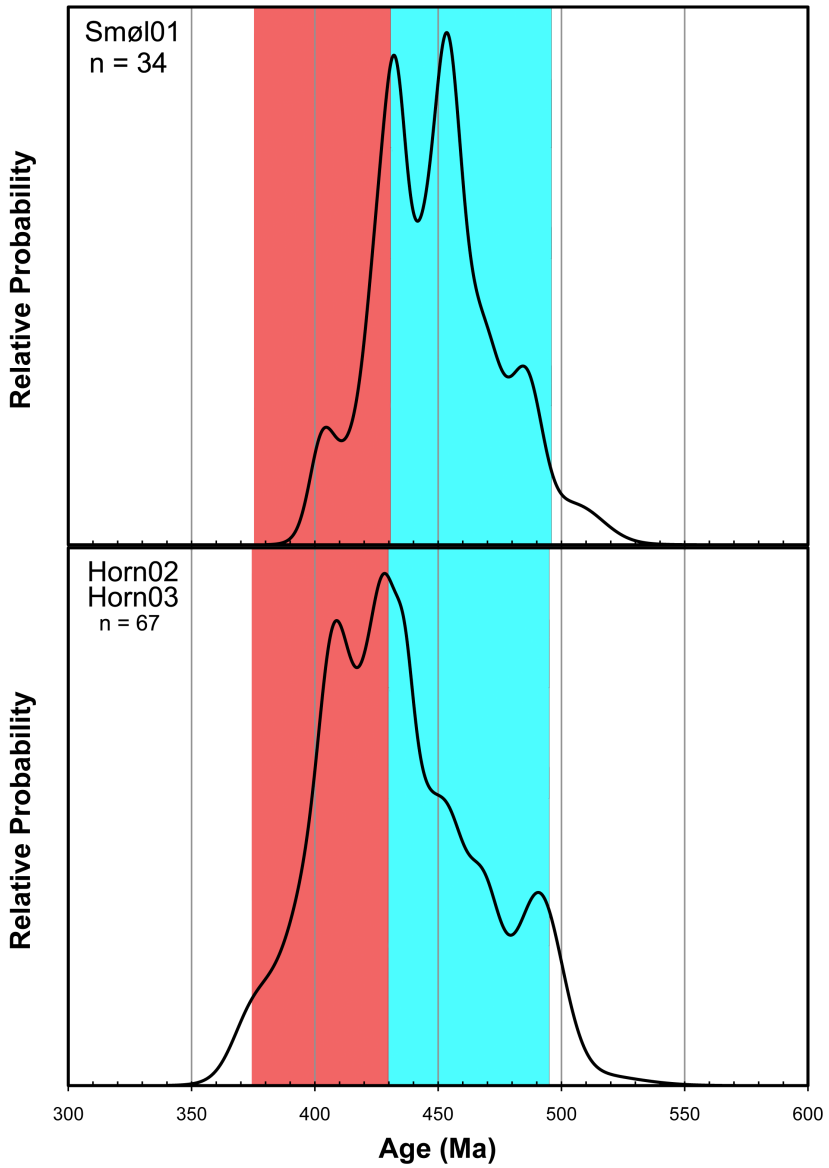

Figur 24. Probability density plot of Caledonian zircons from Hornelen and Smøla. The continent – continent collisional (Scandian) time of the orogeny in red color (430 – 275 Ma), while the oceanic accretion stage is shown in cyan (430 – 495 Ma).

Detrital zircons of pre-Scandian and Scandian age

The Caledonian zircons found in the Devonian basins can be linked to several different periods of the orogeny. The Caledonian orogeny can broadly be subdivided into an oceanic stage – when an oceanic gateway with oceanic crust still separated the two contents – and a continental collisional stage. The oceanic stage is recorded in the Upper Allochthon where magmatic ages range from 495 – 431 Ma (Fig. 24, cyan), and reflects the formation of island arcs, oceanic crust, and microcontinents in the Iapetus Ocean (Furnes et al. 1980; Pedersen &

Dunning 1988; Pedersen & Furnes 1991). The continental collisional stage, known as the Scandian phase, includes continent-continent collision and the following orogenic collapse and extensional tectonics. This Scandian phase of the orogeny (~430 – 375 Ma) is regarded as a "cold" orogeny with relatively little syn- to post-collisional magmatism recorded (Tucker et al 2004; Bingen & Solli 2009 and references therein). However, in recent years a number of migmatites, pegmatite bodies and minor intrusions present within the basement gneisses and the Middle Allochton has been reported to be of late Silurian and Devonian age (Bingen & Solli 2009 and references therein; Lundmark & Corfu 2007; Lundmark et al. 2007; Nordgulen et al. 2002; Tucker et al. 2004).

The Caledonian zircon population in the Hornelen Basin includes ages that are older and younger than 431 Ma. Due to the uncertainty of the measured ages, which is on average ca. 16 Ma (1 sigma) for Caledonian zircons, it is problematic to assign individual grains to a particular Caledonian event. However, the precision of the analyses seems to be good enough to conclude that the youngest Caledonian zircons cannot represent older oceanic terrain and that the oldest Caledonian zircons cannot have formed during the late Scandian magmatic events. It therefore appears that detritus from both the oceanic and the collisional stages of the orogeny are present in the basin.

Source of the Pre-Scandian zircons

The ophiolitic terrain exposed in the hangingwall of the Nordfjord-Sogn detachment fault includes rocks formed during the oceanic stage of the Caledonides. To the south of Hornelen basin this terrain includes the Solund-Stavfjord ophiolite complex (443Ma) with associated sedimentary and volcanosedimentary sequences, while to the north it incorporate the Kalvåg Mélange, the Bremanger Granodiorite (443 ± 4 Ma) and the Gåsøy Intrusion (440 ± 5 Ma).

Quartz-diorite clasts from these intrusive rocks are often present within the fanglomorates that are located in the northern fringes of the basin, and are especially dominating the clast composition close to the sample locations in Hornelen (Fig. 5; Cuthbert 1991).

The most pronounced peak of the Hornelen samples is at ca. 430 Ma (Fig. 24), which is within the error consistent with the age of granitoid bodies in the region (Bremanger Granodiorite 440 ± 5 Ma and the Sogneskollen Granodiorite 434 ± 4).

The Hornelen samples exhibit a population of zircons that are older than 450 Ma, with a relative probability peak around 480-490 (Fig. 24). The ophiolitic terrain of the Nordfjord-Sunfjord area includes only rock units younger then 443 Ma, while older ophiolitic terrains with magmatic histories from 500-440 Ma are present in southwest Norway and in the Trøndelag area. These older oceanic rock units include a phase of arc magmatism at around 490-480 Ma (Dunning and Pedersen 1988; Pedersen and Dunning 1997). It seems likely that rock complexes of this age were present in the drainage area of the basin.

The Devonian deposits on Smøla are associated with the Smøla-Hitra Batholith (446 - 438 Ma). The batholith intrudes metasedimentary and metavolcanic units of Arenig-Llanvirn age (478-462 Ma) that are linked to the early Ordovician ophiolite complexes of the Trøndelag region (Gautneb and Robert 1989; Tucker, et al 2004).

The Caledonian zircons from the Smøla sample represent ~70% of the population, 2/3 of this Caledonian population are within the age of the Smøla-Hitra Batholith with 1 sigma uncertainty, while the older zircons can be attributed to the early Ordovician ophiolite complex.

The remaining population of the Caledonian zircons is younger than these sources from Upper – Uppermost Allochthon and may therefore be derived from rocks formed during the Scandian phase of the Caledonides.

Finally, the increase in the Caledonian component from the Solund/Fensfjorden/Kvamshesten basins to the Hornelen basin, followed by a further increase to the Smøla (Fig. 22), indicate a south-north shift from the Middle Allochthon to the Upper Allocthon as the major source of the zircons. This could again reflect that deeper levels of the Caledonian Nappe stack had been exhumed to surface in the southern region.

The distribution of granitoids within the Upper Allochthon may represent another explanation to this observation. The fact that clast materials from the ophiolitic terrain (e.g. basalt and peridotite) are abundant in the Solund-Fensfjorden basin show that the Upper Allocthon also was a major source of detrital material to these southern basins despite the detrital zircon patterns being totally dominated by Proterozoic grains.

Sources of Scandian age zircons

A significant proportion (~52%) of the zircons from the Hornelen samples are younger then 430 Ma, which is regarded as a divide between the oceanic and the continental collisional stages of the Scandinavian Caledonides. Due to the uncertainty of the analyses, it is impossible to assign zircons close to the division line to either of these two orogenic phases. However, 19 of the 67 Caledonian grains (28%) are younger then 431 Ma outside their 1-sigma uncertainties, and in the relative probability plot these young zircons also define a peak centered at 410-415Ma (Fig. 24, red). This suggests that detrital zircons of Scandian age are present in the Hornelen Basin.

Magmatic rocks formed during the Scandian phase has of yet not been reported from the Upper Allochthon, or Middle Allochthon units close to the Hornelen basin. Scandian magmatic rocks reported from intrusions found in the Middle Allochthon units of the Lindås Nappe and the Jotun Nappe, which yield ages of ~425 Ma (Kühn et al. 2002) and 427 ± 1 Ma (Lundmark & Corfu 2007), respectively. Also minor pegmatite bodies and felsic dykes ranging in age from 436 – 391 Ma are common in the Seve-Kalak and Jotun Nappes (Bingen & Solli 2009 and references therein). Also reported are granitic pegmatites of Scandian age in WGR, ranging in age between 409 – 390 Ma (Bingen & Solli 2009 and references therein). These rock units were probably the source rocks for the Scandian zircons, and a part of the drainage area of the Hornelen basin in Devonian times.

Based on detrital zircon geochronology, Sm-Nd isotope systematics and major and trace element geochemistry of the Hornelen basin, Fonneland (2002) questioned if parts of the WGR could have been exhumed to the surface already

in Devonian time. The Sm-Nd isotopes of the Hornelen deposits yield predominantly Gothian model ages (Fig. 25 a) indicating that the Proterozoic rocks either in the basement or the lower and middle nappe units represent a dominant source. An increase in negative Eu-anomalies, when going from the base towards the northern fringe of the basin, indicate an increase in detritus from more highly fractionated magmatic rocks up stratigraphy and/or towards the northern margin of the basin. Fonneland (2002) proposed that this could be explained by a change in the source rocks from deeper crustal rocks from the Middle Allocthon (anorthosites, mangerites, jotunites etc) to upper crustal rocks in the WGR (granitic plutons and gneisses).

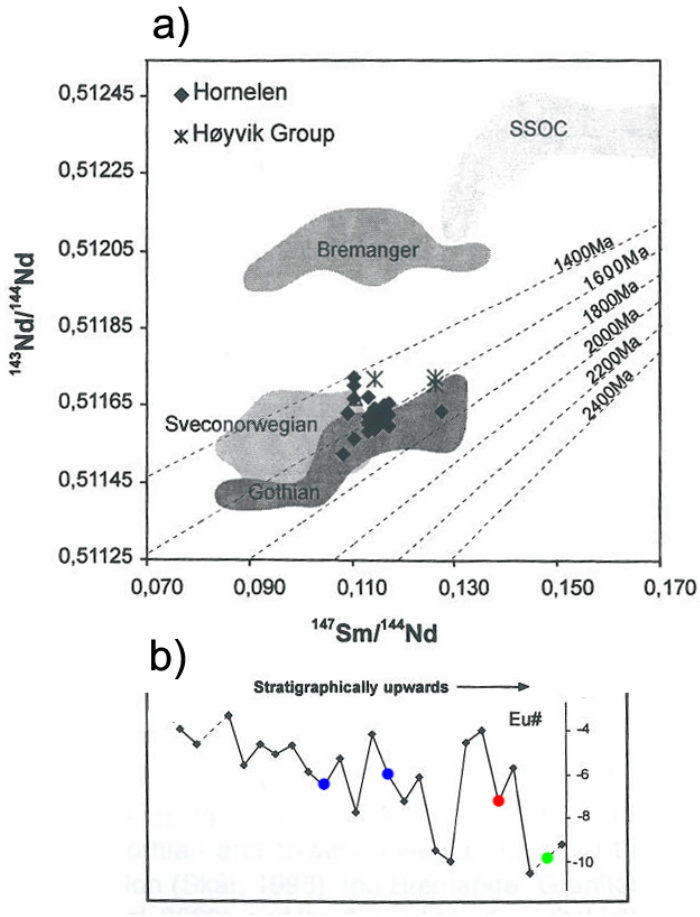

Figure 25. A) *147Sm/144Nd versus 143Nd/144Nd diagram that compares the Hornelen and the Høyvik Groups data with the Sm-Nd isotopic range of: Gothian and Sveconorwegian rocks of the Western Gneiss Region (Skår 1998), the Bremanger Granitoid Complex (Hansen et al. 2002), and the Solund-Stavfjord Ophiolite Complex (Furnes et al. 1990). The dashed lines correspond to isochrons that are labeld by ages in Ma. Sm/Nd values are back calculated to 400 Ma (Fonneland 2002).* **B**) *Variations with stratigraphy of Eu# (Eu-(Sm + Gd)/2)) through the Hornelen basin. In the diagram the samples are equally spaced, and do not strictly follow the Hornelen basin stratigraphy. The samples used by Fonneland for Pb/Pb zircon ages shown in blue, while the U/Pb zircon in this study are shown in red and green, Horn 02 and Horn 03, respectively (Fonneland 2002).*

While the Gothian and Sveconorwegian zircon populations are dominating the two samples from the axial part of the basin analyzed by Fonneland (2002; Fig. 25 B, blue dots), Caledonian zircons represent a significant population in one of the samples analyzed in this study (24%; Fig. 5, Horn 02; Fig. 25 B, red dot) - and the most significant component in the other sample, which was taken close to the northern margin of the basin (41%; Fig. 5, Horn 03; Fig. 25 B, green dot). The Caledonian component seems to increase accordingly from the axial part to the northern boundary of the basin (Fig. 25 b). This is consistent with the abundance of quartzdioritic clasts that were presumably derived from the Bremanger intrusion within the fanglomerates present along the northern boundary of the basin. The decrease in Eu-anomaly towards the northern margin, as documented by Fonneland (2002), may also be explained by a larger contribution from a granitic source in the Upper Allochthon, rather than indicating a shift in the source from the Middle Allochthon to the WGR.

The present provenance data indicate that the marginal and the axial deposits of the Hornelen basin have somewhat different sources. The sample closest to the northern margin has a large input of Caledonian material from Upper Allochthon in the hanging wall. This Caledonian signature diminishes towards the axial parts of the basin, which is dominated by an eastern Sveconorwegian - Gothian source of Middle – Lower Allochthon from the hanging wall and/or footwall.

Presently it is not possible to provide an unambiguous conclusion as to origin nature of the Scandian zircon populations that appears to be present in the Hornelen samples and to a lesser extent in the Smøla sample. In order to decipher the provenance of these young zircon populations, further investigation with a more precise analytical technique such as the TIMS would be necessary. This could help to constrain the maximum age of the Devonian deposits and if the zircons that formed during late Caledonian exhumation had been exhumed to the surface already in Devonian time.

Conclusion

The provenance of fine-grained gravel conglomerates to siltstones samples collected from the five different Devonian basins in western Norway have been studied by detrital zircon geochronology. By comparing these data with previous geological studies done in western Norway, differences in the basins provenance of detrital U/Pb age signature as well as geological aspects of their main source can be distinguished:

The Solund – Fensfjorden basins have an Sveconorwegian main source interpreted to be the Lindås Nappe, while the Kvamshesten basin has a Gothian main source interpreted to be the Dalsfjord Suite. The difference in age spectra between the Lindås Nappe (Sveconorwegian) and its correlatives (Gothian) supports the suggestion proposed by Lundmark et al. (2007) that the Lindås Nappe experienced a higher degree of Sveconorwegian reworking.

The Hornelen basin has a component of zircons formed during rifting of Laurentia in Middle-Late Neoproterozoic times (530 – 870 Ma). Potential source rocks in the vicinity of the basin are the Sunnarvik Complex and the Seve Nappe, but they can only partly account for some of the zircons of this age range that are present in the basin. Thus there are additional sources from this time period that are not yet found or that have been removed by erosion since Devonian times.

The samples from the Hornelen and the Smøla basins have a large component of Caledonian zircons as a result of granitoids present in the drainage area. The Smøla sample is totally dominated by Caledonian detritus from its Upper Allochthonous basement (The Smøla-Hitra Batholith and Støren Nappe), whereas the Hornelen samples show internal differences in Caledonian component linked to the position of the samples relative to the northern basin boundary. This corresponds well with REE data and systematic variations in the Eu anomlies reported by Fonneland (2002). The Sveconorwegian and Gothian zircons in the Hornelen deposits is most likely derived from the Middle Allochthons, possibly the Eikfjord Group and Jotun Nappe.

The laser ablation ICP-MS analyses show that a population of young zircons of Scandian age is present particularly in the Hornelen basins. More precise analytical techniques are needed to reveal the exact age of this population. This could help to constrain the maximum age of the Devonian deposits and if the zircons that formed during late Caledonian exhumation had been exhumed to the surface already in Devonian time.

References

Alsaker, E.& Furnes, H. (1994). *Geochemistry of the Sunnfjord Melange: sediment mixing from different sources during obduction of the Solund-Stavfjord Ophiolite Complex, Norwegian Caledonides*. Geological Magazine131: 105-121.

Andersen, T. & Taylor, P. N. (1988). *Lead isotope geochemistry of the Fen carbonatite complex, SE Norway: Age and petrogenetic implications*. Geochimica et Cosmochimica Acta 52: 209-215.

Andersen, T. (2005). *Detrital zircons as tracers of sedimentary provenance: limiting conditions from statistics and numerical simulation*. Chemical Geology 216: 249-270.

Andersen, T.B., Berry IV, H.N., Lux, D.R. & Andresen, A. (1998). *The tectonic significance of pre-Scandian $^{40}Ar/^{39}Ar$ phengite cooling ages in the Caledonides of western Norway.* Journal of the Geological Society 155: 297-309.

Andersen, T.B., Osmundsen, P. T. & Jolivet, L. (1994). *Deep crustal fabrics and a model for the extensional collapse of the southwest Norwegian Caledonides.* Journal of Structural Geology 16: 1191-1203.

Andersen, T. B., Skjerlie, K.P. & Furnes, H. (1990). *The Sunnfjord Melange, evidence of Silurian ophiolite accretion in the West Norwegian Caledonides.* Journal of the Geological Society 147: 59-68.

Andréasson, P.G., Svenningsen, O. M.& Albrecht, L. (1998). *Dawn of Phanerozoic orogeny in the North Atlantic tract; Evidence from the Seve-Kalak Superterrane, Scandinavian Caledonides.* GFF 20: 159-172.

Anderson, D.S. & Cross, T.A. (2001). *Large-Scale cycle architecture in continental strata, Hornelen Basin (Devonian), Norway.* Journal of Sedimentary Research, 71: 255-271.

Atakan, K. (1989). *The sedimentary and structural development of the Devonian Smøla Group, West Central Norway.* Unpublished cand. scient. thesis, University of Bergen, 308.

Austrheim, H. & Corfu, F. (2008). *Formation of planar deformation features (PDFs) in zircon during coseismic faulting and an evaluation of potential effects on U-Pb systematics.* Chemical Geology 261: 25-31.

Bingen, B., Davis, W. J. & Austrheim, H. (2001). *Zircon U-Pb geochronology in the Bergen arc eclogites and their Proterozoic protoliths, and implications for the pre-Scandian evolution of the Caledonides in western Norway*. Geological Society of America Bulletin 113: 640-649.

Bingen, B. & Solli, A. (2009).*Geochronology of magmatism in the Caledonian and Sveconorwegian belts of Baltica: synopsis for detrital zircon provenance studies.* Norwegian Journal of Geology, 89: 267-290.

Brekke, H. & Solberg, P.O. (1987). *The geology of Atløy, Sunnfjord, western Norway.* Norges Geologiske Undersøkelser, Bulletin 410: 73-94.

Braathen, A., Nordgulen, Ø., Osmundsen, P.T., Andersen, T.B, Solli, A.& Roberts, D. (2000). *Devonian, orogen-parallel, opposed extension in the Central Norwegian Caledonides.* Geology 28: 615-618.

Corfu, F. & Andersen, T.B. (2002). *U/Pb ages of the Dalsfjord Complex SW Norway, and their bearing on the correlation of allochtonous crystalline segments of the Scandinavian Caledonides.* International Journal of Earth Science 91: 955-963.

Corfu, F., Roberts, R.J., Torsvik, T.H., Ashwal, L.D. & Ramsay, D.M. (2007). *Peri Gondwanan elements in the Caledonian nappes of Finnmark, northern Norway: implications for the paleogeographic framework of the Scandinavian Caledonides*. American Journal of Science 307: 434-458.

Cuthbert, S.J. (1991). *Evolution of the Devonian Hornelen Basin, west Norway: new constraints from petrological studies of metamorphic clasts*. Geological Society, London, Special Publications, 57: 343-360.

Dunstan, L.P., Gramch J.W., Barnes, I.L. & Purdy, W.C. (1980). *The absolute abundance and the atomic weight of a reference sample of thallium*. Journal of research of the National Bureau of Standards, 85: 1-10.

Dunning, G.R. & Pedersen, R. B. (1988). *U/Pb ages of ophiolites and arc-related plutons of the Norwegian Caledonides: implications for the development of Iapetus.* Contributions to Mineralogy and Petrology 98: 13-23.

Eide, E.A., Torsvik, T.H. & Andersen, T.B. (1997). *Absolute dating of brittle fault movements: Late Permian and late Jurassic extensional fault breccias in western Norway.* Terra Nova 9: 135-139.

Fonneland, H.C. (2002). *Radiogenic Isotope Systematics of Clastic Sedimentary Rocks – with Emphasis on Detrital Zircon Geochronology*. Unpublished Doctor Scient. thesis, Department of Geology, University of Bergen, 216.

Fossen, H. (1992). *The role of extensional tectonics in the Caledonides of South Norway.* Journal of Structure Geology, 14: 1033-1046.

Fossen, H. (2000). *Extensional tectonics in the Caledonides: Synorogenic or postorogenic?* Tectonics 19: 213-224.

Fossen, H. (2010). *Extensional tectonics in the North Atlantic Caledonides: a regional view.* Geological Society of London, Special Publications 335: 767-793.

Furnes, H., Roberts, D., Sturt, B.A., Thon, A. & Gale, G.H. (1980). *Ophiolite fragments in the Scandinavian Caledonides.* In: Ophiolites, Proceedings International Ophiolite Symposium Cyprus 1979. Cyprus Geological Survey Department 1980. 582-599.

Furnes, H., Skjerlie, K.P., Pedersen, R.B., Andersen, T.B., Stillman, C.J., Suthren, R.J., Tysseland, M. & Garmann, L.B. (1990). *The Solund-Stavfjord Ophiolite Complex and associated rocks: geology, geochemistry and tectonic environment*. Geological Magazine 127: 209-224.

Gee D.G., Fossen H., Henriksen N. & Higgins A.K. (2008). *From the Early Paleozoic Platforms of Baltica and Laurentia to the Caledonide Orogen of Scandinavia and Greenland.* Episodes 31: 1-8.

Gee, D.G., Kumpulainen, R., Roberts, D., Stephens, M.B. & Zachrisson, E. (1985). *Scandinavian Caledonides - Tectonostratigraphic Map. The Caledonide Orogen - Scandinavia and Related areas*. Gee D.G.& Sturt B.A., John Wiley & Sons, England.

Hacker, B.R., Andersen, T.B., Root, D.B., Mehl, L., Mattinson, J.M. & Wooden, J.L. (2003). *Exhumation of high-pressure rocks beneath the Solund Basin, Western Gneiss Region of Norway.* Journal of Metamorphic Geology, 21: 613-629.

Hacker, B.R. (2007). *Ascent of the ultrahigh-pressure Western Gneiss Region, Norway.* Geological Society of America Special Paper.

Hansen, J., Skjerlie, K.P., Pedersen, R.B. & De La Rosa, J. (2002). *Crustal melting in the lower parts of island arcs: an example from the Bremanger Granitoid Complex, west Norwegian Caledonides.* Contrib Mineral Petrol 143: 316-335.

Horn, I., Rudnick, R.L. & McDonough, W.F. (2000). *Precise elemental and isotope ratio measurement by simultaneous solution nebulisation and laser ablation-ICP-MS: application to U-Pb geochronology*. Chemical Geology 164: 281-301.

Hövelmann, J. & Austrheim, H. (2009). *Guidelines for experiments on CO2 sequestration in peridotites based on a natural example.* Goldschmidt Conference Abstracts 2009.

Jackson, S.E., Pearson, N., Griffin, W.L. & Belousova, E.A. (2004) The application of laser ablation-inductively coupled plasma-mass spectrometry to in situ U–Pb zircon geochronology. Chemical Geology, 211: 47–69.

Jarvik, E. (1949). *On the Middle Devonian crossopterygians from the Hornelen field in western Norway*. Universitetet i Bergen Årbok 1948, Naturvidensk. Rekke, No. 8, 1-48.

Johnston, S.M., Hacker, B.R. & Andersen, T.B. (2007). *Exhuming Norwegian ultrahigh-pressure rocks: Overprinting extensional structures and the role of the Nordfjord-Sogn Detachment Zone*. Tectonics 26: 1-12.

Johnston, S.M. (2006). *Exhumation of Norwegian Ultrahigh-Pressure Rocks*. Unpublished Doctor Scient. thesis, Department of Earth Science, University of California, 132.

Kirkland, C.L., Daly, J.S. & Whitehouse, M.J. (2006). *Granitic magmatism of Grenvillian and late Neoproterozoic age in Finn- mark, Arctic Norway – Constraining pre-Scandian deformation in the Kalak Nappe Complex*. Precambrian Research 145: 24-52.

Kirkland, C.L., Daly, J.S. & Whitehouse, M.J. (2008). *Basement-cover relationships of the Kalak Nappe Complex, Arctic Norwegian Caledonides and constraints on Neoproterozoic terrane assembly in the North Atlantic region*. Precambrian Research 160: 245-276.

Kolderup, C. F. (1922). *Der Mangeritsyenit und ungebende Gesteine.* Bergens Museums Aarbok 1920-21.

Kolderup, N.H. (1928). *Fjellbygningen i kyststrøket mellom Nordfjord og Sognefjord.* Bergens Museum Aarbok 1928.

Kosler, J., Fonneland, H., Sylvester, P., Tubrett, M. & Pedersen, R.B. (2002). *U-Pb dating of detrital zircons for sediment provenance studies – a comparison of laser ablation ICPMS and SIMS techniques*. Chemical Geology 182: 605-618.

Kosler, J. & Sylvester, P. (2003). *Present trends and the future of zircon in geochronology: laser ablation ICPMS.* Reviews in Mineralogy & Geochemistry 53: 243-275.

Kühn, A., Glodny, J., Austrheim, H. & Råheim, A. (2002). *The Caledonian tectono-metamorphic evolution of the Lindås nappe: constraints from U/Pb, Sm/Nd and Rb/Sr ages of granitoid dykes.* Norwegian Journal of Geology, 82: 45–57.

Kylander-Clark, A., Hacker, B., Mattinson, J. & Rioux, M. (2006). *U-Pb Titanite ages of decompression melting during exhumation of the western gneiss region ultrahigh-pressure terrane.* Geological Society of America 38: 237.

Kylander-Clark, A., Hacker, B. & Mattinson, J.M. (2008). *Slow exhumation of UHP terranes: Titanite and rutile ages of Western Gneiss Region, Norway*. Earth and Planetary Science Letters 272: 531-540.

Ludwig, K.R. (1999) IsoplotEx v. 2.6. Berkeley Geochronological Center Special Publication no. 1a.

Lundmark, A.M., Corfu, F., Spürgin, S. & Selbekk, R. (2007). *Proterozoic evolution and provenance of the high-grade Jotun Nappe Complex, SW Norway: U–Pb geochronology*. Precambrian Research 159(3–4): 133-154.

Lundmark, A.M. & Corfu, F. (2007). *Age and origin of the Årdal dike complex, SW Norway: False isochrons, incomplete mixing, and the origin of Caledonian granites in basement nappes.* Tectonics 26: 1-13.

Moecher, D.P. & Samson, S. D. (2006). *Differential zircon fertility of source terranes and natural bias in the detrital zircon record: Implications for sedimentary provenance analysis.* Earth and Planetary Science Letters 247: 252-266.

Nilsen, T.H. (1968). *The relationship of sedimentation to tectonics in the Solund Devonian district of southwestern Norway*. Norges Geologiske Undersøkelse, 259: 108.

Nordgulen, Ø., Braathen, A., Corfu, F., Osmundsen, P.T. & Husmo, T. (2002). *Polyphase kinematics and geochronology of the late-Caledonian Kollstraumen detachment, north-central Norway*. Norwegian Journal of Geology, 82: 299-316.

Norton, M.G. (1986). *Late Caledonide extension in western Norway: A response to extreme crustal thickening.* Tectonics, 5: 195-204.

Norton, M.G. (1987). *The Nordfjord-Sogn Detachment, W. Norway.* Norsk Geologisk Tidsskrift 67: 93-106.

Milnes, A.G., Dietler, T.N. & Koestler, A.G. (1988). *The Sognefjorden north shore log – a 25 km depth section through Caledonized basement in western Norway.* Norges Geologiske Undersøkelse, Special Publication 3: 114-121.

Osmundsen, P.T., Andersen, T. B., Markussen, S., & Svendby, A.K. (1998). *Tectonics and sedimantation in the hangingwall of a major extensional detachment: the Devonian Kvamshesten Basin, western Norway.* Basin Research 10: 213-234.

Osmundsen, P.T., Bakke, B., Svendby, A.K. & Andersen, T.B. (2000). *Architecture of the Middle Devonian Kvamshesten Group, western Norway: sedimentary response to deformation above a ramp-flat extensional fault*. Geological Society, London, Special Publications 180: 503-535.

Osmundsen, P.T. & Andersen, T. B. (2001). *The middle Devonian basins of western Norway: sedimantary response to large-scale transtensional tectonics?* Tectonophysics 332: 51-68.

Paulsson, O. & Andréasson, P.G. (2002). *Attempted break-up of Rodinia at 850 Ma: geochronological evidence from the Seve-Kalak Superterrane, Scandinavian Caledonides.* Journal of the Geological Society, London 159: 751-761.

Pedersen, R. B. & Dunning, G. R. (1988). *Some Norwegian ophiolite complexes reconsidered.* Norges Geologiske Undersøkelser, Special Publication 3: 80-85.

Pedersen, R.B., Dunning, G.R. & Robins, B. (1989). *U-Pb ages of nepheline syenite pegmatites from the Seiland Magmatic Province, N Norway.* In: R.A. Gayer, Ed. The Caledonide geology of Scandinavia, 3-8. Graham & Trotman, London.

Pedersen, R.B. & Furnes, H. (1991). *Geology, magmatic affinity and geotectonic environment of some Caledonian ophiolites in Norway*. Journal of Geodynamics, 13: 183-203.

Pedersen, R. B. & Dunning, G. R. (1993). *Provenance of turbiditic cover to the Caledonian Solund-Stavfjorden ophiolite from U-Pb single zircon dating.* Journal Geological Society London, 150: 673-676.

Rankin, D. W. (1976). *Appalachian Salients and Recesses: Late Precambrian Continental Breakup and the Opening of the Iapetus Ocean*. Journal of Geophysical Research, 81(32): 5605–5619.

Roberts, R. & Gee, D.G. (1985). *An introduction to the structure of the Scandinavian Caledonides.* John Wiley & Sons Ltd.

Roberts, R.J., Corfu, F., Torsvik, T.H., Ashwal, L.D. & Ramsay, D.M. (2006). *Short-lived mafic magmatism at 560-570 Ma in the northern Norwegian Caledonides: U-Pb zircon ages from the Seiland Igneous Province*. Geological Magazine 143: 887-903.

Séranne, M. & Séguret, M. (1987). *The Devonian basins of western Norway: tectonics and kinematics of an extending crust.* Geological Society of London 28: 537-548.

Séranne, M. (1992). *Late Paleozoic kinematics of the Møre-Trøndelag Fault Zone and adjacent areas, central Norway*. Norsk Geologisk Tidsskrift, 72: 141-158.

Skår, Ø., Furnes, H. & Claesson, S. (1994). *Proterozoic orogenic magmatism within the Western Gneiss Region, Sunnfjord, Western Norway*. Norsk Geologisk Tidsskrift 74: 114-126.

Skår, Ø., Pedersen, R. B. (2003). *Relations between granitoid magmatism and migmatization: U-Pb geochronological evidence from the Western Gneiss Complex, Norway.* Journal of the Geological Society 160: 935-946.

Slama, J., Kosler, J., Condon, D.J., Crowley, J.L., Gerdes, A., Hanchar, J.M., Horstwood, M., Morris, G.A., Nasdala, L., Norbert, N., Schaltegger, U., Schoene, B., Tubrett, M.N. & Whitehouse, M.J. (2008). *Plešovice zircon – a new natural reference material for U-Pb and Hf isotopic microanalysis*. Chemical Geology, 249: 1-35.

Smith, D. C. (1984). *Coesite in clinopyroxene in the Caledonides and its implications for geodynamics* . Nature 310: 641-644.

Smith, D. C. (1988). *A review of the peculiar mineralogy of the "Norwegian Coesite Eclogite Province", with crystal-chemical, petrological geochemical and geodynamical notes and an extensive bibliography*. Elsevier.

Steel, R.J., Mæhle, S., Røe, S.L., Spinnanger, Å. & Nilsen, H.R. (1977). *Coarsening-upward cycles in the alluvium of Hornelen Basin (Devonian) Norway: Sedimentary response to tectonic events.* Bulletin of Geological Society of America, 88: 1124-1134.

Steel, R.J. & Gloppen, T.G. (1980). *Late Caledonian Devonian basin formation, western Norway: signs of strike-slip tectonics during infilling*. Special Publications the International Association of Sedimentology, 4: 79-103.

Svenningsen, O.M. (2001). *Onset of seafloor spreading in the Iapetus Ocean at 608 Ma: precise age of the Sarek Dyke Swarm, northern Swedish Caledonides.* Precambrian Research 110: 241-254.

Tillung, M. (1999). *Structural and metamorphic development of the Hyllestad-Lifjorden area, western Norway.* University of Bergen. Cand.scient. thesis, 266.

Tucker, R.D., Robinson, P., Solli, A., Gee, D.G., Thorsnes, T., Krogh, T.E., Nordgulen, Ø. & Bickford, M.E. (2004). *Thrusting and extension in the Scandian hinterland, Norway: New U-Pb ages and tectonostratigraphic evidence.* American Journal of Science, 304: 477-532.

Wennberg, O.P. & Milnes, A.G. (1994). *Interpretation of kinematic indicators along the northeastern margin of Bergen Arc System: a preliminary field study*. Norsk Geologisk Tidsskrift (NGT), 74: 166-173.

Wiedenbeck, M., Alle, P., Corfu, F., Griffin, W.L., Meier, M., Oberli, F., von Quadt, A., Roddick, J.C. & Spiegel, W. (1995). *Three natural zircon standards for U-Th-Pb, Lu-Hf, trace element and REE analyses*. Geost Newslet 19: 1-23.

Appendix

Table 1.

Analysis	ISOTOPIC RATIOS						CALCULATED AGES Ma					
	$^{207}Pb/^{235}U$	± 1 sigma	$^{206}Pb/^{238}U$	± 1 sigma	$^{207}Pb/^{206}Pb$	± 1 sigma	$^{207}Pb/^{235}U$	± 1 sigma	$^{206}Pb/^{238}U$	± 1 sigma	$^{207}Pb/^{206}Pb$	± 1 sigma
	Sample Fens 01											
100304LEPa08	1.7447	0.0642	0.1661	0.0051	0.0760	0.0023	1025.2	23.7	990.4	28.2	1093.8	61.6
100304LEPa08	1.7447	0.0642	0.1661	0.0051	0.0760	0.0023	1025.2	23.7	990.4	28.2	1093.8	61.6
100304LEPa09	2.0847	0.1017	0.1900	0.0074	0.0793	0.0030	1143.8	33.5	1121.2	40.1	1180.8	75.5
100304LEPa10	1.6951	0.0539	0.1642	0.0052	0.0734	0.0014	1006.7	20.3	980.0	28.7	1023.8	39.6
100304LEPa11	2.6746	0.1566	0.2223	0.0089	0.0851	0.0024	1321.5	43.3	1294.2	46.7	1318.7	54.9
100304LEPa16	4.3054	0.2434	0.2987	0.0172	0.0974	0.0043	1694.4	46.6	1684.7	85.6	1574.3	83.1
100304LEPa18	4.2535	0.2109	0.3040	0.0157	0.1001	0.0031	1684.4	40.8	1711.0	77.8	1626.7	56.9
100304LEPa19	2.5940	0.1480	0.2165	0.0170	0.0831	0.0025	1298.9	41.8	1263.5	90.3	1270.8	58.4
100304LEPa21	3.2620	0.1689	0.2595	0.0119	0.0900	0.0015	1472.0	40.2	1487.3	60.8	1425.6	31.3
100304LEPa22	2.2867	0.1311	0.2022	0.0126	0.0796	0.0017	1208.2	40.5	1187.0	67.8	1187.7	41.2
100304LEPa31	2.5416	0.1812	0.2127	0.0166	0.0845	0.0017	1284.0	52.0	1243.4	88.2	1303.5	39.5
100304LEPa37	0.5783	0.0345	0.0697	0.0027	0.0597	0.0021	463.4	22.2	434.4	16.5	592.5	75.2
100304LEPa39	1.8198	0.0738	0.1746	0.0062	0.0748	0.0013	1052.6	26.6	1037.6	33.8	1062.3	34.3
100304LEPa41	2.2414	0.0979	0.1928	0.0065	0.0819	0.0033	1194.1	30.7	1136.7	34.9	1242.3	79.5
100304LEPa46	2.7113	0.1100	0.2266	0.0086	0.0855	0.0014	1331.6	30.1	1316.5	45.3	1326.5	31.4
100304LEPa56	2.2379	0.1408	0.1987	0.0084	0.0812	0.0029	1193.0	44.2	1168.2	45.3	1226.8	71.0
100304LEPa70	1.7233	0.1246	0.1738	0.0100	0.0744	0.0037	1017.3	46.5	1033.0	54.9	1051.8	100.6
100304LEPa76	1.8006	0.1433	0.1751	0.0079	0.0748	0.0042	1045.7	52.0	1039.9	43.3	1062.9	112.7
100304LEPa86	1.4636	0.1489	0.1526	0.0063	0.0692	0.0072	915.5	61.4	915.5	35.3	905.4	215.3
100304LEPa93	2.0777	0.1378	0.1930	0.0102	0.0782	0.0023	1141.5	45.5	1137.8	55.3	1152.1	59.3
100304LEPa94	1.8926	0.0943	0.1760	0.0088	0.0773	0.0012	1078.5	33.1	1045.1	48.5	1129.1	29.9
100304LEPa95	1.5787	0.1981	0.1603	0.0089	0.0722	0.0048	961.9	78.0	958.7	49.7	992.0	134.7
100304LEPa96	1.8881	0.0666	0.1720	0.0075	0.0805	0.0023	1076.9	23.4	1022.9	41.2	1209.0	55.7
100304LEPa56	2.2379	0.1408	0.1987	0.0084	0.0812	0.0029	1193.0	44.2	1168.2	45.3	1226.8	71.0
100304LEPa70	1.7233	0.1246	0.1738	0.0100	0.0744	0.0037	1017.3	46.5	1033.0	54.9	1051.8	100.6
100304LEPa76	1.8006	0.1433	0.1751	0.0079	0.0748	0.0042	1045.7	52.0	1039.9	43.3	1062.9	112.7
100304LEPa86	1.4636	0.1489	0.1526	0.0063	0.0692	0.0072	915.5	61.4	915.5	35.3	905.4	215.3
100304LEPa93	2.0777	0.1378	0.1930	0.0102	0.0782	0.0023	1141.5	45.5	1137.8	55.3	1152.1	59.3
100304LEPa94	1.8926	0.0943	0.1760	0.0088	0.0773	0.0012	1078.5	33.1	1045.1	48.5	1129.1	29.9

100304LEPa95	1.5787	0.1981	0.1603	0.0089	0.0722	0.0048	961.9	78.0	958.7	49.7	992.0	134.7
100304LEPa96	1.8881	0.0666	0.1720	0.0075	0.0805	0.0023	1076.9	23.4	1022.9	41.2	1209.0	55.7
100304LEPa101	1.8151	0.1120	0.1720	0.0081	0.0769	0.0027	1050.9	40.4	1023.3	44.5	1117.3	70.1
100304LEPa111	1.6171	0.0793	0.1688	0.0062	0.0684	0.0028	976.9	30.8	1005.4	34.0	881.2	85.8
100304LEPa115	1.4934	0.1091	0.1499	0.0085	0.0747	0.0012	927.7	44.4	900.2	47.5	1061.1	33.3
100304LEPa122	1.7863	0.1029	0.1706	0.0083	0.0772	0.0018	1040.5	37.5	1015.5	45.9	1127.3	45.4
100304LEPa132	1.6635	0.0824	0.1616	0.0045	0.0755	0.0034	994.7	31.4	965.6	25.1	1082.8	89.3
100304LEPa135	2.9186	0.2253	0.2352	0.0168	0.0912	0.0025	1386.7	58.4	1361.6	87.7	1450.4	51.8
100304LEPa136	1.8203	0.0857	0.1773	0.0080	0.0755	0.0012	1052.8	30.8	1052.0	44.0	1082.4	30.7
100304LEPa140	2.3623	0.0772	0.2032	0.0059	0.0949	0.0139	1231.3	23.3	1192.5	31.7	1526.1	275.3
100304LEPa142	2.2020	0.2309	0.2006	0.0180	0.0819	0.0035	1181.7	73.2	1178.8	96.7	1243.2	83.8
100304LEPa146	3.6570	0.1549	0.2676	0.0111	0.1011	0.0026	1562.0	33.8	1528.5	56.6	1643.7	48.4
100304LEPa148	1.7984	0.1575	0.1675	0.0042	0.0787	0.0076	1044.9	57.1	998.2	23.3	1163.6	192.2
100304LEPa149	1.7042	0.0912	0.1738	0.0074	0.0724	0.0024	1010.1	34.2	1032.8	40.8	996.7	66.3
100304LEPa150	1.5000	0.1207	0.1489	0.0097	0.0721	0.0060	930.4	49.0	894.7	54.5	988.2	168.7
100304LEPa163	2.1609	0.1248	0.1922	0.0103	0.0797	0.0026	1168.6	40.1	1133.5	55.9	1188.7	65.4
100304LEPa166	2.9737	0.1941	0.2380	0.0166	0.0895	0.0025	1400.9	49.6	1376.4	86.2	1414.7	52.6
100304LEPa169	1.8639	0.0892	0.1704	0.0108	0.0772	0.0021	1068.4	31.6	1014.5	59.3	1125.8	53.8
100304LEPa176	2.3859	0.2092	0.2044	0.0149	0.0848	0.0026	1238.4	62.7	1199.0	80.0	1312.0	58.5
100304LEPa178	0.8131	0.3735	0.0886	0.0146	0.0637	0.0261	604.2	209.2	547.5	86.5	730.9	867.8
100304LEPa179	3.6615	0.1548	0.2635	0.0102	0.1010	0.0019	1563.0	33.7	1507.8	52.0	1643.0	35.3
100304LEPa181	1.8794	0.1186	0.1775	0.0098	0.0749	0.0036	1073.9	41.8	1053.3	53.8	1066.3	95.7
100304LEPa182	2.1153	0.1424	0.1923	0.0111	0.0805	0.0013	1153.8	46.4	1134.1	60.0	1208.7	32.1
100304LEPa183	1.6033	0.1536	0.1646	0.0099	0.0721	0.0027	971.5	59.9	982.0	54.7	989.0	75.8
100304LEPa188	2.6538	0.2202	0.2216	0.0164	0.0858	0.0051	1315.7	61.2	1290.6	86.8	1333.7	114.7
100304LEPa190	1.8276	0.1412	0.1745	0.0166	0.0771	0.0052	1055.4	50.7	1036.9	91.3	1124.2	134.2
100304LEPa194	1.8231	0.1126	0.1700	0.0078	0.0806	0.0089	1053.8	40.5	1012.1	43.1	1210.5	218.0
100304LEPa196	3.5997	0.2274	0.2755	0.0179	0.0938	0.0024	1549.5	50.2	1568.9	90.6	1505.1	49.1
100304LEPa197	1.9890	0.1015	0.1860	0.0056	0.0782	0.0027	1111.8	34.5	1099.6	30.6	1152.5	67.7
100304LEPa199	2.0644	0.0823	0.1943	0.0055	0.0778	0.0030	1137.1	27.3	1144.9	29.5	1142.5	76.5
100304LEPa204	1.7752	0.1459	0.1686	0.0139	0.0765	0.0012	1036.4	53.4	1004.7	76.8	1109.1	32.2
100304LEPa205	3.1783	0.1387	0.2434	0.0118	0.0949	0.0034	1451.9	33.7	1404.3	61.0	1526.2	67.9
100304LEPa207	1.7487	0.1748	0.1769	0.0083	0.0721	0.0040	1026.7	64.6	1049.8	45.7	988.3	113.9
100304LEPa209	1.9089	0.1512	0.1886	0.0133	0.0735	0.0028	1084.2	52.8	1113.7	72.2	1026.9	75.9

100304LEPa210	2.7108	0.1961	0.2300	0.0132	0.0854	0.0025	1331.4	53.7	1334.3	68.9	1325.0	57.4
100304LEPa215	2.0775	0.1176	0.1949	0.0075	0.0786	0.0043	1141.4	38.8	1148.0	40.6	1161.9	109.2
100304LEPa218	1.8223	0.1458	0.1817	0.0067	0.0736	0.0046	1053.5	52.5	1076.2	36.3	1031.4	127.2
100304LEPa219	2.7259	0.1370	0.2389	0.0091	0.0836	0.0023	1335.5	37.3	1381.1	47.3	1284.4	52.4
100304LEPa220	2.4239	0.1291	0.2155	0.0090	0.0827	0.0018	1249.7	38.3	1258.0	47.9	1262.2	43.3
100304LEPa221	3.0910	0.1996	0.2458	0.0120	0.0901	0.0025	1430.5	49.5	1416.5	62.2	1428.4	52.3
100304LEPa222	3.5808	0.1768	0.2719	0.0108	0.0970	0.0020	1545.3	39.2	1550.6	55.0	1567.4	39.1
100304LEPa223	2.2311	0.1192	0.1988	0.0101	0.0820	0.0027	1190.9	37.5	1168.7	54.2	1244.5	64.3
100304LEPa224	1.8095	0.1041	0.1715	0.0082	0.0773	0.0034	1048.9	37.6	1020.4	45.3	1129.3	88.1
100304LEPa233	1.9512	0.1226	0.1895	0.0083	0.0774	0.0021	1098.8	42.2	1118.4	45.1	1130.8	53.6
100304LEPa235	2.9889	0.2027	0.2434	0.0129	0.0906	0.0043	1404.8	51.6	1404.3	66.7	1438.6	90.0
100304LEPa238	2.0356	0.0851	0.1830	0.0084	0.0795	0.0018	1127.5	28.5	1083.5	45.7	1185.2	45.8

Table 2.

	ISOTOPIC RATIOS						CALCULATED AGES Ma					
Analysis	$^{207}Pb/^{235}U$	± 1 sigma	$^{206}Pb/^{238}U$	± 1 sigma	$^{207}Pb/^{206}Pb$	± 1 sigma	$^{207}Pb/^{235}U$	± 1 sigma	$^{206}Pb/^{238}U$	± 1 sigma	$^{207}Pb/^{206}Pb$	± 1 sigma
					Sample Fens 02							
100302LEPa11	1.6838	0.0751	0.1678	0.0064	0.0728	0.0021	1002.4	28.4	1000.2	35.4	1008.3	57.1
100302LEPa13	1.8588	0.1405	0.1822	0.0136	0.0740	0.0013	1066.6	49.9	1079.0	74.0	1040.1	36.2
100302LEPa14	1.8303	0.0854	0.1848	0.0057	0.0720	0.0019	1056.4	30.6	1093.4	31.1	985.8	54.3
100302LEPa15	1.8658	0.0672	0.1820	0.0059	0.0746	0.0018	1069.0	23.8	1077.6	32.2	1057.1	49.4
100302LEPa16	1.8063	0.0877	0.1789	0.0053	0.0732	0.0024	1047.7	31.7	1061.0	28.8	1018.2	65.1
100302LEPa18	1.7492	0.2104	0.1828	0.0121	0.0709	0.0037	1026.9	77.7	1082.3	66.0	954.0	106.7
100302LEPa20	1.6782	0.1431	0.1737	0.0102	0.0706	0.0028	1000.3	54.2	1032.6	56.0	945.0	80.5
100302LEPa21	1.6186	0.1463	0.1729	0.0096	0.0689	0.0022	977.5	56.7	1028.0	52.6	896.8	67.3
100302LEPa22	1.9676	0.0736	0.1822	0.0048	0.0782	0.0027	1104.5	25.2	1078.8	26.1	1152.7	69.1
100302LEPa27	1.7943	0.0691	0.1770	0.0048	0.0737	0.0018	1043.4	25.1	1050.7	26.3	1033.4	48.8
100302LEPa29	1.7797	0.0955	0.1828	0.0062	0.0704	0.0023	1038.1	34.9	1082.1	34.0	939.8	68.2
100302LEPa31	2.0015	0.1132	0.2051	0.0081	0.0729	0.0018	1116.0	38.3	1202.7	43.1	1010.9	50.6
100302LEPa32	1.8991	0.0783	0.1835	0.0051	0.0734	0.0019	1080.8	27.4	1086.3	27.6	1024.9	53.0
100302LEPa33	1.6713	0.0659	0.1696	0.0047	0.0718	0.0014	997.7	25.0	1009.6	25.7	980.7	41.0
100302LEPa35	1.6298	0.0759	0.1684	0.0046	0.0715	0.0020	981.8	29.3	1003.1	25.6	972.3	58.2
100302LEPa37	2.9519	0.3047	0.2418	0.0146	0.0890	0.0038	1395.3	78.3	1396.3	75.9	1403.8	82.1

100302LEPa39	2.0277	0.1068	0.1880	0.0101	0.0780	0.0015	1124.9	35.8	1110.5	55.0	1148.0	37.7
100302LEPa46	1.8614	0.1324	0.1777	0.0098	0.0762	0.0022	1067.5	47.0	1054.3	53.9	1100.9	57.8
100302LEPa47	1.6514	0.1180	0.1663	0.0084	0.0732	0.0021	990.1	45.2	991.9	46.3	1020.5	59.4
100302LEPa48	1.9707	0.1841	0.1825	0.0070	0.0808	0.0054	1105.6	62.9	1080.8	38.3	1215.5	132.2
100302LEPa51	2.0331	0.0792	0.1933	0.0069	0.0761	0.0012	1126.7	26.5	1139.3	37.4	1097.3	31.6
100302LEPa54	2.1529	0.2230	0.1945	0.0098	0.0804	0.0085	1166.0	71.8	1145.7	52.6	1207.4	209.1
100302LEPa56	2.0721	0.1526	0.1884	0.0103	0.0764	0.0031	1139.6	50.4	1112.7	55.9	1105.7	81.6
100302LEPa57	4.3160	0.2682	0.3030	0.0160	0.1035	0.0023	1696.4	51.2	1706.3	79.2	1687.0	41.3
100302LEPa58	1.8648	0.1274	0.1810	0.0125	0.0748	0.0009	1068.7	45.2	1072.5	68.3	1062.9	23.0
100302LEPa59	2.6389	0.1799	0.2277	0.0097	0.0856	0.0032	1311.5	50.2	1322.3	51.0	1329.6	71.7
100302LEPa60	1.8999	0.1053	0.1917	0.0061	0.0716	0.0026	1081.1	36.9	1130.8	33.2	973.8	73.1
100302LEPa65	1.8628	0.1533	0.1827	0.0129	0.0738	0.0015	1068.0	54.4	1081.8	70.5	1037.2	39.7
100302LEPa68	2.0879	0.1671	0.1896	0.0088	0.0769	0.0047	1144.8	54.9	1118.9	47.9	1119.4	122.4
100302LEPa71	1.7377	0.1117	0.1640	0.0089	0.0764	0.0018	1022.6	41.4	979.0	49.2	1106.6	47.4
100302LEPa72	1.7299	0.1001	0.1663	0.0055	0.0754	0.0027	1019.7	37.2	991.5	30.4	1078.6	72.4
100302LEPa73	1.7458	0.1185	0.1694	0.0117	0.0755	0.0044	1025.6	43.8	1008.8	64.7	1082.6	117.0
100302LEPa74	1.7223	0.0881	0.1695	0.0063	0.0745	0.0023	1016.9	32.9	1009.3	35.0	1055.4	62.7
100302LEPa75	3.1625	0.2087	0.2500	0.0162	0.0924	0.0024	1448.1	50.9	1438.3	83.4	1475.1	49.9
100302LEPa76	0.6650	0.0271	0.0809	0.0022	0.0601	0.0019	517.7	16.5	501.3	12.9	608.6	69.4
100302LEPa77	1.6573	0.1615	0.1698	0.0095	0.0709	0.0046	992.4	61.7	1011.1	52.5	955.4	133.9
100302LEPa78	1.7424	0.1523	0.1758	0.0129	0.0716	0.0015	1024.4	56.4	1044.0	70.7	975.3	43.5
100302LEPa79	1.7250	0.1185	0.1717	0.0109	0.0727	0.0013	1017.9	44.2	1021.4	60.1	1004.5	37.0
100302LEPa80	1.8084	0.0849	0.1768	0.0071	0.0742	0.0012	1048.5	30.7	1049.4	38.9	1046.9	33.2
100302LEPa81	1.9127	0.1719	0.1718	0.0078	0.0831	0.0053	1085.5	59.9	1022.2	43.0	1271.6	125.3
100302LEPa86	1.9946	0.0869	0.1866	0.0077	0.0782	0.0017	1113.7	29.5	1103.1	41.9	1152.3	44.4
100302LEPa87	1.9487	0.1031	0.1829	0.0087	0.0776	0.0021	1098.0	35.5	1082.6	47.5	1136.8	53.7
100302LEPa89	1.7853	0.0595	0.1622	0.0067	0.0774	0.0017	1040.1	21.7	969.0	37.4	1130.3	43.1
100302LEPa90	1.9943	0.0858	0.1842	0.0074	0.0778	0.0020	1113.6	29.1	1089.8	40.2	1141.5	50.6
100302LEPa91	1.6896	0.1359	0.1669	0.0103	0.0726	0.0035	1004.6	51.3	995.1	57.2	1002.7	96.5
100302LEPa95	0.5680	0.0591	0.0760	0.0040	0.0554	0.0034	456.7	38.3	472.5	24.2	429.7	137.7
100302LEPa96	1.9286	0.1261	0.1786	0.0081	0.0789	0.0021	1091.1	43.7	1059.3	44.2	1168.6	51.6
100302LEPa97	1.6794	0.1456	0.1736	0.0100	0.0709	0.0024	1000.8	55.2	1032.2	54.8	953.3	70.6
100302LEPa98	2.7057	0.2029	0.2291	0.0167	0.0862	0.0012	1330.0	55.6	1329.8	87.4	1342.4	26.5
100302LEPa99	1.8024	0.1644	0.1783	0.0142	0.0739	0.0012	1046.3	59.6	1057.4	77.6	1038.9	33.0

100302LEPa101	1.9137	0.1702	0.1840	0.0166	0.0746	0.0047	1085.9	59.3	1088.9	90.4	1058.4	128.0
100302LEPa106	2.0377	0.1932	0.1929	0.0179	0.0770	0.0022	1128.2	64.6	1136.8	96.9	1120.2	57.2
100302LEPa108	1.8957	0.1051	0.1812	0.0092	0.0756	0.0013	1079.6	36.9	1073.5	50.5	1083.2	33.4
100302LEPa110	1.6458	0.1721	0.1762	0.0111	0.0701	0.0033	988.0	66.1	1046.3	60.9	931.2	97.9
100302LEPa111	1.7705	0.1099	0.1686	0.0119	0.0748	0.0028	1034.7	40.3	1004.4	65.5	1062.0	74.2
100302LEPa112	1.6817	0.0860	0.1658	0.0068	0.0741	0.0014	1001.6	32.6	989.1	37.5	1044.5	37.0
100302LEPa116	1.7998	0.0839	0.1786	0.0076	0.0713	0.0021	1045.4	30.4	1059.5	41.4	965.9	58.7
100302LEPa117	2.0080	0.0994	0.1889	0.0069	0.0764	0.0024	1118.2	33.6	1115.2	37.2	1106.0	62.3
100302LEPa125	2.1360	0.1784	0.1964	0.0161	0.0794	0.0021	1160.5	57.8	1156.1	86.6	1182.5	52.0
100302LEPa127	1.6881	0.1324	0.1734	0.0075	0.0715	0.0028	1004.1	50.0	1030.7	41.4	971.7	80.0
100302LEPa128	1.5841	0.1349	0.1669	0.0134	0.0703	0.0029	964.0	53.0	995.0	74.3	937.5	83.7
100302LEPa129	2.0576	0.0771	0.1889	0.0054	0.0805	0.0018	1134.8	25.6	1115.6	29.3	1208.9	44.2
100302LEPa134	1.7571	0.0799	0.1699	0.0074	0.0768	0.0017	1029.8	29.4	1011.4	40.8	1115.6	44.3
100302LEPa136	1.8694	0.0891	0.1749	0.0074	0.0773	0.0026	1070.3	31.5	1039.2	40.8	1128.1	66.6
100302LEPa138	1.8662	0.1852	0.1736	0.0093	0.0800	0.0064	1069.2	65.6	1032.0	50.9	1197.9	157.1
100302LEPa139	2.0278	0.0811	0.1862	0.0083	0.0792	0.0014	1124.9	27.2	1100.5	45.0	1177.6	34.4
100302LEPa140	1.6936	0.2207	0.1713	0.0178	0.0722	0.0035	1006.1	83.2	1019.3	97.8	991.1	99.1

Table 3.

	ISOTOPIC RATIOS						CALCULATED AGES Ma					
Analysis	$^{207}Pb/^{235}U$	± 1 sigma	$^{206}Pb/^{238}U$	± 1 sigma	$^{207}Pb/^{206}Pb$	± 1 sigma	$^{207}Pb/^{235}U$	± 1 sigma	$^{206}Pb/^{238}U$	± 1 sigma	$^{207}Pb/^{206}Pb$	± 1 sigma
					Sample Sol 01							
100910LEPa08	2.5987	0.1238	0.2173	0.0055	0.0867	0.0044	1300.3	34.9	1267.4	29.0	1354.9	97.2
100910LEPa10	1.7154	0.1070	0.1717	0.0050	0.0734	0.0036	1014.3	40.0	1021.5	27.5	1025.5	98.3
100910LEPa11	2.7256	0.1270	0.2271	0.0068	0.0875	0.0024	1335.5	34.6	1319.3	35.7	1371.8	51.8
100910LEPa14	2.1144	0.1108	0.1919	0.0035	0.0845	0.0056	1153.5	36.1	1131.7	19.0	1305.1	128.9
100910LEPa17	3.3203	0.1517	0.2485	0.0082	0.0949	0.0030	1485.8	35.6	1430.7	42.5	1526.5	59.6
100910LEPa18	1.5153	0.0595	0.1508	0.0052	0.0747	0.0014	936.6	24.0	905.2	29.1	1061.3	37.4
100910LEPa20	1.9719	0.1608	0.1963	0.0074	0.0746	0.0033	1106.0	55.0	1155.2	40.1	1057.9	90.3
100910LEPa25	1.6485	0.0802	0.1688	0.0051	0.0734	0.0040	989.0	30.8	1005.3	28.1	1025.5	110.2
100910LEPa26	1.9520	0.0495	0.1912	0.0031	0.0738	0.0024	1099.1	17.0	1127.6	16.7	1036.1	66.0
100910LEPa27	2.0609	0.1264	0.2012	0.0082	0.0748	0.0028	1135.9	41.9	1181.7	44.1	1062.5	76.4
100910LEPa28	3.0505	0.1027	0.2399	0.0077	0.0935	0.0022	1420.4	25.8	1386.2	40.2	1497.7	43.6

100910LEPa30	2.1294	0.0831	0.1905	0.0061	0.0817	0.0018	1158.4	27.0	1123.8	32.9	1237.2	42.7
100910LEPa32	1.7559	0.0850	0.1790	0.0050	0.0726	0.0034	1029.3	31.3	1061.5	27.6	1002.0	94.6
100910LEPa34	1.7071	0.0807	0.1720	0.0053	0.0735	0.0029	1011.2	30.3	1023.0	28.9	1028.3	78.6
100910LEPa35	1.6946	0.1105	0.1699	0.0057	0.0731	0.0028	1006.5	41.7	1011.7	31.2	1017.5	77.0
100910LEPa36	1.9819	0.1283	0.1915	0.0088	0.0762	0.0031	1109.4	43.7	1129.4	47.5	1099.1	81.9
100910LEPa37	0.5762	0.0311	0.0760	0.0017	0.0565	0.0023	462.0	20.1	472.3	10.2	473.8	89.7
100910LEPa38	1.7106	0.0892	0.1696	0.0042	0.0737	0.0033	1012.5	33.4	1009.7	23.0	1034.5	89.3
100910LEPa39	1.8098	0.1079	0.1738	0.0053	0.0761	0.0045	1049.0	39.0	1032.8	29.3	1098.5	117.1
100910LEPa40	1.9415	0.1080	0.1929	0.0058	0.0750	0.0032	1095.5	37.3	1136.9	31.5	1068.1	84.9
100910LEPa49	1.8146	0.0821	0.1773	0.0069	0.0757	0.0027	1050.7	29.6	1052.1	37.9	1086.7	70.7
100910LEPa50	2.1773	0.1065	0.1973	0.0054	0.0806	0.0031	1173.8	34.0	1160.7	28.9	1211.4	75.9
100910LEPa55	2.3110	0.1495	0.2052	0.0085	0.0820	0.0034	1215.7	45.9	1203.1	45.4	1245.6	81.5
100910LEPa56	1.8240	0.0653	0.1734	0.0037	0.0756	0.0024	1054.1	23.5	1030.6	20.4	1084.3	63.0
100910LEPa57	1.6119	0.0515	0.1592	0.0053	0.0742	0.0018	974.9	20.0	952.2	29.4	1045.9	49.7
100910LEPa58	2.6117	0.1071	0.2157	0.0051	0.0859	0.0026	1303.9	30.1	1259.3	27.1	1336.0	59.5
100910LEPa59	1.7902	0.1511	0.1724	0.0112	0.0763	0.0017	1041.9	55.0	1025.1	61.6	1102.0	45.3
100910LEPa60	2.0951	0.0960	0.1870	0.0041	0.0809	0.0035	1147.2	31.5	1105.1	22.1	1218.5	84.3
100910LEPa66	1.9216	0.1362	0.1846	0.0126	0.0749	0.0025	1088.6	47.3	1092.3	68.3	1065.8	67.7
100910LEPa67	1.7315	0.1200	0.1687	0.0054	0.0731	0.0043	1020.3	44.6	1005.1	29.9	1015.5	120.3
100910LEPa68	1.8518	0.1418	0.1715	0.0066	0.0785	0.0057	1064.1	50.5	1020.5	36.2	1160.2	144.7
100910LEPa70	1.6782	0.0680	0.1627	0.0045	0.0748	0.0030	1000.3	25.8	971.5	24.9	1064.2	81.8
100910LEPa71	1.6536	0.1752	0.1573	0.0113	0.0791	0.0101	990.9	67.0	942.0	62.8	1175.8	252.9
100910LEPa72	0.5945	0.0381	0.0748	0.0019	0.0571	0.0031	473.8	24.2	464.7	11.5	493.8	121.6
100910LEPa73	1.9095	0.1060	0.1812	0.0073	0.0765	0.0025	1084.4	37.0	1073.3	40.0	1107.3	65.5
100910LEPa74	1.8380	0.0556	0.1777	0.0042	0.0757	0.0015	1059.1	19.9	1054.6	23.2	1085.9	39.6
100910LEPa75	1.7094	0.0920	0.1610	0.0073	0.0776	0.0024	1012.1	34.5	962.5	40.4	1137.2	60.6
100910LEPa77	1.5573	0.0709	0.1524	0.0054	0.0747	0.0018	953.4	28.1	914.2	30.1	1061.4	49.1
100910LEPa85	0.5753	0.0273	0.0744	0.0016	0.0556	0.0023	461.4	17.6	462.8	9.8	437.2	91.7
100910LEPa86	1.9088	0.0808	0.1851	0.0057	0.0750	0.0022	1084.2	28.2	1094.9	31.1	1068.1	58.9
100910LEPa88	1.8572	0.0707	0.1746	0.0039	0.0771	0.0030	1066.0	25.1	1037.2	21.6	1123.1	78.2
100910LEPa89	2.1732	0.1278	0.1942	0.0069	0.0788	0.0041	1172.5	40.9	1144.1	37.2	1166.2	102.1
100910LEPa90	1.7315	0.1654	0.1671	0.0053	0.0757	0.0065	1020.3	61.5	996.0	29.1	1086.6	172.4
100910LEPa91	2.9913	0.1346	0.2395	0.0095	0.0906	0.0023	1405.4	34.3	1384.2	49.2	1438.1	49.4
100910LEPa92	1.7171	0.0618	0.1725	0.0035	0.0723	0.0018	1014.9	23.1	1026.0	19.3	994.8	51.8

100910LEPa94	0.6295	0.0476	0.0740	0.0026	0.0611	0.0042	495.8	29.6	460.5	15.6	644.4	146.6
100910LEPa97	1.6360	0.0719	0.1664	0.0037	0.0712	0.0029	984.2	27.7	992.2	20.5	963.7	82.3
100910LEPa108	2.1773	0.1594	0.1878	0.0101	0.0838	0.0029	1173.8	50.9	1109.4	54.9	1288.6	67.4
100910LEPa110	1.7254	0.1167	0.1687	0.0070	0.0760	0.0046	1018.0	43.5	1005.1	38.5	1095.2	122.4
100910LEPa111	1.9519	0.0979	0.1840	0.0086	0.0768	0.0044	1099.1	33.7	1088.5	47.0	1116.0	114.0
100910LEPa112	2.7519	0.1106	0.2315	0.0081	0.0854	0.0027	1342.6	29.9	1342.3	42.2	1324.4	61.8
100910LEPa113	2.0876	0.0863	0.2029	0.0051	0.0757	0.0029	1144.7	28.4	1190.7	27.2	1087.1	76.7
100910LEPa114	2.9553	0.1609	0.2536	0.0105	0.0871	0.0033	1396.2	41.3	1457.2	54.2	1361.9	73.9
100910LEPa116	1.7890	0.1722	0.1716	0.0133	0.0755	0.0053	1041.5	62.7	1021.1	73.1	1082.2	142.0
100910LEPa117	1.9867	0.0577	0.1902	0.0041	0.0785	0.0017	1111.0	19.6	1122.5	22.0	1159.4	43.6
100910LEPa119	4.0208	0.1495	0.2917	0.0058	0.1007	0.0032	1638.4	30.2	1650.0	28.9	1637.3	58.6
100910LEPa120	1.9423	0.1012	0.1852	0.0056	0.0763	0.0035	1095.8	34.9	1095.5	30.6	1101.8	92.6
100910LEPa126	1.8217	0.0908	0.1702	0.0044	0.0791	0.0043	1053.3	32.7	1013.5	24.4	1175.7	107.3
100910LEPa127	2.2610	0.1419	0.2075	0.0089	0.0769	0.0028	1200.2	44.2	1215.6	47.4	1118.5	72.2
100910LEPa128	1.8511	0.0817	0.1794	0.0044	0.0757	0.0037	1063.8	29.1	1063.4	24.3	1087.4	96.9
100910LEPa129	2.4024	0.2417	0.2125	0.0065	0.0900	0.0028	1243.3	72.1	1242.3	34.8	1425.6	58.6
100910LEPa130	2.5715	0.1467	0.2139	0.0111	0.0858	0.0021	1292.6	41.7	1249.4	59.0	1333.4	47.7
100910LEPa131	2.0709	0.0524	0.1889	0.0046	0.0792	0.0012	1139.2	17.3	1115.4	24.8	1178.1	29.5
100910LEPa132	0.5145	0.0489	0.0685	0.0027	0.0565	0.0024	421.5	32.8	427.0	16.3	472.8	95.7
100910LEPa133	2.1271	0.1002	0.1936	0.0059	0.0814	0.0035	1157.6	32.5	1140.6	32.0	1231.8	85.1
100910LEPa134	1.9865	0.0717	0.1916	0.0062	0.0788	0.0017	1110.9	24.4	1130.0	33.8	1168.2	42.9
100910LEPa136	2.0746	0.2408	0.1946	0.0072	0.0812	0.0057	1140.4	79.5	1146.1	38.8	1226.6	138.4
100910LEPa137	2.6413	0.1043	0.2215	0.0063	0.0870	0.0033	1312.2	29.1	1290.0	33.2	1360.8	72.9
100910LEPa138	1.6926	0.0966	0.1722	0.0031	0.0715	0.0037	1005.8	36.4	1024.2	17.1	971.1	105.6
100910LEPa139	2.0245	0.1085	0.1931	0.0054	0.0774	0.0033	1123.8	36.4	1138.1	29.3	1132.7	83.8
100910LEPa140	2.8919	0.1654	0.2294	0.0120	0.0935	0.0019	1379.8	43.1	1331.5	62.9	1498.9	38.5
100910LEPa145	1.9465	0.1853	0.1847	0.0125	0.0771	0.0038	1097.2	63.9	1092.6	68.0	1124.7	97.9
100910LEPa147	1.9544	0.1473	0.1850	0.0089	0.0769	0.0063	1099.9	50.6	1094.4	48.6	1118.4	162.7
100910LEPa148	1.5088	0.0805	0.1596	0.0040	0.0792	0.0093	934.0	32.6	954.8	22.2	1176.7	231.7
100910LEPa149	1.9000	0.0603	0.1824	0.0049	0.0762	0.0019	1081.1	21.1	1080.3	26.7	1099.3	49.2
100910LEPa152	1.7489	0.1043	0.1789	0.0080	0.0766	0.0020	1026.8	38.5	1061.0	43.8	1110.4	52.6
100910LEPa153	1.8537	0.0895	0.1857	0.0052	0.0730	0.0029	1064.7	31.9	1098.1	28.1	1013.3	81.8
100910LEPa154	2.9764	0.1463	0.2484	0.0077	0.0864	0.0028	1401.6	37.4	1430.4	39.8	1347.5	61.6
100910LEPa155	0.8408	0.0595	0.1025	0.0028	0.0607	0.0040	619.6	32.8	628.8	16.4	628.4	141.9

100910LEPa160	1.4479	0.1312	0.1518	0.0105	0.0708	0.0022	909.0	54.4	911.0	59.0	952.2	63.3
100910LEPa165	1.8514	0.0987	0.1825	0.0078	0.0748	0.0034	1063.9	35.2	1080.5	42.4	1063.2	92.5
100910LEPa169	2.0769	0.1688	0.1999	0.0079	0.0749	0.0044	1141.2	55.7	1175.0	42.6	1066.3	119.1
100910LEPa171	1.6792	0.0808	0.1686	0.0047	0.0717	0.0029	1000.7	30.6	1004.3	26.1	978.5	82.0
100910LEPa172	1.7974	0.0481	0.1700	0.0041	0.0753	0.0025	1044.5	17.5	1012.0	22.5	1076.6	66.1
100910LEPa175	2.1449	0.1056	0.1868	0.0094	0.0792	0.0044	1163.4	34.1	1104.1	51.1	1177.5	108.9
100910LEPa176	2.2609	0.0705	0.1959	0.0043	0.0830	0.0025	1200.2	22.0	1153.4	23.0	1268.9	59.2
100910LEPa177	1.8169	0.0751	0.1822	0.0039	0.0714	0.0020	1051.6	27.1	1079.1	21.1	967.6	56.3
100910LEPa178	2.7228	0.1030	0.2229	0.0047	0.0860	0.0031	1334.7	28.1	1297.0	24.7	1338.8	69.2
100910LEPa179	1.9076	0.0711	0.1794	0.0044	0.0756	0.0036	1083.8	24.8	1063.7	24.1	1085.4	94.9
100910LEPa187	1.8058	0.1071	0.1682	0.0046	0.0733	0.0043	1047.5	38.8	1002.2	25.2	1021.4	117.7
100910LEPa188	1.7454	0.1831	0.1689	0.0055	0.0729	0.0064	1025.5	67.7	1006.1	30.6	1011.9	176.7
100910LEPa189	1.9548	0.0895	0.1846	0.0050	0.0764	0.0034	1100.1	30.8	1092.0	27.4	1104.7	87.8
100910LEPa190	2.0234	0.0954	0.1851	0.0056	0.0765	0.0035	1123.4	32.0	1094.7	30.5	1107.2	91.7
100910LEPa191	0.5407	0.0463	0.0699	0.0023	0.0555	0.0039	438.9	30.5	435.4	13.8	431.5	156.3
100910LEPa192	1.9318	0.0985	0.1855	0.0035	0.0744	0.0034	1092.2	34.1	1097.2	19.1	1051.1	92.6
100910LEPa193	2.2092	0.0918	0.1961	0.0067	0.0792	0.0020	1184.0	29.0	1154.1	36.2	1177.7	49.3
100910LEPa194	2.0780	0.1191	0.1898	0.0059	0.0757	0.0034	1141.6	39.3	1120.0	32.2	1086.9	88.9
100910LEPa197	4.4742	0.1980	0.2964	0.0102	0.1061	0.0026	1726.2	36.7	1673.4	50.8	1733.2	45.1
100910LEPa198	1.8062	0.1031	0.1739	0.0064	0.0717	0.0042	1047.7	37.3	1033.8	35.0	976.2	120.9
100910LEPa199	1.7925	0.1111	0.1755	0.0057	0.0719	0.0041	1042.8	40.4	1042.5	31.3	983.4	116.7
100910LEPa200	1.7300	0.1382	0.1790	0.0048	0.0712	0.0059	1019.7	51.4	1061.3	26.1	963.4	169.5
100910LEPa205	0.8986	0.0314	0.1007	0.0030	0.0645	0.0023	651.0	16.8	618.7	17.6	759.6	73.8
100910LEPa206	1.6404	0.0980	0.1672	0.0046	0.0724	0.0035	985.9	37.7	996.7	25.7	996.2	97.1
100910LEPa208	2.9980	0.2828	0.2469	0.0134	0.0895	0.0037	1407.1	71.8	1422.6	69.2	1415.5	78.0
100910LEPa209	1.8425	0.0893	0.1740	0.0055	0.0753	0.0037	1060.7	31.9	1033.9	30.0	1076.2	99.6
100910LEPa210	2.1677	0.0854	0.1900	0.0062	0.0839	0.0027	1170.7	27.4	1121.4	33.4	1291.1	62.5
100910LEPa211	3.1227	0.0811	0.2454	0.0048	0.0914	0.0021	1438.3	20.0	1414.8	24.7	1455.9	43.1
100910LEPa216	2.0034	0.0797	0.1858	0.0049	0.0779	0.0027	1116.7	26.9	1098.4	26.6	1144.9	68.8
100910LEPa217	3.9209	0.1975	0.2759	0.0160	0.1013	0.0030	1618.0	40.8	1570.6	81.0	1648.6	55.0
100910LEPa219	2.2443	0.1144	0.1985	0.0057	0.0809	0.0027	1195.0	35.8	1167.1	30.9	1219.1	65.5
100910LEPa227	2.5462	0.1149	0.2209	0.0080	0.0849	0.0020	1285.3	32.9	1286.4	42.4	1313.6	45.6
100910LEPa228	2.0387	0.0712	0.1933	0.0044	0.0784	0.0018	1128.5	23.8	1139.0	23.7	1156.6	44.5
100910LEPa230	2.5551	0.1316	0.2238	0.0106	0.0830	0.0022	1287.9	37.6	1301.7	55.8	1269.5	51.9

100910LEPa231	2.1202	0.0863	0.1899	0.0075	0.0805	0.0019	1155.4	28.1	1120.9	40.8	1209.3	47.4
100910LEPa232	3.2933	0.1177	0.2616	0.0060	0.0927	0.0023	1479.5	27.8	1498.0	30.7	1481.0	47.5
100910LEPa236	2.6912	0.0908	0.2304	0.0060	0.0851	0.0019	1326.0	25.0	1336.6	31.5	1318.7	43.8
100910LEPa237	2.9913	0.1963	0.2402	0.0104	0.0908	0.0029	1405.4	49.9	1387.8	54.0	1442.4	60.2
100910LEPa238	1.8085	0.0823	0.1789	0.0060	0.0758	0.0024	1048.5	29.7	1061.0	32.5	1090.9	62.4
100910LEPa239	1.9059	0.1134	0.1724	0.0039	0.0796	0.0048	1083.2	39.6	1025.1	21.6	1187.0	119.8
100910LEPa240	2.0266	0.1123	0.1830	0.0052	0.0782	0.0031	1124.5	37.7	1083.2	28.6	1151.9	78.1
100910LEPa245	2.9867	0.1337	0.2424	0.0081	0.0901	0.0038	1404.2	34.1	1399.1	42.2	1427.3	80.9
100910LEPa247	1.9007	0.0676	0.1828	0.0036	0.0763	0.0026	1081.3	23.7	1082.1	19.6	1103.6	68.7
100910LEPa249	2.1322	0.0748	0.1944	0.0033	0.0816	0.0027	1159.3	24.2	1145.1	17.7	1236.0	65.3
100910LEPa251	2.3678	0.1112	0.2053	0.0050	0.0812	0.0036	1232.9	33.5	1203.9	27.0	1226.3	86.1
100910LEPa252	2.1190	0.0945	0.1999	0.0057	0.0757	0.0022	1155.0	30.8	1174.6	30.6	1086.8	57.4
100910LEPa254	2.2182	0.1164	0.2012	0.0072	0.0791	0.0022	1186.8	36.7	1182.0	38.5	1174.2	56.0
100910LEPa255	1.7819	0.1202	0.1851	0.0041	0.0694	0.0045	1038.9	43.9	1094.7	22.2	911.5	133.0
100910LEPa256	1.7659	0.2067	0.1695	0.0110	0.0746	0.0035	1033.0	75.9	1009.4	60.4	1056.8	94.3
100910LEPa257	1.9877	0.0717	0.1821	0.0048	0.0778	0.0029	1111.3	24.4	1078.5	26.0	1140.6	74.3
100910LEPa259	1.8268	0.1910	0.1930	0.0062	0.0730	0.0038	1055.1	68.6	1137.5	33.3	1014.0	104.3
100910LEPa263	1.9334	0.1500	0.1818	0.0065	0.0773	0.0050	1092.7	51.9	1076.7	35.3	1127.9	127.9
100910LEPa265	2.1630	0.1322	0.1981	0.0056	0.0771	0.0044	1169.2	42.4	1165.3	30.3	1122.5	113.1

Table 4.

	ISOTOPIC RATIOS						CALCULATED AGES Ma					
Analysis	$^{207}Pb/^{235}U$	± 1 sigma	$^{206}Pb/^{238}U$	± 1 sigma	$^{207}Pb/^{206}Pb$	± 1 sigma	$^{207}Pb/^{235}U$	± 1 sigma	$^{206}Pb/^{238}U$	± 1 sigma	$^{207}Pb/^{206}Pb$	± 1 sigma
	Sample Sol 04											
100305LEPa10	4.5670	0.1813	0.3111	0.0146	0.1069	0.0021	1743.3	33.1	1746.0	71.6	1747.4	35.9
100305LEPa11	4.0897	0.1866	0.2969	0.0113	0.0973	0.0036	1652.2	37.2	1675.9	55.9	1573.5	70.2
100305LEPa13	2.3861	0.2067	0.2152	0.0142	0.0821	0.0035	1238.5	62.0	1256.3	75.4	1248.6	82.5
100305LEPa20	2.1452	0.1053	0.1979	0.0095	0.0801	0.0018	1163.5	34.0	1164.1	51.2	1200.3	43.4
100305LEPa21	3.2090	0.1491	0.2541	0.0119	0.0931	0.0017	1459.3	36.0	1459.8	60.9	1489.1	34.1
100305LEPa23	1.6950	0.0752	0.1703	0.0074	0.0736	0.0019	1006.6	28.3	1013.6	40.6	1031.3	50.9
100305LEPa25	4.0948	0.2048	0.2960	0.0089	0.1063	0.0034	1653.3	40.8	1671.5	44.3	1736.9	58.2
100305LEPa26	2.0699	0.1172	0.1958	0.0100	0.0776	0.0018	1138.9	38.8	1152.8	53.9	1136.5	46.5
100305LEPa28	2.4354	0.1753	0.2192	0.0131	0.0793	0.0024	1253.1	51.8	1277.9	69.4	1180.0	60.0

100305LEPa30	1.8116	0.0811	0.1752	0.0065	0.0761	0.0013	1049.6	29.3	1040.8	35.9	1097.3	34.9
100305LEPa33	1.0741	0.1434	0.1190	0.0082	0.0687	0.0024	740.7	70.2	724.9	47.1	890.3	71.2
100305LEPa34	3.1031	0.2191	0.2491	0.0166	0.0909	0.0022	1433.5	54.2	1433.7	85.5	1444.3	46.3
100305LEPa47	3.1607	0.1655	0.2513	0.0104	0.0928	0.0023	1447.6	40.4	1445.1	53.8	1483.2	47.9
100305LEPa48	1.7930	0.1425	0.1720	0.0071	0.0780	0.0045	1042.9	51.8	1022.9	39.3	1147.6	115.0
100305LEPa49	4.3981	0.1698	0.3095	0.0144	0.1036	0.0020	1712.0	31.9	1738.5	70.9	1690.0	35.8
100305LEPa50	1.8842	0.0931	0.1888	0.0074	0.0745	0.0049	1075.5	32.8	1114.8	40.2	1056.0	131.5
100305LEPa58	2.9317	0.1241	0.2307	0.0075	0.0925	0.0013	1390.1	32.0	1338.3	39.2	1478.6	25.8
100305LEPa60	2.0043	0.1369	0.1810	0.0082	0.0801	0.0036	1117.0	46.3	1072.5	44.5	1199.6	87.6
100305LEPa65	3.2785	0.1380	0.2480	0.0086	0.0950	0.0021	1476.0	32.7	1428.2	44.6	1528.1	41.7
100305LEPa68	1.8966	0.1257	0.1724	0.0081	0.0797	0.0034	1079.9	44.1	1025.6	44.6	1189.3	84.7
100305LEPa74	3.8279	0.2092	0.2690	0.0165	0.1007	0.0018	1598.6	44.0	1535.8	84.0	1637.1	33.3
100305LEPa76	2.4046	0.2052	0.2079	0.0167	0.0837	0.0023	1244.0	61.2	1217.7	89.4	1285.0	53.1
100305LEPa77	4.2672	0.2447	0.2874	0.0161	0.1081	0.0014	1687.1	47.2	1628.5	80.6	1767.1	23.7
100305LEPa80	2.2427	0.1250	0.2028	0.0106	0.0798	0.0011	1194.5	39.1	1190.1	56.9	1192.1	27.1
100305LEPa82	1.8339	0.1496	0.1731	0.0087	0.0759	0.0031	1057.7	53.6	1029.2	47.9	1092.5	81.6
100305LEPa83	3.1063	0.2647	0.2386	0.0165	0.0985	0.0017	1434.3	65.4	1379.4	86.1	1595.1	32.1
100305LEPa89	2.7152	0.2071	0.2180	0.0168	0.0912	0.0021	1332.6	56.6	1271.3	89.2	1451.4	44.7
100305LEPa92	2.0642	0.1455	0.1869	0.0112	0.0795	0.0022	1137.0	48.2	1104.3	60.6	1184.5	54.3
100305LEPa95	1.8584	0.1511	0.1772	0.0100	0.0791	0.0033	1066.4	53.7	1051.7	55.0	1174.4	82.4
100305LEPa96	1.8500	0.1248	0.1678	0.0092	0.0785	0.0021	1063.4	44.5	1000.1	50.8	1160.0	52.6
100305LEPa98	1.9132	0.2327	0.1648	0.0112	0.0836	0.0058	1085.7	81.1	983.5	62.3	1283.8	135.8
100305LEPa99	1.8818	0.1757	0.1734	0.0131	0.0790	0.0021	1074.7	61.9	1030.8	72.1	1171.7	52.8
100305LEPa101	2.2171	0.0674	0.2099	0.0064	0.0771	0.0013	1186.4	21.3	1228.4	34.3	1123.8	34.2
100305LEPa109	2.0710	0.1755	0.1968	0.0127	0.0755	0.0026	1139.3	58.0	1158.3	68.7	1082.5	68.1
100305LEPa110	2.1770	0.1338	0.2005	0.0082	0.0795	0.0033	1173.7	42.7	1178.1	43.9	1185.7	82.7
100305LEPa111	1.6959	0.0915	0.1648	0.0061	0.0756	0.0029	1007.0	34.4	983.5	33.8	1085.6	77.7
100305LEPa114	1.9187	0.1673	0.1907	0.0116	0.0735	0.0018	1087.6	58.2	1125.3	62.8	1026.9	50.5
100305LEPa115	1.8698	0.0877	0.1804	0.0074	0.0756	0.0018	1070.4	31.0	1069.3	40.4	1084.4	46.6
100305LEPa116	3.1113	0.2024	0.2500	0.0143	0.0907	0.0016	1435.5	50.0	1438.5	73.9	1440.9	33.3
100305LEPa117	1.7709	0.1713	0.1803	0.0129	0.0719	0.0022	1034.9	62.8	1068.4	70.4	983.8	61.5
100305LEPa119	1.7923	0.1597	0.1827	0.0105	0.0733	0.0020	1042.6	58.1	1081.9	57.3	1021.7	55.2
100305LEPa120	2.3302	0.1244	0.2083	0.0084	0.0804	0.0023	1221.5	37.9	1219.8	44.7	1206.6	55.8
100305LEPa121	1.7600	0.1842	0.1745	0.0162	0.0729	0.0018	1030.9	67.8	1037.1	88.8	1012.1	51.1

100305LEPa124	2.9954	0.2224	0.2433	0.0190	0.0889	0.0023	1406.5	56.5	1403.8	98.4	1402.5	49.0
100305LEPa126	4.0444	0.2053	0.2810	0.0173	0.1041	0.0029	1643.2	41.3	1596.4	87.1	1698.2	52.0
100305LEPa127	2.1148	0.1344	0.1943	0.0080	0.0775	0.0028	1153.6	43.8	1144.6	43.4	1134.8	73.1
100305LEPa128	3.6829	0.2589	0.2817	0.0170	0.0982	0.0018	1567.7	56.1	1600.0	85.6	1590.0	33.8
100305LEPa130	3.3026	0.1743	0.2586	0.0130	0.0922	0.0027	1481.7	41.1	1482.7	66.4	1471.3	55.4
100305LEPa131	1.7035	0.1024	0.1759	0.0079	0.0714	0.0043	1009.8	38.5	1044.7	43.4	969.0	124.3
100305LEPa133	1.8398	0.1821	0.1829	0.0130	0.0725	0.0036	1059.8	65.1	1082.7	71.1	998.9	101.1
100305LEPa134	1.6412	0.1158	0.1756	0.0073	0.0688	0.0026	986.2	44.5	1043.0	40.0	893.5	76.7
100305LEPa136	2.1817	0.1486	0.2108	0.0171	0.0733	0.0046	1175.2	47.4	1233.0	91.2	1022.8	126.8

Table 5.

	ISOTOPIC RATIOS						CALCULATED AGES Ma					
Analysis	$^{207}Pb/^{235}U$	± 1 sigma	$^{206}Pb/^{238}U$	± 1 sigma	$^{207}Pb/^{206}Pb$	± 1 sigma	$^{207}Pb/^{235}U$	± 1 sigma	$^{206}Pb/^{238}U$	± 1 sigma	$^{207}Pb/^{206}Pb$	± 1 sigma
					Sample Hest 03							
100909LEPa08	3.9462	0.3112	0.2801	0.0157	0.1010	0.0037	1623.2	63.9	1591.8	79.0	1643.5	68.2
100909LEPa10	1.6803	0.2183	0.1696	0.0148	0.0742	0.0032	1001.1	82.7	1009.9	81.3	1047.2	86.5
100909LEPa12	3.6942	0.2403	0.2701	0.0169	0.0988	0.0019	1570.1	52.0	1541.2	85.7	1600.7	36.7
100909LEPa14	0.4612	0.0789	0.0605	0.0059	0.0572	0.0031	385.1	54.8	378.7	36.1	497.9	118.3
100909LEPa18	1.7481	0.0641	0.1721	0.0066	0.0737	0.0014	1026.5	23.7	1023.5	36.0	1032.1	37.3
100909LEPa25	3.5669	0.2525	0.2655	0.0156	0.1001	0.0021	1542.2	56.1	1518.1	79.7	1626.0	38.2
100909LEPa27	3.7960	0.2995	0.2727	0.0151	0.1012	0.0037	1591.9	63.4	1554.3	76.3	1646.1	68.4
100909LEPa28	2.0950	0.2401	0.1930	0.0137	0.0792	0.0036	1147.2	78.8	1137.4	74.0	1175.9	89.5
100909LEPa33	3.5747	0.1294	0.2635	0.0105	0.0989	0.0022	1543.9	28.7	1507.5	53.4	1603.5	41.0
100909LEPa34	4.0385	0.1323	0.2889	0.0081	0.1000	0.0019	1642.0	26.7	1635.9	40.4	1624.9	36.1
100909LEPa35	1.8139	0.1181	0.1722	0.0093	0.0742	0.0043	1050.5	42.6	1024.5	51.4	1047.9	116.9
100909LEPa36	2.3479	0.1112	0.2072	0.0072	0.0818	0.0027	1226.9	33.7	1213.9	38.4	1240.9	63.6
100909LEPa39	1.7231	0.1502	0.1670	0.0067	0.0737	0.0039	1017.2	56.0	995.5	36.8	1034.2	105.7
100909LEPa40	3.9379	0.1255	0.2854	0.0078	0.1007	0.0015	1621.5	25.8	1618.5	39.3	1637.9	27.8
100909LEPa45	3.7287	0.2075	0.2667	0.0151	0.1012	0.0022	1577.6	44.6	1524.2	76.7	1645.6	39.8
100909LEPa46	3.4662	0.3201	0.2655	0.0163	0.0952	0.0036	1519.6	72.8	1518.0	82.9	1531.5	71.4
100909LEPa47	4.0212	0.2234	0.2915	0.0139	0.1011	0.0020	1638.5	45.2	1649.2	69.2	1644.9	37.2
100909LEPa48	0.5247	0.0234	0.0673	0.0017	0.0568	0.0028	428.3	15.6	419.7	10.3	484.0	108.8
100909LEPa49	3.8995	0.1895	0.2788	0.0137	0.1019	0.0032	1613.6	39.3	1585.3	69.3	1659.8	58.5

100909LEPa51	4.4144	0.1856	0.3034	0.0111	0.1043	0.0038	1715.0	34.8	1708.0	54.8	1701.7	67.4
100909LEPa57	4.2260	0.1417	0.2930	0.0080	0.1024	0.0019	1679.1	27.5	1656.5	39.7	1668.7	34.4
100909LEPa59	3.6435	0.1869	0.2656	0.0115	0.0999	0.0023	1559.1	40.9	1518.2	58.7	1622.4	42.3
100909LEPa65	3.9302	0.1599	0.2829	0.0098	0.1009	0.0021	1619.9	32.9	1605.8	49.1	1640.0	38.8
100909LEPa66	4.2151	0.2009	0.2977	0.0139	0.1016	0.0030	1677.0	39.1	1680.1	69.2	1653.5	54.2
100909LEPa70	3.7869	0.1187	0.2785	0.0076	0.0987	0.0019	1590.0	25.2	1583.8	38.2	1600.3	36.8
100909LEPa73	3.9645	0.3450	0.2739	0.0111	0.1010	0.0043	1627.0	70.6	1560.4	56.0	1642.6	79.2
100909LEPa74	3.9169	0.1567	0.2846	0.0099	0.1006	0.0018	1617.2	32.3	1614.3	49.7	1634.5	33.9
100909LEPa80	4.1595	0.2107	0.2956	0.0091	0.1015	0.0039	1666.1	41.5	1669.5	45.4	1652.5	71.9
100909LEPa92	3.8569	0.1878	0.2828	0.0123	0.1006	0.0021	1604.7	39.3	1605.5	62.0	1635.4	39.6
100909LEPa96	1.9952	0.1083	0.1838	0.0069	0.0791	0.0031	1113.9	36.7	1087.5	37.8	1175.7	77.3
100909LEPa98	3.8542	0.1972	0.2762	0.0117	0.0997	0.0027	1604.2	41.3	1572.2	59.0	1618.8	49.7
100909LEPa99	3.6469	0.2169	0.2685	0.0133	0.0982	0.0025	1559.8	47.4	1533.1	67.7	1590.7	47.0
100909LEPa105	2.7871	0.1572	0.2299	0.0061	0.0860	0.0050	1352.1	42.2	1334.2	31.8	1338.0	111.8
100909LEPa108	2.9306	0.1206	0.2328	0.0081	0.0916	0.0025	1389.8	31.2	1349.2	42.2	1459.3	51.8
100909LEPa110	3.7088	0.1922	0.2770	0.0083	0.0982	0.0043	1573.3	41.4	1576.4	42.1	1590.6	82.3
100909LEPa116	3.9746	0.1328	0.2819	0.0095	0.1021	0.0028	1629.0	27.1	1600.8	47.8	1663.5	50.2
100909LEPa118	0.6190	0.0495	0.0723	0.0022	0.0598	0.0043	489.2	31.1	450.2	13.5	595.4	156.4
100909LEPa119	4.2002	0.1502	0.3043	0.0096	0.1072	0.0064	1674.1	29.3	1712.4	47.3	1751.6	108.9
100909LEPa127	3.6258	0.1358	0.2703	0.0073	0.0983	0.0022	1555.2	29.8	1542.1	37.2	1591.4	41.7
100909LEPa135	3.6004	0.1633	0.2683	0.0105	0.0996	0.0026	1549.6	36.0	1532.4	53.2	1616.4	48.7
100909LEPa146	3.7249	0.2639	0.2756	0.0159	0.1000	0.0022	1576.7	56.7	1569.0	80.6	1624.7	41.1
100909LEPa148	3.9272	0.1201	0.2810	0.0101	0.0988	0.0022	1619.3	24.7	1596.5	50.9	1601.4	42.4
100909LEPa150	1.7171	0.1897	0.1700	0.0094	0.0742	0.0043	1014.9	70.9	1012.3	51.8	1046.8	116.5
100909LEPa166	1.9024	0.1886	0.1766	0.0102	0.0785	0.0036	1081.9	66.0	1048.6	55.7	1160.7	91.8
100909LEPa174	3.6725	0.1754	0.2790	0.0086	0.0972	0.0041	1565.4	38.1	1586.2	43.3	1571.9	79.3
100909LEPa176	4.2720	0.1601	0.2995	0.0101	0.1042	0.0034	1688.0	30.8	1688.7	50.2	1700.9	60.0
100909LEPa177	4.0563	0.1826	0.2877	0.0101	0.1023	0.0029	1645.6	36.7	1629.9	50.3	1665.8	53.1
100909LEPa199	4.0726	0.1227	0.2898	0.0086	0.1012	0.0018	1648.8	24.6	1640.8	43.2	1646.2	32.8
100909LEPa206	4.0767	0.1057	0.2880	0.0058	0.1021	0.0019	1649.7	21.1	1631.8	29.2	1663.4	34.6
100909LEPa207	4.0427	0.1895	0.2900	0.0080	0.1019	0.0038	1642.8	38.2	1641.8	40.1	1658.5	69.6
100909LEPa208	4.5017	0.3236	0.3191	0.0169	0.1037	0.0044	1731.3	59.7	1785.4	82.8	1691.9	77.4
100909LEPa212	4.0460	0.1355	0.2843	0.0076	0.1037	0.0024	1643.5	27.3	1612.9	38.1	1691.0	43.0
100909LEPa213	4.3560	0.1710	0.3093	0.0109	0.1027	0.0020	1704.0	32.4	1737.2	53.4	1673.8	35.6

100909LEPa214	3.4092	0.1795	0.2567	0.0101	0.0956	0.0034	1506.5	41.3	1473.2	51.6	1540.9	67.0
100909LEPa215	2.4740	0.1568	0.2188	0.0097	0.0804	0.0058	1264.5	45.8	1275.4	51.5	1205.6	143.2
100909LEPa216	3.7453	0.2085	0.2742	0.0114	0.1006	0.0033	1581.1	44.6	1562.2	57.8	1635.9	61.3
100909LEPa217	4.1310	0.2355	0.2892	0.0141	0.1046	0.0023	1660.5	46.6	1637.3	70.3	1707.6	40.7
100909LEPa220	4.1698	0.1800	0.2917	0.0132	0.1043	0.0021	1668.1	35.4	1650.1	66.1	1701.6	36.7
100909LEPa223	4.1852	0.1193	0.2970	0.0088	0.1041	0.0021	1671.1	23.4	1676.6	44.0	1699.1	37.7
100909LEPa224	2.5996	0.1645	0.2283	0.0111	0.0826	0.0041	1300.5	46.4	1325.8	58.5	1259.2	96.4
100909LEPa225	3.9064	0.1889	0.2821	0.0126	0.1032	0.0025	1615.0	39.1	1602.2	63.2	1682.3	45.2
100909LEPa226	4.2385	0.1531	0.2921	0.0082	0.1060	0.0024	1681.5	29.7	1652.1	40.8	1731.5	41.1
100909LEPa227	4.0169	0.1694	0.2840	0.0097	0.1037	0.0031	1637.6	34.3	1611.5	48.7	1691.0	54.8
100909LEPa228	4.1541	0.2163	0.2867	0.0134	0.1061	0.0041	1665.0	42.6	1625.0	67.2	1732.8	70.5

Table 6.

	ISOTOPIC RATIOS						CALCULATED AGES Ma					
Analysis	$^{207}Pb/^{235}U$	± 1 sigma	$^{206}Pb/^{238}U$	± 1 sigma	$^{207}Pb/^{206}Pb$	± 1 sigma	$^{207}Pb/^{235}U$	± 1 sigma	$^{206}Pb/^{238}U$	± 1 sigma	$^{207}Pb/^{206}Pb$	± 1 sigma
					Sample Hest 04							
100908LEPa12	2.6893	0.1788	0.2226	0.0090	0.0872	0.0039	1325.5	49.2	1295.6	47.5	1364.3	85.5
100908LEPa17	3.9522	0.1532	0.2825	0.0133	0.1039	0.0043	1624.5	31.4	1604.1	66.7	1695.4	76.4
100908LEPa19	3.1382	0.2743	0.2538	0.0133	0.0958	0.0037	1442.1	67.3	1458.2	68.5	1543.5	73.4
100908LEPa21	3.5653	0.2617	0.2644	0.0154	0.0967	0.0025	1541.8	58.2	1512.2	78.7	1561.6	47.7
100908LEPa22	3.0400	0.1891	0.2376	0.0122	0.0932	0.0047	1417.7	47.5	1374.3	63.7	1491.1	95.0
100908LEPa27	3.9490	0.0789	0.2848	0.0046	0.1033	0.0017	1623.8	16.2	1615.3	22.9	1683.9	31.0
100908LEPa28	3.7753	0.1269	0.2743	0.0063	0.1002	0.0021	1587.5	27.0	1562.4	31.8	1628.7	39.1
100908LEPa29	3.6808	0.1012	0.2698	0.0071	0.1009	0.0015	1567.2	21.9	1539.5	36.0	1641.3	28.3
100908LEPa30	3.8356	0.1352	0.2902	0.0069	0.0976	0.0028	1600.2	28.4	1642.4	34.6	1578.3	54.2
100908LEPa31	3.4536	0.1637	0.2573	0.0098	0.0986	0.0028	1516.7	37.3	1475.9	50.4	1597.9	52.3
100908LEPa33	3.9598	0.1106	0.2814	0.0081	0.1039	0.0025	1626.0	22.6	1598.3	40.8	1695.2	44.9
100908LEPa37	4.1225	0.1451	0.2911	0.0083	0.1029	0.0024	1658.8	28.8	1647.1	41.4	1677.3	42.7
100908LEPa40	3.7436	0.2231	0.2707	0.0117	0.0998	0.0035	1580.7	47.8	1544.2	59.5	1619.6	65.3
100908LEPa46	3.5906	0.1497	0.2700	0.0099	0.0976	0.0026	1547.4	33.1	1540.7	50.0	1577.8	49.3
100908LEPa48	3.0738	0.1359	0.2493	0.0074	0.0912	0.0026	1426.2	33.9	1434.8	38.3	1451.5	53.7
100908LEPa49	1.6609	0.1297	0.1652	0.0114	0.0734	0.0039	993.7	49.5	985.6	63.2	1024.2	106.8
100908LEPa68	3.7953	0.1331	0.2731	0.0087	0.1010	0.0022	1591.7	28.2	1556.6	43.9	1642.7	39.8

100908LEPa69	4.0804	0.1645	0.2880	0.0092	0.1009	0.0018	1650.4	32.9	1631.4	46.1	1640.4	33.8
100908LEPa70	1.8649	0.0920	0.1750	0.0076	0.0761	0.0031	1068.7	32.6	1039.8	41.9	1098.1	81.4
100908LEPa73	3.9072	0.0900	0.2756	0.0050	0.1023	0.0019	1615.2	18.6	1569.0	25.1	1666.7	34.3
100908LEPa74	3.7808	0.1353	0.2748	0.0086	0.0999	0.0018	1588.7	28.7	1565.1	43.6	1621.9	33.5
100908LEPa77	3.0796	0.2118	0.2401	0.0113	0.0955	0.0023	1427.6	52.7	1387.1	58.5	1537.1	45.6
100908LEPa79	3.8467	0.1487	0.2758	0.0071	0.1017	0.0025	1602.6	31.2	1570.2	35.8	1654.6	45.7
100908LEPa80	2.5749	0.2950	0.2241	0.0092	0.0873	0.0058	1293.5	83.8	1303.5	48.2	1366.1	128.3
100908LEPa87	3.9051	0.2219	0.2758	0.0134	0.0996	0.0047	1614.7	45.9	1570.2	67.5	1617.3	86.9
100908LEPa89	4.1234	0.1203	0.2939	0.0076	0.1010	0.0023	1658.9	23.8	1661.0	37.7	1642.6	42.5
100908LEPa90	3.3521	0.1381	0.2563	0.0072	0.0959	0.0023	1493.3	32.2	1471.1	36.8	1546.3	44.2
100908LEPa91	3.5897	0.1621	0.2609	0.0102	0.1022	0.0022	1547.3	35.9	1494.6	52.3	1663.9	39.3
100908LEPa92	3.7494	0.0877	0.2722	0.0059	0.0995	0.0014	1582.0	18.8	1552.0	29.8	1614.0	26.6
100908LEPa93	3.1233	0.2288	0.2451	0.0124	0.0938	0.0030	1438.4	56.4	1413.0	64.2	1503.9	61.3
100908LEPa96	3.5916	0.1211	0.2578	0.0077	0.1001	0.0019	1547.7	26.8	1478.3	39.5	1626.5	35.2
100908LEPa105	3.7389	0.1417	0.2680	0.0086	0.1005	0.0034	1579.7	30.4	1530.6	43.7	1633.9	63.6
100908LEPa109	3.5527	0.1783	0.2581	0.0117	0.0971	0.0023	1539.0	39.8	1480.1	59.7	1569.1	44.6
100908LEPa110	3.3119	0.2427	0.2506	0.0110	0.0967	0.0039	1483.9	57.2	1441.6	56.7	1561.6	76.2
100908LEPa127	3.3551	0.1645	0.2586	0.0099	0.0931	0.0029	1494.0	38.4	1482.6	50.9	1489.2	59.7
100908LEPa128	4.0175	0.2108	0.2931	0.0166	0.1007	0.0016	1637.8	42.7	1657.1	82.6	1638.0	30.2
100908LEPa132	3.7773	0.1382	0.2776	0.0111	0.0983	0.0017	1587.9	29.4	1579.3	56.1	1591.5	32.4
100908LEPa134	3.0243	0.1897	0.2385	0.0114	0.0934	0.0035	1413.8	47.9	1378.7	59.1	1495.7	70.5
100908LEPa136	3.5470	0.1664	0.2676	0.0098	0.0968	0.0026	1537.8	37.2	1528.6	49.9	1563.2	49.9
100908LEPa137	4.1645	0.1488	0.3004	0.0099	0.1012	0.0020	1667.1	29.3	1693.3	49.1	1645.8	35.8
100908LEPa150	3.0862	0.1994	0.2462	0.0097	0.0923	0.0051	1429.3	49.6	1418.7	50.0	1474.3	104.7
100908LEPa151	3.4751	0.1187	0.2746	0.0064	0.0918	0.0020	1521.6	26.9	1564.2	32.5	1464.2	41.9
100908LEPa154	3.8909	0.1077	0.2820	0.0077	0.1015	0.0015	1611.8	22.4	1601.2	38.9	1651.0	27.0
100908LEPa156	1.5147	0.0421	0.1521	0.0044	0.0722	0.0011	936.3	17.0	912.6	24.4	991.5	31.5
100908LEPa158	1.5789	0.1320	0.1575	0.0059	0.0741	0.0051	962.0	52.0	943.1	33.0	1043.9	139.7
100908LEPa165	4.5004	0.2492	0.2997	0.0111	0.1032	0.0027	1731.0	46.0	1689.9	55.1	1683.1	47.8
100908LEPa167	3.8313	0.2302	0.2719	0.0069	0.1021	0.0030	1599.3	48.4	1550.5	35.1	1661.9	55.2
100908LEPa173	3.2828	0.2172	0.2488	0.0108	0.0964	0.0035	1477.0	51.5	1432.2	55.9	1556.5	68.4
100908LEPa180	3.6952	0.1503	0.2677	0.0083	0.1005	0.0019	1570.3	32.5	1529.2	42.2	1634.0	34.8
100908LEPa188	3.9460	0.0670	0.2819	0.0056	0.1025	0.0014	1623.2	13.8	1601.1	28.2	1670.6	25.1
100908LEPa190	3.7305	0.1808	0.2709	0.0117	0.1014	0.0030	1577.9	38.8	1545.1	59.3	1650.6	54.3

100908LEPa191	1.7633	0.0956	0.1679	0.0047	0.0757	0.0040	1032.1	35.1	1000.7	26.0	1088.0	104.7
100908LEPa200	2.0681	0.0960	0.1850	0.0073	0.0821	0.0021	1138.3	31.8	1094.2	39.7	1247.7	49.7
100908LEPa206	3.8067	0.1022	0.2799	0.0063	0.0996	0.0020	1594.2	21.6	1590.6	31.7	1616.9	36.7
100908LEPa216	3.8136	0.0838	0.2767	0.0058	0.0987	0.0016	1595.6	17.7	1574.6	29.4	1599.0	29.9
100908LEPa218	3.5029	0.1849	0.2596	0.0105	0.0972	0.0017	1527.9	41.7	1487.9	53.5	1570.9	32.0
100908LEPa220	1.5686	0.1013	0.1654	0.0086	0.0687	0.0032	957.9	40.0	986.8	47.4	888.8	95.2
100908LEPa229	3.3847	0.1595	0.2605	0.0072	0.0946	0.0052	1500.9	36.9	1492.6	36.8	1520.1	103.6
100908LEPa232	3.6664	0.1162	0.2671	0.0071	0.0993	0.0013	1564.1	25.3	1525.9	36.1	1611.0	24.6
100908LEPa235	1.9479	0.1279	0.1797	0.0069	0.0797	0.0030	1097.7	44.0	1065.1	37.6	1188.5	73.3
100908LEPa237	3.8708	0.1192	0.2745	0.0064	0.0998	0.0016	1607.6	24.8	1563.8	32.1	1619.5	30.2
100908LEPa238	3.6326	0.1810	0.2686	0.0101	0.0998	0.0028	1556.7	39.7	1533.5	51.2	1620.3	51.9
100908LEPa239	3.7422	0.1188	0.2797	0.0094	0.0999	0.0022	1580.5	25.4	1590.0	47.4	1622.5	41.0

Table 7.

	ISOTOPIC RATIOS						CALCULATED AGES Ma					
Analysis	$^{207}Pb/^{235}U$	± 1 sigma	$^{206}Pb/^{238}U$	± 1 sigma	$^{207}Pb/^{206}Pb$	± 1 sigma	$^{207}Pb/^{235}U$	± 1 sigma	$^{206}Pb/^{238}U$	± 1 sigma	$^{207}Pb/^{206}Pb$	± 1 sigma
					Sample Horn 02							
110201LEPa012	4.3167	0.2376	0.3010	0.0097	0.1030	0.0049	1696.6	45.4	1696.3	48.1	1679.6	87.4
110201LEPa016	2.0866	0.2604	0.1905	0.0069	0.0808	0.0104	1144.4	85.6	1124.0	37.5	1217.3	253.8
110201LEPa017	1.7538	0.2113	0.1639	0.0146	0.0767	0.0045	1028.6	77.9	978.3	80.8	1114.5	117.3
110201LEPa030	3.7320	0.1370	0.2694	0.0077	0.0991	0.0031	1578.3	29.4	1537.6	39.2	1607.2	58.9
110201LEPa036	0.5846	0.0603	0.0742	0.0038	0.0565	0.0055	467.4	38.6	461.1	22.5	473.1	217.1
110201LEPa038	0.6465	0.0594	0.0744	0.0044	0.0630	0.0035	506.3	36.6	462.4	26.6	707.7	118.5
110201LEPa039	0.5353	0.0481	0.0674	0.0021	0.0581	0.0040	435.3	31.8	420.3	12.5	532.1	151.3
110201LEPa040	1.7373	0.0988	0.1666	0.0056	0.0758	0.0041	1022.5	36.7	993.3	31.0	1089.9	107.3
110201LEPa045	2.2754	0.2698	0.1981	0.0183	0.0853	0.0060	1204.7	83.7	1165.2	98.4	1322.7	136.6
110201LEPa047	0.6947	0.0749	0.0788	0.0030	0.0627	0.0055	535.6	44.9	489.0	18.1	698.3	185.3
110201LEPa050	1.4307	0.1471	0.1547	0.0064	0.0686	0.0073	901.8	61.4	927.2	35.9	886.4	220.8
110201LEPa054	0.5030	0.0520	0.0737	0.0030	0.0545	0.0059	413.8	35.1	458.3	17.7	390.9	242.9
110201LEPa055	3.6611	0.2138	0.2887	0.0137	0.0989	0.0036	1562.9	46.6	1634.8	68.7	1603.4	68.2
110201LEPa057	0.5953	0.0483	0.0749	0.0023	0.0636	0.0053	474.3	30.7	465.6	13.8	729.0	176.8
110201LEPa060	1.7014	0.0835	0.1754	0.0100	0.0746	0.0038	1009.1	31.4	1042.1	55.0	1056.5	102.6
110201LEPa066	3.0777	0.1591	0.2478	0.0116	0.0956	0.0036	1427.2	39.6	1427.2	59.8	1539.9	71.7

110201LEPa073	0.5793	0.0433	0.0823	0.0063	0.0566	0.0028	464.0	27.8	509.7	37.7	476.5	108.2
110201LEPa074	2.0783	0.1417	0.1982	0.0084	0.0786	0.0025	1141.7	46.7	1165.9	45.1	1162.1	64.3
110201LEPa088	3.7423	0.1957	0.2906	0.0168	0.0970	0.0035	1580.5	41.9	1644.7	83.9	1567.4	67.2
110201LEPa094	3.1988	0.2524	0.2621	0.0110	0.0970	0.0057	1456.9	61.0	1500.3	56.0	1566.6	110.3
110201LEPa105	4.3684	0.2522	0.3132	0.0118	0.1033	0.0048	1706.4	47.7	1756.4	57.8	1683.5	86.5
110201LEPa106	3.2077	0.1562	0.2469	0.0093	0.0952	0.0034	1459.0	37.7	1422.5	47.9	1532.5	67.8
110201LEPa109	2.8984	0.1504	0.2326	0.0067	0.0907	0.0038	1381.5	39.2	1348.2	34.8	1439.9	79.9
110201LEPa111	3.9133	0.2172	0.2934	0.0121	0.0976	0.0030	1616.4	44.9	1658.7	60.4	1579.0	56.6
110201LEPa114	3.9995	0.2429	0.2979	0.0128	0.0993	0.0048	1634.1	49.3	1680.6	63.5	1611.7	90.1
110201LEPa119	4.0226	0.2334	0.2955	0.0103	0.1015	0.0044	1638.8	47.2	1669.1	51.1	1651.7	80.8
110201LEPa127	3.5697	0.1853	0.2642	0.0101	0.0974	0.0035	1542.8	41.2	1511.5	51.5	1574.1	68.2
110201LEPa128	1.4987	0.1135	0.1584	0.0060	0.0697	0.0052	929.9	46.1	947.8	33.4	919.1	152.5
110201LEPa129	3.1821	0.3215	0.2413	0.0189	0.0935	0.0028	1452.8	78.1	1393.3	98.2	1498.2	55.9
110201LEPa130	3.7315	0.1332	0.2751	0.0089	0.0985	0.0041	1578.2	28.6	1566.4	45.2	1596.7	77.2
110201LEPa131	3.8928	0.1868	0.2861	0.0087	0.0974	0.0037	1612.2	38.8	1621.8	43.5	1574.2	71.7
110201LEPa133	0.7077	0.0457	0.0866	0.0031	0.0594	0.0038	543.4	27.2	535.4	18.5	583.2	140.1
110201LEPa135	2.1003	0.1164	0.1888	0.0072	0.0809	0.0038	1148.9	38.1	1114.7	39.1	1220.2	91.4
110201LEPa140	3.2672	0.1667	0.2611	0.0079	0.0880	0.0044	1473.3	39.7	1495.6	40.6	1381.9	95.8
110415aLEP009	4.2217	0.1089	0.2937	0.0072	0.1042	0.0015	1678.2	43.3	1660.1	40.8	1701.1	26.1
110415aLEP010	0.4896	0.0378	0.0676	0.0019	0.0525	0.0012	404.6	31.2	421.6	11.8	309.0	53.0
110415aLEP013	2.2803	0.0802	0.2031	0.0065	0.0814	0.0011	1206.2	42.4	1191.9	38.4	1232.0	27.5
110415aLEP014	2.2422	0.0598	0.2051	0.0044	0.0793	0.0012	1194.3	31.9	1202.8	26.1	1179.1	29.4
110415aLEP016	0.5630	0.0211	0.0754	0.0018	0.0541	0.0007	453.5	17.0	468.8	11.3	376.6	30.1
110415aLEP017	2.6955	0.1022	0.2260	0.0077	0.0865	0.0013	1327.2	50.3	1313.7	44.6	1349.1	28.0
110415aLEP018	3.8959	0.1572	0.2769	0.0091	0.1020	0.0014	1612.8	65.1	1575.7	52.0	1661.6	25.4
110415aLEP025	0.7325	0.0930	0.0875	0.0044	0.0607	0.0016	558.0	70.9	540.9	27.4	628.5	56.5
110415aLEP026	1.6415	0.0470	0.1655	0.0041	0.0719	0.0010	986.3	28.3	987.5	24.6	983.5	28.4
110415aLEP030	4.2119	0.1239	0.2956	0.0086	0.1033	0.0015	1676.3	49.3	1669.6	48.4	1684.8	26.9
110415aLEP033	4.3474	0.1236	0.3092	0.0076	0.1020	0.0014	1702.4	48.4	1736.6	42.5	1660.6	25.2
110415aLEP034	2.8353	0.0905	0.2257	0.0059	0.0911	0.0012	1364.9	43.6	1311.8	34.1	1449.1	25.5
110415aLEP035	3.9871	0.1845	0.2757	0.0126	0.1049	0.0015	1631.6	75.5	1569.5	71.6	1712.6	27.1
110415aLEP036	2.0694	0.1065	0.1928	0.0051	0.0778	0.0020	1138.7	58.6	1136.7	30.0	1142.6	52.2
110415aLEP038	3.2916	0.1040	0.2608	0.0062	0.0915	0.0014	1479.1	46.7	1494.1	35.3	1457.6	28.1
110415aLEP040	4.4691	0.1976	0.3058	0.0127	0.1060	0.0015	1725.3	76.3	1720.0	71.4	1731.6	26.1

110415aLEP045	4.0057	0.1726	0.2925	0.0116	0.0993	0.0013	1635.4	70.5	1654.0	65.6	1611.4	25.2
110415aLEP047	4.0390	0.1797	0.2921	0.0074	0.1003	0.0015	1642.1	73.0	1651.9	42.1	1629.5	26.9
110415aLEP049	0.5785	0.0193	0.0734	0.0017	0.0572	0.0012	463.5	15.5	456.3	10.4	499.2	44.9
110415aLEP065	0.6298	0.0321	0.0805	0.0023	0.0568	0.0012	496.0	25.3	498.9	14.3	482.2	46.6
110415aLEP066	1.0233	0.1108	0.1166	0.0089	0.0636	0.0008	715.6	77.5	711.0	54.2	729.9	28.2
110415aLEP070	0.5079	0.0269	0.0651	0.0021	0.0566	0.0007	417.1	22.1	406.6	13.3	475.2	26.2
110415aLEP072	1.9992	0.1435	0.1933	0.0072	0.0750	0.0012	1115.3	80.1	1139.2	42.4	1069.0	31.0
110415aLEP076	1.9041	0.1452	0.1770	0.0056	0.0780	0.0011	1082.5	82.6	1050.7	33.2	1147.1	28.8
110415aLEP080	3.3959	0.1327	0.2601	0.0079	0.0947	0.0013	1503.4	58.8	1490.5	45.2	1521.7	25.3
110415aLEP098	4.1257	0.1145	0.2949	0.0045	0.1015	0.0013	1659.4	46.0	1666.0	25.2	1651.1	24.3

Table 8.

	ISOTOPIC RATIOS						CALCULATED AGES Ma					
Analysis	$^{207}Pb/^{235}U$	± 1 sigma	$^{206}Pb/^{238}U$	± 1 sigma	$^{207}Pb/^{206}Pb$	± 1 sigma	$^{207}Pb/^{235}U$	± 1 sigma	$^{206}Pb/^{238}U$	± 1 sigma	$^{207}Pb/^{206}Pb$	± 1 sigma
					Sample Horn 03							
110418aLEP008	0.5483	0.0939	0.0706	0.0054	0.0563	0.0013	443.9	76.0	439.9	33.6	464.6	49.5
110418aLEP015	0.8226	0.0298	0.0961	0.0024	0.0621	0.0011	609.5	22.1	591.6	14.8	676.5	37.0
110418aLEP027	0.5179	0.0257	0.0664	0.0030	0.0566	0.0008	423.8	21.0	414.4	18.6	475.0	30.1
110418aLEP031	3.0288	0.1846	0.2449	0.0120	0.0897	0.0010	1414.9	86.2	1411.9	69.3	1419.4	22.2
110418aLEP032	0.4752	0.0727	0.0636	0.0051	0.0542	0.0013	394.8	60.4	397.5	31.7	379.2	52.3
110418aLEP033	0.5421	0.0209	0.0697	0.0019	0.0564	0.0008	439.8	17.0	434.4	11.8	468.3	33.4
110418aLEP034	1.4781	0.0666	0.1545	0.0048	0.0694	0.0008	921.4	41.5	926.0	28.5	910.6	24.6
110418aLEP036	2.8401	0.1369	0.2366	0.0092	0.0871	0.0010	1366.2	65.8	1369.1	53.2	1361.7	21.6
110418aLEP037	3.7391	0.1660	0.2770	0.0108	0.0979	0.0013	1579.8	70.2	1576.0	61.7	1584.8	25.1
110418aLEP045	4.3975	0.2090	0.3061	0.0102	0.1042	0.0012	1711.9	81.3	1721.3	57.2	1700.4	21.4
110418aLEP046	0.5055	0.0235	0.0644	0.0026	0.0569	0.0009	415.4	19.3	402.3	16.1	489.2	33.3
110418aLEP047	0.9527	0.0501	0.1103	0.0035	0.0626	0.0008	679.5	35.8	674.8	21.3	695.2	27.1
110418aLEP049	1.5989	0.0740	0.1599	0.0047	0.0725	0.0011	969.8	44.9	956.2	28.2	1000.7	32.1
110418aLEP050	3.8648	0.1541	0.2799	0.0092	0.1001	0.0013	1606.4	64.1	1590.8	52.4	1626.8	23.7
110418aLEP051	2.5663	0.1239	0.2201	0.0045	0.0846	0.0022	1291.1	62.3	1282.3	26.4	1305.8	50.7
110418aLEP052	1.8478	0.0601	0.1781	0.0055	0.0752	0.0018	1062.6	34.6	1056.8	32.8	1074.6	47.1
110418aLEP054	3.8287	0.1615	0.2774	0.0088	0.1001	0.0022	1598.8	67.5	1578.3	50.0	1625.9	40.3
110418aLEP055	0.5361	0.0234	0.0635	0.0022	0.0612	0.0015	435.8	19.0	396.8	13.5	647.5	53.0

110418aLEP056	0.8230	0.0589	0.0981	0.0058	0.0609	0.0015	609.7	43.7	603.0	35.9	634.8	54.1
110418aLEP057	1.6800	0.0449	0.1682	0.0033	0.0725	0.0016	1001.0	26.8	1002.1	19.7	998.6	43.7
110418aLEP059	0.5275	0.0201	0.0687	0.0018	0.0557	0.0014	430.2	16.4	428.1	11.5	441.0	56.0
110418aLEP068	0.5188	0.0157	0.0685	0.0017	0.0550	0.0012	424.3	12.9	426.8	10.4	410.7	48.0
110418aLEP071	0.5326	0.0170	0.0690	0.0014	0.0560	0.0013	433.5	13.8	429.9	8.7	452.5	51.4
110418aLEP072	1.3269	0.0593	0.1407	0.0056	0.0684	0.0018	857.5	38.3	848.5	33.7	881.0	53.4
110418aLEP074	0.5608	0.0456	0.0764	0.0033	0.0532	0.0020	452.1	36.8	474.8	20.3	338.0	84.9
110418aLEP078	3.9384	0.1041	0.2842	0.0067	0.1005	0.0022	1621.6	42.9	1612.7	38.3	1633.2	41.2
110418aLEP079	0.5636	0.0326	0.0699	0.0018	0.0585	0.0022	453.9	26.2	435.4	11.1	548.5	80.8
110418aLEP086	4.9156	0.1620	0.3292	0.0079	0.1083	0.0028	1804.9	59.5	1834.4	43.8	1771.1	47.6
110418aLEP088	3.7689	0.1549	0.2704	0.0089	0.1011	0.0022	1586.1	65.2	1542.9	50.5	1644.1	40.7
110418aLEP089	5.9671	0.2043	0.3613	0.0095	0.1198	0.0026	1971.1	67.5	1988.1	52.2	1953.2	38.3
110418aLEP090	3.8563	0.1668	0.2822	0.0104	0.0991	0.0021	1604.6	69.4	1602.3	58.8	1607.7	39.5
110418aLEP091	0.5418	0.0451	0.0677	0.0054	0.0581	0.0017	439.6	36.6	422.2	33.9	531.9	63.4
110418aLEP093	0.5020	0.0550	0.0674	0.0025	0.0540	0.0018	413.1	45.3	420.5	15.9	371.7	73.2
110418aLEP094	1.6102	0.0623	0.1600	0.0041	0.0730	0.0017	974.2	37.7	956.7	24.5	1013.9	46.0
110418aLEP096	3.6291	0.0933	0.2751	0.0065	0.0957	0.0023	1555.9	40.0	1566.5	36.8	1541.7	44.8
110418aLEP099	1.6611	0.0753	0.1734	0.0043	0.0695	0.0017	993.8	45.0	1030.8	25.5	913.1	49.2
110418aLEP106	0.5267	0.0330	0.0655	0.0026	0.0583	0.0017	429.6	26.9	409.0	16.3	541.5	64.5
110418aLEP108	2.2328	0.1188	0.1977	0.0068	0.0819	0.0024	1191.4	63.4	1163.0	39.7	1243.3	57.3
110418aLEP112	2.0168	0.1062	0.1898	0.0049	0.0770	0.0024	1121.2	59.1	1120.6	28.9	1122.4	62.1
110418aLEP113	1.5228	0.0867	0.1601	0.0043	0.0690	0.0021	939.6	53.5	957.1	25.5	898.8	63.7
110418aLEP115	2.1922	0.1075	0.1986	0.0057	0.0800	0.0024	1178.6	57.8	1167.9	33.6	1198.2	58.4
110418aLEP116	0.5345	0.0286	0.0679	0.0024	0.0571	0.0019	434.8	23.3	423.3	14.9	496.1	74.0
110418aLEP132	1.5799	0.0801	0.1576	0.0043	0.0727	0.0024	962.3	48.8	943.2	26.0	1006.3	66.9
110418aLEP133	3.9866	0.1873	0.2881	0.0091	0.1004	0.0029	1631.5	76.6	1632.2	51.3	1630.6	54.0
110418aLEP138	1.6973	0.1243	0.1689	0.0088	0.0729	0.0022	1007.5	73.8	1006.3	52.5	1010.1	61.1
110418aLEP139	0.7397	0.0416	0.0871	0.0028	0.0616	0.0019	562.2	31.6	538.1	17.4	661.1	67.0
110418aLEP146	0.5258	0.0383	0.0685	0.0022	0.0556	0.0019	429.0	31.2	427.3	13.4	438.4	76.0
110418aLEP148	0.4834	0.0755	0.0638	0.0035	0.0549	0.0018	400.4	62.5	398.9	21.8	408.8	74.2
110418aLEP149	0.7648	0.0895	0.0928	0.0036	0.0598	0.0023	576.8	67.5	572.2	22.5	594.7	83.8
110418aLEP151	2.7976	0.1501	0.2268	0.0070	0.0894	0.0019	1354.9	72.7	1317.9	40.9	1413.7	41.2
110418aLEP154	0.5560	0.0217	0.0648	0.0022	0.0622	0.0018	448.9	17.5	405.0	13.9	680.5	60.4
110418aLEP155	0.5124	0.0232	0.0700	0.0010	0.0531	0.0014	420.1	19.1	436.4	6.4	331.2	58.5

110418aLEP157	0.5215	0.0285	0.0662	0.0017	0.0571	0.0014	426.2	23.3	413.3	10.8	496.7	55.6
110418aLEP159	0.6125	0.0267	0.0801	0.0028	0.0555	0.0014	485.1	21.1	496.5	17.5	431.7	54.8
110418aLEP160	3.0774	0.1316	0.2459	0.0047	0.0908	0.0020	1427.1	61.0	1417.5	26.9	1441.4	41.8
110418aLEP165	0.4945	0.0431	0.0634	0.0033	0.0566	0.0015	408.0	35.6	396.1	20.5	475.8	59.0
110418aLEP168	0.7316	0.0382	0.0872	0.0029	0.0609	0.0015	557.5	29.1	538.8	18.2	634.7	51.6
110418aLEP170	0.6760	0.0292	0.0793	0.0022	0.0618	0.0015	524.4	22.6	491.9	13.6	668.5	52.8
110418aLEP171	0.9429	0.0523	0.1066	0.0038	0.0642	0.0017	674.4	37.4	653.0	23.4	746.6	55.0
110418aLEP174	0.5607	0.0217	0.0705	0.0015	0.0577	0.0013	452.0	17.5	439.3	9.1	516.8	49.9
110418aLEP180	3.8061	0.1399	0.2739	0.0053	0.1008	0.0024	1594.0	58.6	1560.4	30.4	1638.9	44.8
110418aLEP185	0.4933	0.0433	0.0648	0.0015	0.0552	0.0018	407.1	35.8	405.0	9.5	419.1	73.6
110418aLEP188	0.6291	0.0460	0.0781	0.0033	0.0584	0.0016	495.5	36.2	484.6	20.7	546.1	58.0
110418aLEP191	4.0431	0.1871	0.2850	0.0097	0.1029	0.0024	1642.9	76.0	1616.5	55.1	1676.9	42.3
110418aLEP193	2.6267	0.1192	0.2302	0.0055	0.0828	0.0018	1308.1	59.4	1335.5	32.0	1263.5	43.7
110418aLEP195	3.9576	0.1551	0.2799	0.0066	0.1025	0.0023	1625.5	63.7	1591.0	37.4	1670.6	41.0
110418aLEP197	2.2068	0.1277	0.2016	0.0105	0.0794	0.0020	1183.2	68.5	1184.0	61.8	1181.8	50.7
110418aLEP205	0.5518	0.0286	0.0716	0.0020	0.0559	0.0016	446.2	23.1	445.8	12.3	448.0	62.3
110418aLEP211	4.6150	0.2529	0.3089	0.0127	0.1084	0.0028	1752.0	96.0	1735.1	71.6	1772.2	46.4
110418aLEP213	0.6024	0.0242	0.0710	0.0026	0.0615	0.0017	478.7	19.3	442.4	15.9	656.8	58.7
110418aLEP214	2.2282	0.1252	0.1990	0.0073	0.0812	0.0025	1189.9	66.9	1169.7	42.9	1226.9	60.0
110418aLEP226	3.4766	0.1340	0.2648	0.0080	0.0952	0.0027	1521.9	58.6	1514.1	45.7	1532.8	52.5
110418aLEP228	3.9860	0.2226	0.2865	0.0105	0.1009	0.0027	1631.3	91.1	1623.8	59.5	1641.1	49.9
110418aLEP229	0.5656	0.0239	0.0709	0.0021	0.0579	0.0018	455.2	19.2	441.6	13.0	524.3	68.7
110418aLEP230	0.5950	0.0326	0.0727	0.0022	0.0594	0.0016	474.1	26.0	452.3	13.6	581.1	59.9
110418aLEP232	2.3617	0.0833	0.2117	0.0052	0.0809	0.0021	1231.1	43.4	1238.1	30.4	1218.9	52.0
110418aLEP239	2.1113	0.0901	0.1905	0.0056	0.0804	0.0027	1152.5	49.2	1124.2	33.3	1206.0	66.5
110418aLEP247	2.7757	0.1359	0.2305	0.0098	0.0873	0.0024	1349.0	66.1	1336.9	56.9	1368.2	53.5
110418aLEP249	0.5291	0.0795	0.0652	0.0018	0.0589	0.0018	431.2	64.8	407.1	10.9	562.1	66.8
110418aLEP253	3.3222	0.1431	0.2530	0.0092	0.0953	0.0024	1486.3	64.0	1453.7	52.9	1533.1	46.8
110418aLEP255	0.5729	0.0214	0.0753	0.0022	0.0552	0.0015	459.9	17.2	467.8	13.9	420.8	62.6
110418aLEP258	0.5848	0.0163	0.0726	0.0020	0.0584	0.0015	467.6	13.0	451.9	12.2	545.4	56.2
110418aLEP260	1.4028	0.0534	0.1470	0.0037	0.0692	0.0019	890.1	33.9	884.0	22.3	905.4	55.5
110418aLEP265	5.6723	0.2258	0.3496	0.0137	0.1177	0.0028	1927.2	76.7	1932.8	75.7	1921.1	42.1
110418aLEP266	0.5523	0.0287	0.0726	0.0026	0.0552	0.0013	446.5	23.2	451.9	16.1	418.9	53.0
110418aLEP271	3.6895	0.1471	0.2805	0.0110	0.0954	0.0023	1569.1	62.6	1593.7	62.7	1536.1	45.7

110418aLEP276	0.9397	0.0498	0.1063	0.0033	0.0641	0.0023	672.7	35.7	651.1	20.0	745.7	75.5
110418aLEP277	0.5250	0.0398	0.0718	0.0024	0.0530	0.0029	428.5	32.5	447.0	15.2	330.4	125.7
110418aLEP278	0.5556	0.0151	0.0689	0.0018	0.0585	0.0016	448.7	12.2	429.3	11.0	549.6	60.1
110418aLEP280	0.8770	0.0585	0.1013	0.0058	0.0628	0.0021	639.4	42.6	621.8	35.8	701.9	70.5
101223LEPa8	2.0293	0.2090	0.2025	0.0177	0.0743	0.0032	1125.4	70.0	1188.5	94.8	1049.7	87.4
101223LEPa9	3.4041	0.1746	0.2582	0.0118	0.0938	0.0025	1505.3	40.3	1480.5	60.5	1504.5	50.1
101223LEPa11	1.7361	0.0845	0.1723	0.0049	0.0718	0.0033	1022.0	31.3	1025.0	26.9	980.3	93.2
101223LEPa15	0.4980	0.0508	0.0677	0.0039	0.0545	0.0032	410.3	34.4	422.4	23.3	391.5	129.7
101223LEPa16	0.5781	0.0639	0.0733	0.0055	0.0559	0.0031	463.2	41.1	456.1	33.2	446.6	123.7
101223LEPa25	0.5232	0.0467	0.0627	0.0049	0.0585	0.0020	427.3	31.1	391.8	29.4	550.3	76.2
101223LEPa26	0.5306	0.0229	0.0672	0.0032	0.0554	0.0018	432.2	15.2	419.1	19.4	429.5	72.9
101223LEPa27	0.5269	0.0283	0.0639	0.0037	0.0564	0.0015	429.8	18.8	399.0	22.3	468.0	58.7
101223LEPa30	4.1979	0.2646	0.2959	0.0157	0.1007	0.0020	1673.6	51.7	1670.9	78.2	1636.5	36.3
101223LEPa31	3.4820	0.1462	0.2615	0.0087	0.0931	0.0023	1523.1	33.1	1497.5	44.4	1489.8	45.8
101223LEPa33	3.8524	0.3309	0.2663	0.0164	0.1005	0.0048	1603.8	69.3	1521.7	83.6	1632.9	88.5
101223LEPa35	3.4829	0.5388	0.2629	0.0337	0.0949	0.0049	1523.3	122.0	1504.5	172.1	1527.0	98.1
101223LEPa39	0.5851	0.0555	0.0765	0.0030	0.0549	0.0041	467.7	35.5	475.2	17.9	407.2	165.4
101223LEPa40	4.3653	0.6785	0.2987	0.0416	0.1040	0.0046	1705.8	128.4	1684.6	206.4	1695.8	81.3
101223LEPa49	2.0265	0.0943	0.1854	0.0074	0.0741	0.0024	1124.5	31.7	1096.3	40.4	1043.2	65.3
101223LEPa53	4.0648	0.5119	0.2830	0.0275	0.1025	0.0061	1647.3	102.6	1606.3	138.2	1670.1	109.2
101223LEPa59	1.0956	0.1314	0.1185	0.0115	0.0661	0.0021	751.2	63.7	722.1	66.2	808.8	67.9
101223LEPa64	0.8360	0.0249	0.0963	0.0018	0.0617	0.0014	616.9	13.8	592.8	10.7	665.3	47.6
101223LEPa65	0.5377	0.0307	0.0613	0.0036	0.0607	0.0028	436.9	20.3	383.5	21.8	628.4	98.3
101223LEPa71	0.5124	0.0293	0.0658	0.0018	0.0558	0.0021	420.1	19.7	410.8	10.7	443.1	85.7
101223LEPa73	2.6221	0.1674	0.2157	0.0144	0.0880	0.0020	1306.9	46.9	1259.0	76.2	1382.6	43.6
101223LEPa75	1.2440	0.1207	0.1175	0.0125	0.0686	0.0030	820.7	54.6	716.4	72.0	886.0	91.9
101223LEPa77	0.6495	0.0400	0.0789	0.0026	0.0595	0.0033	508.2	24.6	489.4	15.3	586.5	119.1
101223LEPa78	2.1879	0.1136	0.1834	0.0099	0.0842	0.0025	1177.2	36.2	1085.4	53.7	1297.5	58.2
101223LEPa79	4.6878	0.1691	0.3108	0.0116	0.1078	0.0021	1765.1	30.2	1744.6	56.8	1762.5	35.8
101223LEPa80	3.4243	0.2958	0.2446	0.0239	0.1014	0.0028	1510.0	67.9	1410.4	123.7	1650.8	51.4
101223LEPa85	2.1968	0.0871	0.1990	0.0083	0.0796	0.0017	1180.0	27.7	1169.7	44.5	1187.1	41.1
101223LEPa86	3.8043	0.3070	0.2687	0.0142	0.0984	0.0073	1593.6	64.9	1534.3	72.3	1593.9	138.7
101223LEPa87	0.4734	0.0259	0.0596	0.0024	0.0569	0.0015	393.5	17.8	373.1	14.4	486.3	57.1
101223LEPa89	0.5279	0.0610	0.0670	0.0033	0.0560	0.0044	430.4	40.5	418.0	19.9	453.1	175.1

101223LEPa90	3.3022	0.1565	0.2544	0.0131	0.0946	0.0035	1481.6	36.9	1460.9	67.3	1519.6	69.1
101223LEPa93	2.7178	0.2544	0.2216	0.0244	0.0875	0.0053	1333.3	69.5	1290.5	129.0	1371.7	115.9
101223LEPa96	4.0792	0.1624	0.2879	0.0112	0.1029	0.0019	1650.1	32.5	1630.8	56.3	1676.4	34.5
101223LEPa97	3.9945	0.1827	0.2918	0.0133	0.0987	0.0018	1633.1	37.1	1650.3	66.5	1600.2	34.6
101223LEPa99	3.6685	0.2572	0.2594	0.0160	0.1009	0.0024	1564.5	55.9	1486.7	81.7	1640.9	43.4
101223LEPa106	2.2399	0.0947	0.1912	0.0040	0.0803	0.0027	1193.6	29.7	1128.0	21.4	1204.8	66.5
101223LEPa108	0.5674	0.0224	0.0692	0.0033	0.0569	0.0015	456.3	14.5	431.5	19.6	488.6	57.2
101223LEPa110	2.0539	0.2915	0.1968	0.0242	0.0736	0.0026	1133.6	96.9	1157.9	130.3	1031.5	71.1
101223LEPa111	1.7016	0.2566	0.1623	0.0216	0.0744	0.0034	1009.1	96.5	969.4	119.6	1053.5	91.7
101223LEPa116	2.5616	0.1704	0.1956	0.0097	0.0896	0.0035	1289.8	48.6	1151.9	52.3	1417.3	73.7
101223LEPa117	0.4878	0.0476	0.0621	0.0053	0.0557	0.0016	403.4	32.5	388.3	32.1	440.7	63.1
101223LEPa120	1.3695	0.0676	0.1299	0.0057	0.0759	0.0017	875.9	29.0	787.0	32.6	1091.8	45.3
101223LEPa126	4.0384	0.1696	0.2877	0.0120	0.1017	0.0020	1642.0	34.2	1630.1	59.9	1655.4	36.5
101223LEPa129	2.8529	0.1452	0.2342	0.0131	0.0901	0.0019	1369.6	38.3	1356.3	68.7	1427.2	39.4
101223LEPa130	3.6383	0.3240	0.2871	0.0283	0.0920	0.0030	1558.0	70.9	1627.2	141.8	1467.1	61.2
101223LEPa132	3.1191	0.1153	0.2524	0.0093	0.0892	0.0020	1437.4	28.4	1451.0	48.0	1408.6	42.0
101223LEPa133	3.9003	0.1303	0.2821	0.0083	0.0996	0.0015	1613.7	27.0	1602.1	42.0	1615.7	28.9
101223LEPa136	0.6354	0.0472	0.0789	0.0024	0.0568	0.0034	499.5	29.3	489.8	14.2	482.0	133.5
101223LEPa137	2.0812	0.3055	0.1862	0.0247	0.1014	0.0243	1142.6	100.7	1100.6	134.4	1650.8	443.8
101223LEPa139	3.6730	0.1135	0.2721	0.0087	0.0980	0.0021	1565.5	24.7	1551.7	44.3	1586.8	40.9
101223LEPa140	0.5233	0.0451	0.0614	0.0036	0.0615	0.0027	427.3	30.1	383.8	22.1	656.7	95.8
101223LEPa145	2.0426	0.2806	0.1993	0.0242	0.0752	0.0031	1129.8	93.7	1171.5	130.1	1074.0	82.5
101223LEPa148	0.5353	0.0289	0.0654	0.0017	0.0637	0.0045	435.3	19.1	408.4	10.1	731.0	149.9
101223LEPa149	2.9664	0.1766	0.2322	0.0148	0.0923	0.0013	1399.1	45.2	1345.8	77.4	1473.7	25.8
101223LEPa150	1.6057	0.1388	0.1570	0.0135	0.0732	0.0048	972.4	54.1	939.9	75.0	1019.0	133.2
101223LEPa153	0.5366	0.0383	0.0697	0.0032	0.0565	0.0021	436.2	25.3	434.4	19.3	471.9	82.3
101223LEPa154	2.5709	0.1273	0.2158	0.0090	0.0871	0.0018	1292.4	36.2	1259.8	47.7	1362.7	39.5
101223LEPa156	4.0072	0.1777	0.2882	0.0098	0.1009	0.0023	1635.7	36.0	1632.5	49.1	1641.3	42.0
101223LEPa157	2.3411	0.0840	0.2101	0.0041	0.0803	0.0027	1224.9	25.5	1229.6	22.0	1204.8	66.6
101223LEPa160	0.4991	0.0434	0.0684	0.0026	0.0547	0.0043	411.1	29.4	426.4	15.4	400.2	174.2
101223LEPa171	2.7139	0.1460	0.2265	0.0094	0.0867	0.0036	1332.3	39.9	1316.3	49.6	1354.3	79.3

Table 9.

Analysis	ISOTOPIC RATIOS						CALCULATED AGES Ma					
	$^{207}Pb/^{235}U$	± 1 sigma	$^{206}Pb/^{238}U$	± 1 sigma	$^{207}Pb/^{206}Pb$	± 1 sigma	$^{207}Pb/^{235}U$	± 1 sigma	$^{206}Pb/^{238}U$	± 1 sigma	$^{207}Pb/^{206}Pb$	± 1 sigma
	Sample Smøl 01											
110419aLEP010	1.7296	0.1083	0.1726	0.0068	0.0727	0.0017	1019.6	63.8	1026.7	40.6	1004.4	48.8
110419aLEP016	0.5970	0.0310	0.0736	0.0025	0.0589	0.0017	475.3	24.7	457.5	15.8	562.1	61.7
110419aLEP032	0.6287	0.0245	0.0785	0.0018	0.0581	0.0015	495.3	19.3	487.4	11.0	531.9	58.3
110419aLEP037	0.5873	0.0305	0.0715	0.0025	0.0596	0.0014	469.1	24.4	445.2	15.5	588.2	51.7
110419aLEP038	0.5342	0.0510	0.0691	0.0038	0.0561	0.0016	434.6	41.5	430.5	23.9	456.4	61.7
110419aLEP040	0.6423	0.0401	0.0773	0.0044	0.0603	0.0024	503.8	31.5	479.7	27.5	614.4	85.0
110419aLEP046	0.5214	0.0246	0.0696	0.0012	0.0544	0.0014	426.1	20.1	433.6	7.6	386.0	58.5
110419aLEP048	0.5986	0.0610	0.0725	0.0043	0.0599	0.0023	476.3	48.6	451.3	26.7	598.8	83.8
110419aLEP049	0.5725	0.0686	0.0777	0.0071	0.0535	0.0019	459.6	55.1	482.1	44.1	348.5	82.2
110419aLEP057	0.5825	0.0218	0.0729	0.0017	0.0579	0.0012	466.1	17.5	453.6	10.4	527.8	46.7
110419aLEP058	0.5697	0.0236	0.0734	0.0014	0.0563	0.0013	457.8	19.0	456.8	8.7	463.3	51.1
110419aLEP066	0.5748	0.0344	0.0692	0.0029	0.0602	0.0013	461.1	27.6	431.6	18.2	611.3	47.0
110419aLEP067	0.5185	0.0687	0.0679	0.0017	0.0554	0.0018	424.1	56.2	423.7	10.5	426.8	73.2
110419aLEP069	0.5699	0.0238	0.0693	0.0023	0.0596	0.0015	458.0	19.2	432.1	14.4	589.8	53.2
110419aLEP073	2.6016	0.0907	0.2192	0.0050	0.0861	0.0017	1301.1	45.4	1277.7	29.0	1340.0	39.0
110419aLEP075	4.1623	0.1479	0.2873	0.0082	0.1051	0.0020	1666.6	59.2	1628.0	46.5	1715.7	35.1
110419aLEP089	0.5378	0.0298	0.0690	0.0024	0.0566	0.0014	437.0	24.2	429.9	14.7	474.6	54.3
110419aLEP090	3.2007	0.2017	0.2481	0.0109	0.0936	0.0018	1457.3	91.9	1428.8	62.6	1499.2	35.7
110419aLEP091	1.6684	0.1210	0.1704	0.0053	0.0710	0.0016	996.6	72.3	1014.3	31.4	957.8	46.5
110419aLEP092	4.1846	0.1395	0.2939	0.0063	0.1033	0.0020	1671.0	55.7	1660.8	35.7	1683.8	36.0
110419aLEP094	0.7794	0.0519	0.0937	0.0060	0.0604	0.0020	585.2	39.0	577.1	37.1	616.5	73.2
110419aLEP105	0.5249	0.0339	0.0666	0.0027	0.0572	0.0020	428.4	27.7	415.5	16.5	498.8	76.0
110419aLEP106	0.5524	0.0172	0.0693	0.0012	0.0578	0.0012	446.5	13.9	432.0	7.6	522.1	47.0
110419aLEP108	0.5953	0.0164	0.0759	0.0015	0.0569	0.0012	474.2	13.0	471.5	9.6	487.5	46.2
110419aLEP111	1.3727	0.1242	0.1394	0.0094	0.0714	0.0014	877.3	79.4	841.4	56.5	969.1	40.8
110419aLEP119	0.5157	0.0856	0.0728	0.0013	0.0514	0.0014	422.2	70.1	452.9	7.8	258.3	62.4
110419aLEP125	2.5648	0.0515	0.2208	0.0032	0.0843	0.0015	1290.7	25.9	1286.0	18.6	1298.5	35.5
110419aLEP130	1.8201	0.1333	0.1718	0.0077	0.0768	0.0016	1052.7	77.1	1021.9	46.1	1117.1	41.6
101222LEPa11	0.5508	0.0235	0.0684	0.0015	0.0576	0.0020	445.5	15.4	426.8	8.9	512.9	75.3

101222LEPa12	3.2516	0.2834	0.2673	0.0213	0.0909	0.0070	1469.6	67.7	1526.9	108.4	1443.7	146.3
101222LEPa13	3.0749	0.1663	0.2330	0.0099	0.0959	0.0048	1426.5	41.4	1350.2	52.0	1545.5	93.4
101222LEPa14	0.5261	0.0548	0.0725	0.0021	0.0526	0.0054	429.2	36.4	451.3	12.9	310.2	233.2
101222LEPa15	3.8860	0.1459	0.2894	0.0081	0.0972	0.0036	1610.8	30.3	1638.3	40.4	1571.0	68.6
101222LEPa26	0.6563	0.0358	0.0776	0.0025	0.0583	0.0029	512.3	21.9	481.8	14.8	542.6	107.3
101222LEPa29	0.5511	0.0296	0.0694	0.0020	0.0563	0.0025	445.7	19.3	432.8	11.8	463.5	99.8
101222LEPa30	0.5122	0.0234	0.0644	0.0016	0.0578	0.0019	419.9	15.7	402.6	9.5	523.1	70.8
101222LEPa35	1.6405	0.1239	0.1647	0.0057	0.0728	0.0034	985.9	47.7	983.1	31.3	1007.2	95.8
101222LEPa37	0.5258	0.0197	0.0652	0.0026	0.0606	0.0026	429.0	13.1	407.1	16.0	625.5	92.5
101222LEPa39	0.6231	0.0357	0.0736	0.0020	0.0604	0.0035	491.8	22.3	458.1	12.0	616.9	123.9
101222LEPa40	1.1561	0.0484	0.1264	0.0031	0.0668	0.0022	780.1	22.8	767.3	17.6	833.0	69.5
101222LEPa45	0.5994	0.0401	0.0749	0.0016	0.0580	0.0031	476.9	25.5	465.6	9.8	529.3	116.7
101222LEPa46	0.6468	0.0554	0.0689	0.0037	0.0653	0.0054	506.5	34.1	429.3	22.1	783.6	173.7
101222LEPa47	0.5942	0.0280	0.0716	0.0021	0.0600	0.0020	473.6	17.8	445.9	12.8	603.9	72.5
101222LEPa49	0.5192	0.0928	0.0720	0.0060	0.0521	0.0038	424.6	62.0	448.1	36.3	290.5	168.4
101222LEPa52	0.4068	0.1109	0.0587	0.0067	0.0583	0.0141	346.5	80.0	367.7	41.0	539.7	530.3
101222LEPa54	0.6144	0.0421	0.0779	0.0024	0.0588	0.0026	486.4	26.5	483.8	14.5	559.6	95.9
101222LEPa55	3.9353	0.2567	0.2678	0.0156	0.1078	0.0027	1621.0	52.8	1529.7	79.1	1762.2	45.6
101222LEPa59	0.6391	0.0493	0.0819	0.0035	0.0581	0.0041	501.8	30.6	507.2	20.9	532.4	153.4
101222LEPa60	0.5058	0.0933	0.0718	0.0027	0.0499	0.0107	415.7	62.9	446.9	16.5	191.1	499.5
101222LEPa69	0.5353	0.0450	0.0714	0.0038	0.0549	0.0036	435.3	29.8	444.8	22.7	409.9	147.9
101222LEPa70	5.6934	0.3073	0.3535	0.0128	0.1192	0.0035	1930.4	46.6	1951.2	60.8	1943.8	52.9
101222LEPa76	0.5934	0.0873	0.0748	0.0040	0.0568	0.0055	473.0	55.6	465.1	24.1	483.6	212.3
101222LEPa79	0.6086	0.0259	0.0726	0.0027	0.0599	0.0022	482.7	16.4	451.8	16.4	601.5	78.9
101222LEPa81	1.5354	0.3118	0.1428	0.0176	0.0727	0.0067	944.7	124.9	860.4	99.2	1004.3	186.6